Past and future tsunamis and other extreme longwave oscillations in the Strait of Georgia

Alexander Rabinovich, Richard Thomson, Jadranka Šepić, Lauren Lupton, Stephen Mundschutz and Nicky Hastings

Fisheries and Oceans Canada
Institute of Ocean Sciences
9860 West Saanich Road
Sidney, BC V8L 4B2, CANADA

2023

Canadian Technical Report of
Hydrography and Ocean Sciences 363

Fisheries and Oceans Canada | Pêches et Océans Canada

Canada

Canadian Technical Report of Hydrography and Ocean Sciences

Technical reports contain scientific and technical information of a type that represents a contribution to existing knowledge, but which is not normally found in the primary literature. The subject matter is generally related to programs and interests of the Oceans and Science sectors of Fisheries and Oceans Canada.

Technical reports may be cited as full publications. The correct citation appears above the abstract of each report. Each report is abstracted in the data base Aquatic Sciences and Fisheries Abstracts.

Technical reports are produced regionally but are numbered nationally. Requests for individual reports will be filled by the issuing establishment listed on the front cover and title page.

Regional and headquarters establishments of Ocean Science and Surveys ceased publication of their various report series as of December 1981. A complete listing of these publications and the last number issued under each title are published in the Canadian Journal of Fisheries and Aquatic Sciences, Volume 38: Index to Publications 1981. The current series began with Report Number 1 in January 1982.

Rapport technique canadien sur l'hydrographie et les sciences océaniques

Les rapports techniques contiennent des renseignements scientifiques et techniques qui constituent une contribution aux connaissances actuelles mais que l'on ne trouve pas normalement dans les revues scientifiques. Le sujet est généralement rattaché aux programmes et intérêts des secteurs des Océans et des Sciences de Pêches et Océans Canada.

Les rapports techniques peuvent être cités comme des publications à part entière. Le titre exact figure au-dessus du résumé de chaque rapport. Les rapports techniques sont résumés dans la base de données Résumés des sciences aquatiques et halieutiques.

Les rapports techniques sont produits à l'échelon régional, mais numérotés à l'échelon national. Les demandes de rapports seront satisfaites par l'établissement auteur dont le nom figure sur la couverture et la page de titre.

Les établissements de l’ancien secteur des Sciences et Levés océaniques dans les régions et à l'administration centrale ont cessé de publier leurs diverses séries de rapports en décembre 1981. Vous trouverez dans l'index des publications du volume 38 du Journal canadien des sciences halieutiques et aquatiques, la liste de ces publications ainsi que le dernier numéro paru dans chaque catégorie. La nouvelle série a commencé avec la publication du rapport numéro 1 en janvier 1982.

Canadian Technical Report of
Hydrography and Ocean Sciences 363

2023

PAST AND FUTURE TSUNAMIS AND OTHER EXTREME LONGWAVE OSCILLATIONS IN THE STRAIT OF GEORGIA

Alexander Rabinovich[1], Richard Thomson[1], Jadranka Šepić[2], Lauren Lupton[1], Stephen Mundschutz[1], and Nicky Hastings[3]

[1]Fisheries and Oceans Canada
Institute of Ocean Sciences
9860 West Saanich Road
Sidney, BC V8L 4B2, CANADA

[2]Faculty of Science
University of Split
33 Ruđera Boškovića
Split, 21000, CROATIA

[3]Natural Resources Canada
Geological Survey of Canada - Pacific Division
605 Robson Street
Vancouver, BC V6B 5J3, CANADA

Cat. No. Fs97-18/363E-PDF ISBN 978-0-660-68323-2 ISSN 1488-5417

Correct citation for this publication:

Rabinovich, A., Thomson, R., Šepić, J., Lupton, L., Mundschutz, S., and Hastings, N., 2023. Past and future tsunamis and other extreme longwave oscillations in the Strait of Georgia. Can. Tech. Rep. Hydrogr. Ocean Sci. 363: vi + 89 p.

CONTENTS

ABSTRACT

Rabinovich, A., Thomson, R., Šepić, J., Lupton, L., Mundschutz, S., and Hastings, N., 2023. Past and future tsunamis and other extreme longwave oscillations in the Strait of Georgia. Can. Tech. Rep. Hydrogr. Ocean Sci. 363: vi + 89 p.

The coast of British Columbia is susceptible to tsunamis generated by strong earthquakes within the Pacific Ocean and by local underwater earthquakes. Although the Strait of Georgia is partially sheltered from tsunami waves arriving from the open ocean, past tsunamis from major events, such as the 1964 Alaska and 2011 Tohoku tsunamis, have penetrated into the region. Vancouver Island is also in a seismically active zone; the magnitude 7.3 Vancouver Island Earthquake near Campbell River generated local tsunamis in the strait that caused considerable damage and the death of one person. The east coast of Vancouver Island is further susceptible to landslide-generated tsunamis, meteorological tsunamis and storm surge.

This study examines the risk of marine flooding at Federal Government facilities located in the Saanich Inlet/Pat Bay and Nanaimo regions. Trans-oceanic tsunamis are found to present a substantial, but not major, threat to these two regions. The primary concern is a major tsunami generated by a great earthquake along the Cascadia Subduction Zone.

Submarine landslides, rock falls and avalanches are not uncommon on the British Columbia coast. The two regions having a high risk of future submarine slides are: (1) Roberts Bank, Fraser River delta; and (2) Malaspina Strait. A Roberts Bank slide would produce marked tsunami runup in the Gulf Islands, but only small (< 0.5 m) runup in the Patricia Bay and Nanaimo areas. A Malaspina Strait failure would have a negligible effect on these areas.

Atmospheric processes are the most important factor for flooding in the southern Strait of Georgia. Allowing for an engineering “safety factor” of 1.5, we find that the maximum possible sea level rise associated with meteorological forcing for the study sites is 1.6-1.7 m.

RÉSUMÉ

Rabinovich, A., Thomson, R., Šepić, J., Lupton, L., Mundschutz, S., and Hastings, N., 2023. Past and future tsunamis and other extreme longwave oscillations in the Strait of Georgia. Can. Tech. Rep. Hydrogr. Ocean Sci. 363: vi + 89 p.

La côte de la Colombie-Britannique est sensible aux tsunamis générés par de forts tremblements de terre dans l'océan Pacifique et par des tremblements de terre sous-marins locaux. Bien que le détroit de Géorgie soit partiellement à l'abri des vagues de tsunami arrivant du large, des tsunamis passés lors d'événements majeurs, tels que les tsunamis de l'Alaska en 1964 et du Tohoku en 2011, ont pénétré dans la région. L'île de Vancouver se trouve également dans une zone sismiquement active; le tremblement de terre de magnitude 7,3 sur l'île de Vancouver, près de Campbell River, a généré des tsunamis locaux dans le détroit qui ont causé des dégâts considérables et la mort d'une personne. La côte est de l'île de Vancouver est également vulnérable aux tsunamis provoqués par des glissements de terrain, aux tsunamis météorologiques et aux ondes de tempête.

Cette étude examine le risque d'inondation marine dans les installations du gouvernement fédéral situées dans les régions de Saanich Inlet/Pat Bay et de Nanaimo. Les tsunamis transocéaniques constituent une menace importante, mais pas majeure, pour ces deux régions. La principale préoccupation est un tsunami majeur généré par un grand tremblement de terre le long de la zone de subduction de Cascadia.

Les glissements de terrain sous-marins, les chutes de pierres et les avalanches ne sont pas rares sur la côte de la Colombie-Britannique. Les deux régions présentant un risque élevé de futurs glissements sous-marins sont: (1) Roberts Bank, delta du fleuve Fraser; et (2) le détroit de Malaspina. Un glissement de terrain de Roberts Bank produirait un ruissellement de tsunami marqué dans les îles Gulf, mais seulement un faible ruissellement (< 0,5 m) dans les régions de Patricia Bay et de Nanaimo. Une rupture du détroit de Malaspina aurait un effet négligeable sur ces zones.

Les processus atmosphériques constituent le facteur le plus important d'inondation dans le sud du détroit de Géorgie. En tenant compte d'un «facteur de sécurité» technique de 1,5, nous constatons que l'élévation maximale possible du niveau de la mer associée au forçage météorologique pour les sites d'étude est de 1,6 à 1,7 m.

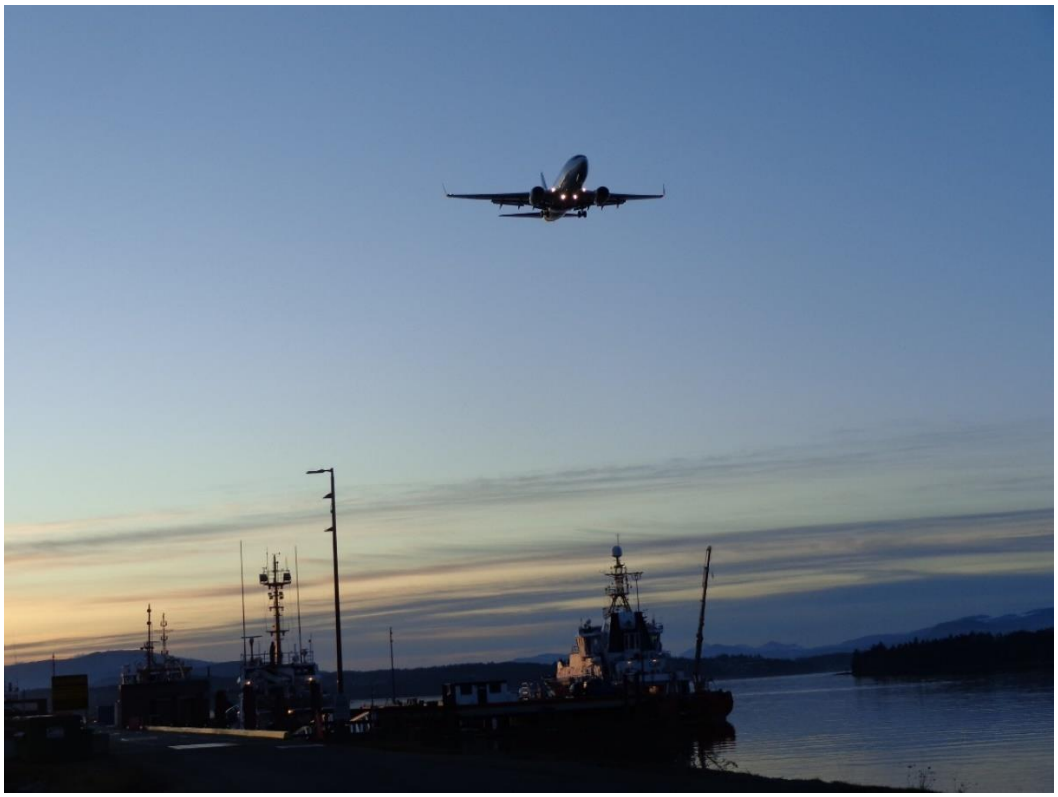

1. INTRODUCTION

Large segments of the British Columbia coast are susceptible to tsunamis generated within the Pacific Ocean and by local underwater earthquakes. The catastrophic tsunamis of the last two decades, including the 2004 Sumatra, 2010 Chile and 2011 Tohoku events, as well as two recent 2018 tsunamis in Indonesia (Sulawesi and Anak-Krakatau), demonstrate the serious threat of major seismically generated tsunamis to coastal communities in southern British Columbia. The 2004 Sumatra tsunami killed roughly 230,000 people in 14 countries bordering the Indian Ocean, and was the deadliest tsunami in recorded history. The 2011 Tohoku tsunami killed nearly 20,000 people, destroyed the Fukushima Dai-ichi nuclear power plant and produced major damage along the Japanese coast. The 2010 Chile tsunami resulted in hundreds of deaths and severe damage on the coast of South America, while two recent local tsunamis in Indonesia killed several thousands of people in that country. The Strait of Georgia are relatively sheltered from tsunami waves incoming from the open ocean, nevertheless, tsunamis from major events (e.g., the 1964 Alaska

and 2011 Tohoku tsunamis) have penetrated this region and were recorded by Canadian Hydrographic Service (CHS) tide gauges. Moreover, Vancouver Island is a seismically active region; the 1946 M_w 7.5 Vancouver Island Earthquake with its epicenter near Campbell River triggered several local landslides and associated tsunamis in the Strait of Georgia that created considerable damage and killed one person.

Submarine landslides, slumps, rock falls, and avalanches can generate significant tsunami waves in coastal areas of the World Ocean. Although landslide-generated tsunamis are more localized than seismically generated tsunamis, they can produce destructive coastal runup and cause severe damage, especially where the wave energy is trapped by the confines of inlets or semi-enclosed embayments. The inlets and narrow straits of the Pacific Coast of North America are the regions, where landslide-generated tsunamis occur most frequently and are accompanied by the largest runup [*Lander*, 1996; *Evans*, 2001; *Rabinovich et al*., 2003]. In general, studies in the coastal areas of North America indicate high instability of deltaic and nearshore sediments [*Prior et al*., 1981, 1984; *Johns et al.*, 1986]. Large accumulations of unstable sediments deposited in the deltas of North American rivers, such as the Fraser, Skeena, and Nisqually, are particularly dangerous. Construction sites, buildings, and submarine cables in these areas are at significant risk to direct damage from subaerial and submarine landslides. In these areas, tsunamis generated by the failure events probably pose an even greater threat in terms of damage and loss of life than tsunamis generated by distant earthquakes. The sediment transported by the Fraser River form a huge body of unstable alluvial deposits at the entrance to the river and could, potentially, produce a destructive tsunami in the southern part of the Strait of Georgia that might impact Patricia Bay and Nanaimo.

Additional risk for the east coast of Vancouver Island is associated with sea level oscillations caused by atmospheric processes. There are two main categories of atmospherically generated hazardous types of such oscillations:

(a) *Storm surge* – a low-frequency sea level displacement with typical duration from several hours to several days produced by the cumulative effect of wind stress and the fall of the air pressure normally associated with passage of a cyclone [*Murty*, 1977; *Pugh and Woodworth*, 2014].

(b) *Meteorological tsunamis (meteotsunamis)* – high-frequency sea level oscillations with typical periods from a few minutes to a couple of hours generated by atmospheric pressure

jumps, internal atmospheric gravity waves, squall lines or frontal passages [*Monserrat et al.*, 2006; *Rabinovich*, 2020].

Several storm surge and meteotsunami events have been measured in the past in the southern part of the Strait of Georgia. The Saanich Inlet/Pat Bay and Nanaimo regions are susceptible to anomalously highwater levels during major southeasterly storms at the time of "King Tides" and heavy rainfall. It is expected that atmospherically forced sea level events will be of increasing importance to low-lying BC communities as sea levels continue to rise through the effects of global warming. The estimation of the potential flood risk to the inner coast of Vancouver Island initiated by storm surges and meteotsunamis is clearly of considerable importance to low-lying coastal areas.

We can conclude that the following types of marine hazardous sea level events could potentially affect the areas of the Institute of Ocean Sciences (IOS) in Patricia Bay and the Pacific Biological Station (PBS) in Nanaimo:

(1) Major trans-oceanic seismically generated tsunamis

(2) Local seismically generated tsunamis

(3) Landslide-generated tsunamis

(4) Storm surges

(5) Meteorological tsunamis

These five types of events will be considered in the current report in turn. Our main concern is the possible superposition of several types of strong sea level oscillations, in particular tsunamis, high tides and storm surge. Estimation of the potential tsunami risk to the British Columbia coast from a superposition of storm surges, meteotsunamis and tides, is vitally important, especially for areas being considered for new construction or major renovations [*Leonard et al*., 2014].

The purpose of this project is to investigate historical tsunamis, storm surges and meteotsunamis in the southern and central parts of the Strait of Georgia, in general, and specifically in the area of Patricia Bay and Nanaimo based on tide gauge measurements from this region. Unfortunately, there has not been a permanent tide gauge station at Nanaimo and only temporary sea level observations are available for this region. That is why sea level statistics for Nanaimo are relatively poor. The situation for Patricia Bay (Pat Bay) is much better as a result of permanent observations at this station since 1974, i.e., for more than 45 years. However, even this statistic is insufficient in that it missed all five of the great tsunamis of the 20th century (1946, 1952, 1957,

1960 and 1964; cf. *Rabinovich et al.* [2019]). For this reason, the present study uses information and data from other stations located in this region. We also examine all other available information regarding marine hazardous events in this region, including tsunami catalogues, papers, reports and media information.

2. OBSERVATIONS

The present report is mainly based on analysis of the Canadian Hydrographic Service (CHS) tide gauge records from the instruments in the southern Strait of Georgia and at the head of Juan de Fuca Strait. The instrument sites are shown in Figure 1. Before the end of 1990s all tide gauges were analogue ("pen-and-paper") instruments. As a result of the destructive tsunamis of the 1990s in the Pacific Ocean, the CHS in 1997 initiated a major upgrade of the existing network of tide gauges on the BC coast, including those located in the Strait of Georgia. The new digital instruments were designed to continuously measure sea levels with much higher precision and time resolution than earlier analogue gauges, and to store recorded values with 1-min sampling intervals [*Rabinovich and Stephenson*, 2004].

One of our reference stations, **Patricia Bay**, was deployed as a permanent CHS station in June 1976 and since that time has been working continuously. Until 1997, the tide gauge provided analogue data digitized with 1-hour sampling. In July 1997, a new high-resolution digital gauge was installed at this station with 1 min sampling. Thus, for this station there are 21 years of paper and 1-hour records and about 22.5 years of 1-min data. There are only a few short gaps in the data. These data can be used to examine oceanic processes in a broad frequency range, including tsunamis, storm surge and meteotsunamis.

Regular sea level measurements at **Nanaimo** began in January 1997, when a digital tide gauge with 3-min sampling was deployed at this station. Continuous measurements at Nanaimo lasted until October 2003 and were then stopped. A tide gauge at Nanaimo was restored in July 2014 and since that time the instrument has been providing continuous data series with 1-min sampling.

Unfortunately, the Nanaimo tide gauge was not in operation during all major tsunami events that occurred in the Pacific Ocean during last 100 years, while the Pat Bay tide gauge worked only during the 2010 and 2011 events. However, we can use some other stations located in this region:

(1) **Point Atkinson**, located on the northern coast of Burrard Inlet, at the entrance to the Strait of Georgia (see inset in Figure 1a). This is one of the oldest CHS stations; it started in 1914, so the sea level record at this station is one of the longest for the coast of British Columbia [*Rabinovich et al.*, 2019]. A precise high-resolution instrument with 1-min sampling has been working at this station since 1997.

(2) The principal station for the region is **Victoria** – a permanent CHS tide gauge station in operation since 1906 [*Rabinovich et al.*, 2019]. All tsunamis from the Pacific Ocean enter the southern Strait of Georgia through Juan de Fuca Strait, passing Victoria. So, for all stations located in the Strait of Georgia, Victoria is the *gate station.* Tsunamis observed in the Strait of Georgia were first recorded at Victoria. However, because the San Juan Islands (USA) and the Gulf Islands (BC) shelter the Strait of Georgia from incoming tsunami waves, not all waves observed at Victoria entered the Strait of Georgia. As with Point Atkinson, sea level measurements at Victoria up to the middle of 1997 were analogue and after that high-resolution digital with 1-min sampling.

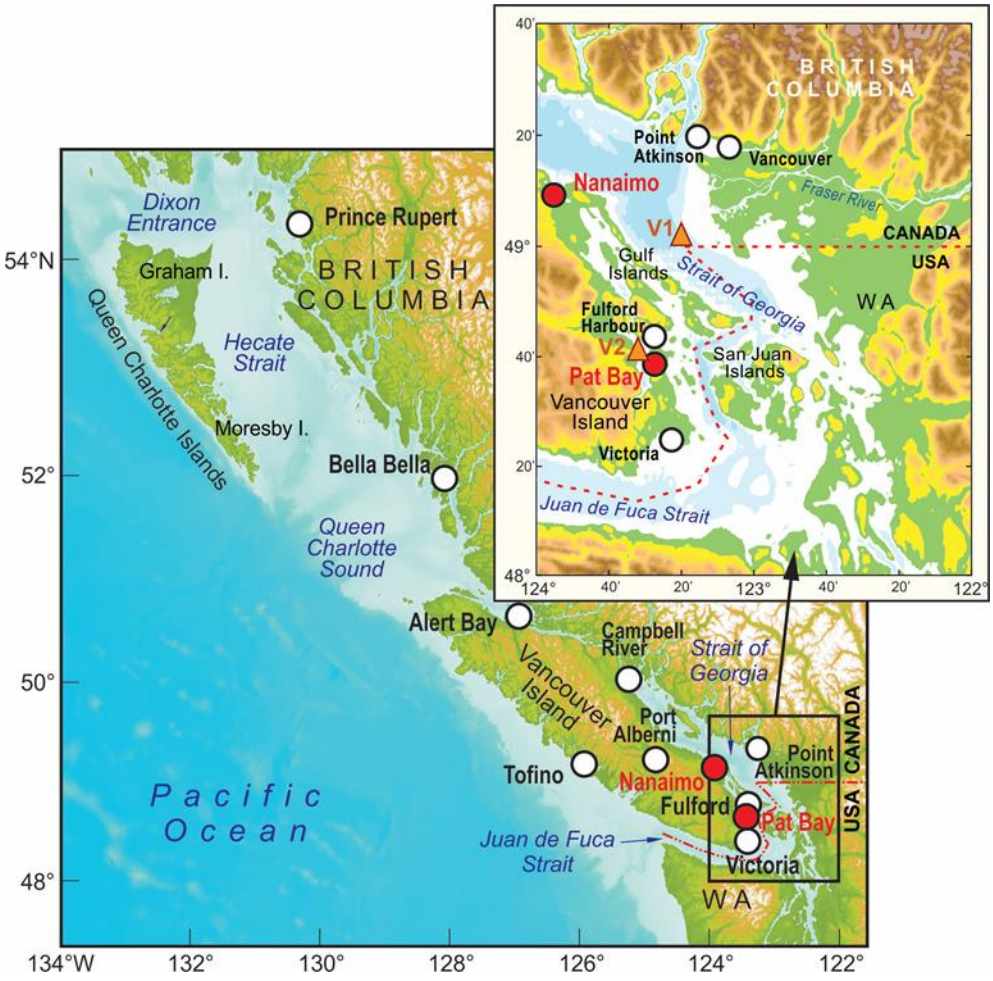

Figure 1. Map of British Columbia showing locations of the Canadian Hydrographic Service (CHS) coastal tide gauges: *Red circles* indicate Patricia Bay and Nanaimo tide gauges, *white circles* indicate other tide gauge stations, *orange triangles* show the locations of two Ocean Network Canada (ONC) VENUS bottom pressure recorders (BPRs).

In addition to Point Atkinson and Victoria, we used historical analogue records from **Fulford Harbour** on Salt Spring Island (an old station that was in operation during the 1952-1992 period). For comparison, we also used information on historical tsunamis recorded at stations located on the outer and northern coast of Vancouver Island and on the mainland coast: Tofino, Alert Bay, Bella Bella and Prince Rupert (Figure 1).

All available analogue records for the time of five great tsunamis of the 20th century (1946, 1952, 1957, 1960 and 1964), in particular, Victoria, Point Atkinson and Fulford Harbour, were

digitized with a sampling interval of 1 min and examined by *Rabinovich et al.* [2019]; the results of that study are used in the present report.

The only tsunami that was clearly recorded at the head (northernmost part) of the Strait of Georgia was the 2011 Tohoku tsunami measured at **Campbell River**. This record, together with the records of this tsunami from Point Atkinson and Patricia Bay, were used to estimate the 2011 tsunami wave height at Nanaimo. Other major tsunamis either did not reach the Campbell River station (in particular, the 2010 Chilean tsunami) or occurred when this station was not in operation, as in the cases of the (tsunamis of 1946-1964.

We also used data from two Ocean Network Canada (ONC), Victoria Experimental Network Under the Sea (VENUS) bottom pressure stations. One of them (V1) is located in the southern part of the Strait of Georgia, close to Nanaimo, the other one (V2) in Saanich Inlet near Patricia Bay (Figure 1). Both stations have been in operation since February 2006 (https://www.oceannetworks.ca/venus-data-now-available-oceans-20); the data have a time step of 1 min.

In addition, we used paleotsunami data and various information and data from the tsunami catalogues of *Lander and Lockridge* [1989], *Lander et al.* [1993] and *Stephenson et al.* [2007] and from several papers [cf. *Rabinovich et al.*, 2019].

3. HISTORICAL AND RECENT TRANS-OCEANIC TSUNAMIS

In this section, we examine all available information on Pacific tsunamis that could affect the coasts of the Strait of Georgia. The data from the existing tsunami catalogues [*Lander and Lockridge*, 1989; *Lander et al.*, 1993; *Stephenson et al.*, 2007] and from specific papers [cf. *Rabinovich et al.*, 2019] indicate that only major trans-oceanic tsunamis can penetrate into this region. During the entire instrumental period of 1900-2020 there have been seven such events: (1) the 1946 Aleutian Islands tsunami (initiated by an earthquake with a momentum magnitude M_w 8.6); (2) the 1952 Kamchatka tsunami (M_w 9.0); (3) the 1957 Andreanof Islands (M_w 8.6); (4) the 1960 Great Chile tsunami (M_w 9.5); (5) the 1964 Alaska tsunami (M_w 9.2); (6) the 2010 Chile (Maule) tsunami (M_w 8.8); and (7) the 2011 Tohoku (East Japan) tsunami (M_w 9.0) [*Gusiakov*, 2014; *Rabinovich et al.*, 2019]. Also from paleotsunami field survey studies on the coasts of British

Columbia, Washington and Oregon [cf. *Wang et al.*, 2003; *Clague et al.*, 2003] and from historical chronicles in Japan [cf. *Atwater et al.*, 2005], we know about a major trans-oceanic tsunami that was generated in 1700 by a great earthquake with an estimated magnitude of M_w 9.0 in the Cascadia Subduction Zone (CSZ). The epicenters of all these eight major earthquakes are shown in Figure 2.

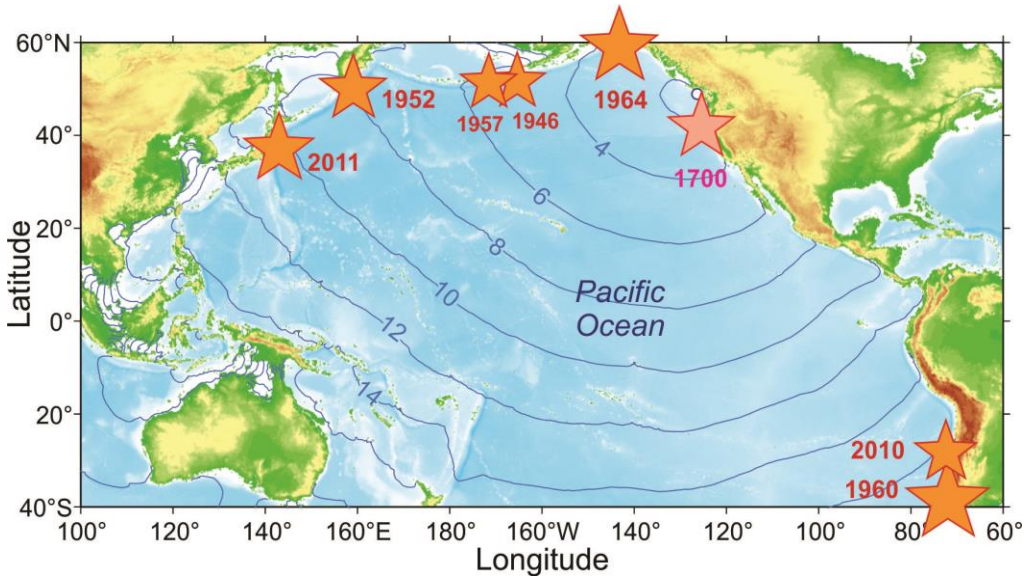

Figure 2. Epicenters (orange stars) of the five great earthquakes of the 20th century (1946 Aleutian Islands, 1952 Kamchatka, 1957 Andreanof Islands., 1960 Chile and 1964 Alaska) and the two of the 21st century (2010 Chile and 2011 Tohoku) in the Pacific Ocean that produced major trans-oceanic tsunamis. Also shown by a pink star is the epicenter of the 1700 Cascadia Subduction Zone (CSZ) earthquake. The size of the star is proportional to the earthquake momentum magnitude (M_w). The solid blue lines are inverted isochrones of the tsunami travel time (in hours) from various parts in the Pacific Ocean to Tofino, British Columbia (modified from *Rabinovich et al.* [2019]).

Possible waveforms in the Strait of Georgia (SoG) associated with the eight tsunamis are examined in the following text (Sections 3.1–3.8). As indicated above, the San Juan and Gulf islands shelter the SoG from incoming trans-oceanic waves. Therefore, these waves either do not penetrate into this region or they were strongly attenuated. As an example, Figure 3 shows maximum tsunami wave heights recorded during the last 110 years at Victoria and Point Atkinson. While the Victoria tide gauge recorded 39 tsunamis during this period , including all seven major events, the tide gauge at Point Atkinson recorded only three tsunamis (1960, 1964 and 2011) and

the measured tsunami heights for these events at Point Atkinson were 5-10 times smaller than at Victoria.

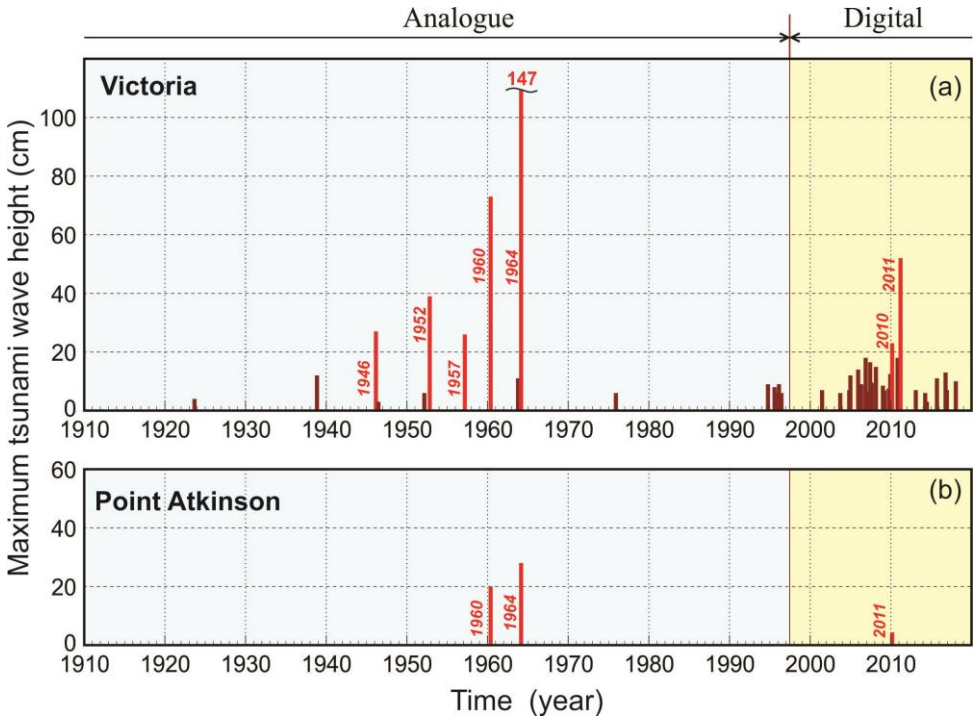

Figure 3. Maximum wave heights of tsunamis recorded at (a) Victoria and (b) Point Atkinson during the period 1910–2019. Up to 1997, measurements were made by analogue tide gauges; since July 1997, digital tide gauges have been used. The *red bars* indicate tsunami wave heights for the five great tsunamis of the 20th century (1946, 1952, 1957, 1960 and 1964) and two of the 21st century (2010 and 2011); all the others are indicated by the *magenta bars*.

3.1. The 1700 Cascadia Tsunami

The Cascadia Subduction Zone (CSZ) is a convergent plate boundary that stretches from central Vancouver Island (Canada) to Northern California (USA). It is a huge, sloping subduction zone where the Explorer, Juan de Fuca, and Gorda plates move to the east and slide below the continental North American Plate (Figure 4). The most important tsunami threat for the southern coast of British Columbia is from this zone [*Ng et al.*, 1991; *Wang et al.*, 2003; *Clague et al.*, 2003;

Leonard et al., 2014]. The Great CSZ earthquake of 26 January 1700, which had an estimated magnitude M_w = 9.0, generated a major trans-oceanic tsunami (Figure 5) that caused significant destruction in Japan, on the opposite side of the Pacific Ocean [cf. *Atwater et al.,* 2005], and strongly affected the outer coast of British Columbia.

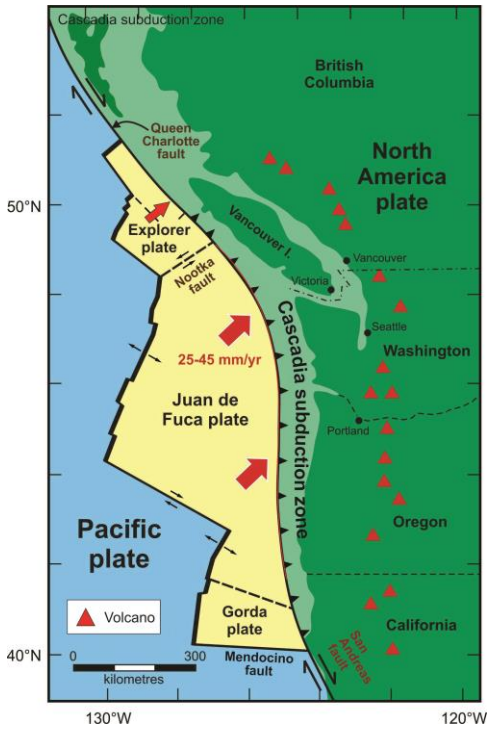

Figure 4. The Cascadia subduction zone, a convergent plate boundary stretching 1000 km from northern Vancouver Island (BC) to northern California. The Juan de Fuca Plate and two smaller plates are sliding beneath the North American Plate.

There is no reliable information or data concerning historical tsunami heights on the coast of British Columbia associated with the 1700 CSZ earthquake. However, paleotsunami findings on the coast of Vancouver Island and the west coast of the USA [*Clague,* 2001; *Clague et al*., 2000, 2003] show that tsunami waves of ~15 m likely struck these coasts at the time of the earthquake. Numerical modelling of the 1700 CSZ tsunami for coastal North America [cf. *Cherniawsky et al*., 2007; *Fine et al*., 2008, 2018; *Cheung et al*., 2011] support these estimates.

Based on the tsunami arrival information for the coast of Japan, researchers back calculated that the earthquake occurred on the west coast of North America in the evening at about 21:00 LT.

Immediately following the earthquake, coastal areas subsided 0.5–2.0 m and, in response, the level of the sea immediately rose by a comparable amount. The first waves impacted the nearest coastal areas 20–30 min after the rupture. Fortunately, the tides were reasonably low and falling along the west coast of Vancouver Island at the time of the earthquake.

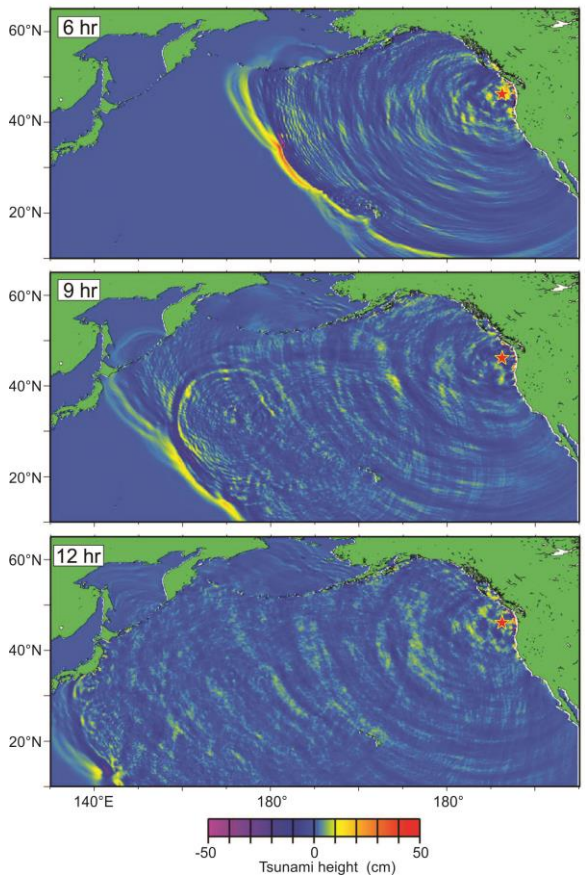

Figure 5. Simulated tsunami waves from a computer model showing the positions of the waves 6, 9 and 12 hours after the Cascadia subduction zone great earthquake in 1700 (from *Satake et al.* [1996]).

Recent paleotsunami studies for the coast of Vancouver Island and the west coast of the USA [cf. *Clague et al*., 2000, *Clague*, 2001], as well as numerical modelling of CSZ tsunamis for coastal North America [cf. *Cherniawsky et al*., 2007; *Fine et al*., 2008], demonstrate the high risk of CSZ tsunamis for southern British Columbia. Numerous seismotectonic studies indicate that great megathrust earthquakes in the CSZ region have occurred on a regular basis in the past and can be expected to occur with an average return period of about 500 years, with an uncertainty of

approximately 200 years [*Witter et al*., 2013; *Wang et al*., 2013; *Wang and Tréhu*, 2016]. The only way to accurately determine the risk of CSZ tsunamis and the maximum expected tsunami wave heights for the SoG is through a series of numerical experiments that apply various scenarios for the source region of a CSZ earthquake. Detailed high-resolution modelling of a possible CSZ tsunami for Victoria Harbour and adjacent regions was carried out by *Fine et al*. [2018]. Similar modelling is needed for the Patricia Bay and Nanaimo regions. On the other hand, numerous paleotsunami studies on Vancouver Island [cf. *Clague*, 2001; *Clague et al*., 2000, 2003] reveal no evidence of tsunami deposits that can be linked with the 1700 event on the inner (SoG) coast of the island.

3.2. The Aleutian Tsunami of 1 April 1946

The 1946 Aleutian tsunami was generated by a $M_w = 8.6$ earthquake with its epicenter located 150 km from Unimak Island in the eastern Aleutian Islands. The earthquake generated one of the largest trans-Pacific tsunamis ever instrumentally recorded, with maximum runup heights on the coasts of Alaska and the Aleutian Islands of up to 40 m. Within 48 minutes of the earthquake, the tsunami struck the area of Scotch Cap, Alaska and completely destroyed a newly built US Coast Guard Lighthouse, surging over the coastal cliff to a height of 42 m above mean sea level. Then, 4.5 hours after the main shock, the destructive waves reached the coast of the Hawaiian Islands, where they were totally unexpected. The maximum runup in the area of Hilo on the Big Island was 17 m; on the islands of Oahu and Maui, the maximum run-up was 11 m and 10 m, respectively. The tsunami was also recorded along the entire west coast of the United States, and crossed the Pacific Ocean to produce 9-m waves at locations in the Marquesas Islands. The tsunami also extended southeastwards, damaging boats in Chile. Altogether, the tsunami killed 167 people, most of them in Hawaii (158), but also at the Scotch Cap lighthouse (5), Marquesas (2), Peru (1) and California (1).

The tsunami was unusually powerful for the size of the earthquake. Due to the large discrepancy between the tsunami magnitude, $M_t = 9.3$ [*Abe*, 1979], and the surface wave magnitude, $M_s = 7.4$, this earthquake was identified as a '*tsunami earthquake*' [*Kanamori*, 1972; *Abe*, 1973], i.e., as an earthquake generating a tsunami that is much larger than it should be based on the earthquake magnitude. The severe destruction and large number of casualties in the

Hawaiian Islands prompted the United States to create, in Honolulu, Hawaii, the Seismic Sea Wave System, which was then converted in 1949 to the Pacific Tsunami Warning Center (PTWC).

The 1946 tsunami was clearly recorded at the Tofino and Victoria tide gauges (Figure 6). The tsunami waves arrived at the Victoria gauge 5 hours 19 minutes after the earthquake, in good agreement with the theoretical travel time and with earlier estimates of arrival times [cf. *Stephenson et al.*, 2007]. The maximum wave height recorded was 27 cm; this is approximately one half of the maximum wave height at Tofino (55 cm) [*Rabinovich et al.*, 2019].

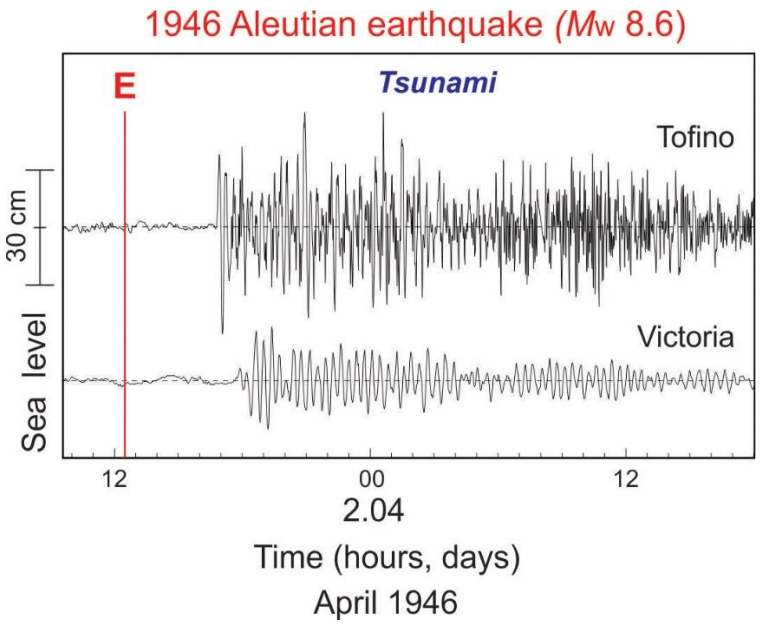

Figure 6. The 1 April 1946 Aleutian tsunami recorded at Tofino and Victoria. The solid vertical red line labelled "E" denotes the time of the earthquake (from *Rabinovich et al.* [2019]).

Station Caulfield (Point Atkinson) was in operation during the event but did not record the 1946 tsunami. The question is: *Why would the 1946 tsunami, which was highly destructive on the coasts of the Hawaiian Islands and some other Pacific islands, relatively weak on the coast of British Columbia and did not impact the southern Strait of Georgia?* The most probable explanation is the narrow focus of the tsunami "beam" was directed southwestward exactly toward the Hawaiian Islands, with little energy propagating southeastward toward British Columbia. In addition, the Caulfield (Point Atkinson) site, as well as other sites in the SoG, were well sheltered from tsunami waves arriving via the San Juan and Gulf islands.

3.3. The Kamchatka Tsunami of 4 November 1952

The 1952 tsunami was generated by a M_w = 9.0 earthquake with its source area located near the southern end of the Kamchatka Peninsula, Russia. The tsunami had wave heights >18 m and killed about 10,000 people in Severo-Kurilsk (Paramushir Island), Baikovo (Shumshu Island) and southern Kamchatka. It was the most devastating tsunami in Russian history [*Gusiakov*, 2013]. Six hours later, 6-8 m waves struck the Hawaiian Islands, with a maximum wave height of 9.1 m on the easternmost coast of Oahu Island. However, no fatalities were reported from the far-field areas affected by this tsunami.

The Kamchatka tsunami was clearly recorded on the coast of British Columbia. The digitized and de-tided records from five tide gauges, including Victoria, are shown in Figure 7; the corresponding statistical information is given in Table 1. The fact that this wave was so clearly recorded at Kitimat is especially remarkable considering that the station is located at the head of Kitimat Arm, the innermost inlet at the end of the long and narrow Douglas Channel, roughly 80 km from Hecate Strait (Figure 7). The tsunami parameters, which were unrecognizable in the original paper record [cf. *Weeks and Studds*, 1953; *Stephenson et al.*, 2007], were easily determined from the digitized and de-tided record (Table 1) [*Rabinovich et al.*, 2019].

A particular property of all records was the very long "ringing" of the tsunami waves for more than three days. Tsunami waves were noticed by shipping in Victoria Harbour but there was no damage [*Stephenson et al.*, 2007]. The District Engineer (CHS, Victoria) reported "This wave was of somewhat greater amplitude on our coast than the one of 1946 and continued to oscillate for a considerably longer time…" [*Weeks and Studds*, 1953]. The maximum tsunami wave height at Victoria estimated from the de-tided record (Figure 7) was 39 cm, in agreement with the historical estimate by *Weeks and Studds* [1953] who reported a maximum wave height of 40 cm. Tsunami travel time was also substantially corrected from 8 hours 12 minutes to 8 hours 42 minutes.

Although the Caulfield (Point Atkinson) station was in operation during the 1952 event, tsunami waves were not been recorded at this station. It appears that the San Juan and Gulf islands effectively sheltered the Strait of Georgia from arriving tsunami waves. There is no evidence that the 1952 tsunami penetrated into the southern Strait of Georgia.

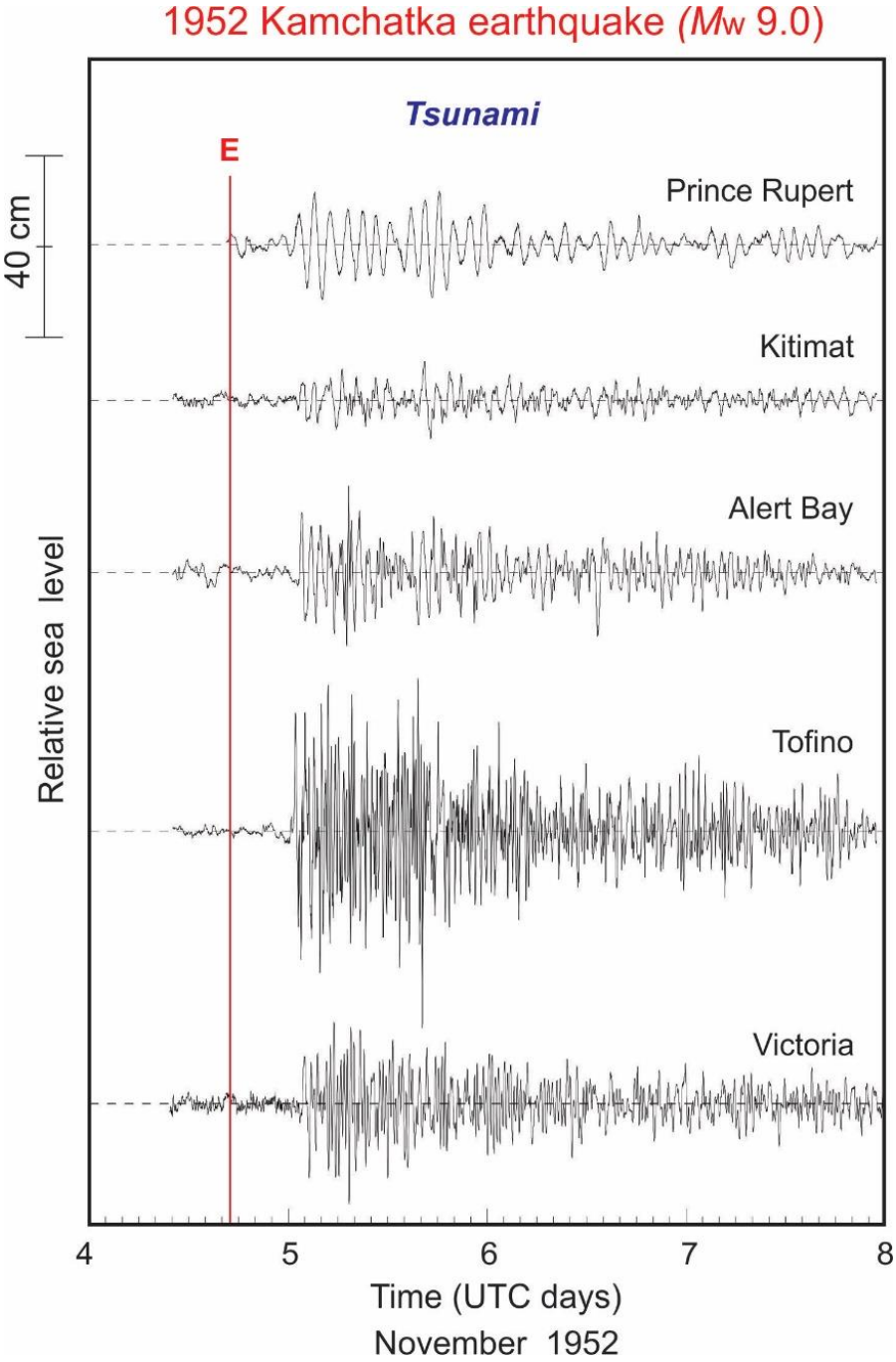

Figure 7. The 4 November 1952 Kamchatka tsunami recorded at Prince Rupert, Kitimat, Alert Bay, Tofino and Victoria on the coast of British Columbia. The solid vertical red line labelled "E" denotes the time of the earthquake (from *Rabinovich et al.* [2019]).

Table 1. Parameters of the Kamchatka tsunami of 4 November 1952 recorded by five analogue CHS tide gauges on the coast of British Columbia (Main shock, M_w = 9.0 at 16:58 UTC)

Station	First wave			Maximum wave			Visible period (min)
	Arrival time (UTC)	Travel time (hh:mm)	Amplitude (cm) & Sign	Amplitude (cm)	Time (UTC) of maximum amplitude	Height (cm)	
Victoria	1:40	8:42	+6.0	18.0	5:30	38.8	25
Tofino	0:30	7:32	+26.2	33.7	15:38	77.0	22
Alert Bay	1:19	8:21	+14.7	19.2	7:16	35.3	25, 70
Kitimat	1:17	8:19	+5.5	8.5	16:26	17.0	30, 100
Prince Rupert	0:43	7:45	+7.0	11.8	18:13	23.7	110

Comments:

(1) The analogue records of these tsunamis were digitized at 1 min sampling.
(2) Arrival and maximum wave times are for 5 November 1952.

3.4. The Andreanof Islands Tsunami of 9 March 1957

The tsunami of 9 March 1957 was generated by a M_w = 8.6 earthquake originating south of the Andreanof Islands group, in the central part of the Aleutian Islands (Figure 2). Based on the aftershock distribution, *Johnson et al.* [1994] estimated the source area of the earthquake as one of the longest of any earthquakes instrumentally recorded, stretching almost 1200 km along the Aleutian Trench. The earthquake generated a major tsunami that was recorded by tide gauges throughout the entire Pacific Ocean [*Salsman*, 1959]. The tsunami wave heights on the coasts of some of the unpopulated Aleutian Islands were estimated to be more than 20 m high; the north coast of Kauai Island (Hawaii) was hit by waves up to 16 m high. The Hawaiian Islands suffered the most, with infrastructure damage of approximately $5 million (in 1957 US dollars). Timely tsunami warnings prevented any direct fatalities, even in the far-field areas affected [*Lander and Lockridge*, 1989].

The effects of the 1957 event are poorly documented for the coast of British Columbia. An analysis of the analogue records by *Wigen* [1983] indicated that the maximum wave height at Tofino was 52 cm, but he did not examine other records, probably because the tsunami signal was

weak and could not be readily extracted from tidal analogue records. *Rabinovich et al.* [2019] digitized all available tide gauge paper records of this event. The thorough analyses of these records showed that the 1952 tsunami was measured at six stations (Table 2), including Tofino, Victoria and Fulford Harbour (Figure 8).

As with the 1952 tsunami event, Tofino was the first station on the BC coast to record the 1957 tsunami. The leading wave arrived at Tofino at 18:46 UTC on 9 March 1957 (4 h 23 min after the earthquake); subsequent recorded arrival times were 19:23 UTC at Alert Bay, 20:05 UTC at Victoria and 20:50 UTC at Fulford Harbour. Once again, the maximum wave height among all stations (~48 cm) was recorded at Tofino. - the station that can be considered as a *beacon station* for all trans-oceanic tsunamis arriving along the coast of British Columbia [*Wigen*, 1983; *Rabinovich et al.*, 2019]. The observed wave heights at other stations were significantly smaller, ranging from 11 cm at Fulford Harbour to 26 cm at Victoria (Table 3).

Table 2. Parameters of the Andreanof Islands tsunami of 9 March 1957 recorded by six analogue CHS tide gauges on the coast of British Columbia (Main shock, M_w = 8.0 at 14:23 UTC)

Station	First wave			Maximum wave			Visible period (min)
	Arrival time (UTC)	Travel time (hh:mm)	Amplitude (cm) & Sign	Amplitude (cm)	Time (UTC) of max amplitude	Wave height (cm)	
Prince Rupert	19:07	4:44	+6.70	7.2	21:43	15.0	110
Bella Coola	19:44	5:21	+4.8	6.3	4:00*	15.0	24
Alert Bay	19:23	5:00	+8.3	11.0	2:51*	22.2	24
Tofino	18:46	4:23	+20.2	24.9	1:14*	48.2	24
Victoria	20:05	5:42	+6.3	12.2	3:55*	25.7	22
Fulford Harbour	20:50	6:27	+3.5	6.1	10:30*	11.2	25

Comments:

(1) The analogue records for this tsunami were digitized at 1 min sampling.
(2) Maximum wave times indicated by "*" are on 10 March 1957.
(3) Tide gauge record at Port San Juan (Port Renfrew) was very noisy and no tsunami signal was recognizable.

The maximum 1952 tsunami wave height at Victoria was ~0.53 of the wave height at Tofino. *Rabinovich et al.* [2019] based on 7 major tsunamis estimated that

$$H_{max}\ (\text{Victoria}) = (0.57 \pm 0.03)\ H_{max}\ (\text{Tofino}),$$

while according to Table 2, H_{max} (Fulford) ≈ 0.43H_{max} (Victoria). In general, the 1957 Andreanof Islands tsunami was the first trans-oceanic tsunami that was recorded within the Strait of Georgia (in Fulford Harbour).

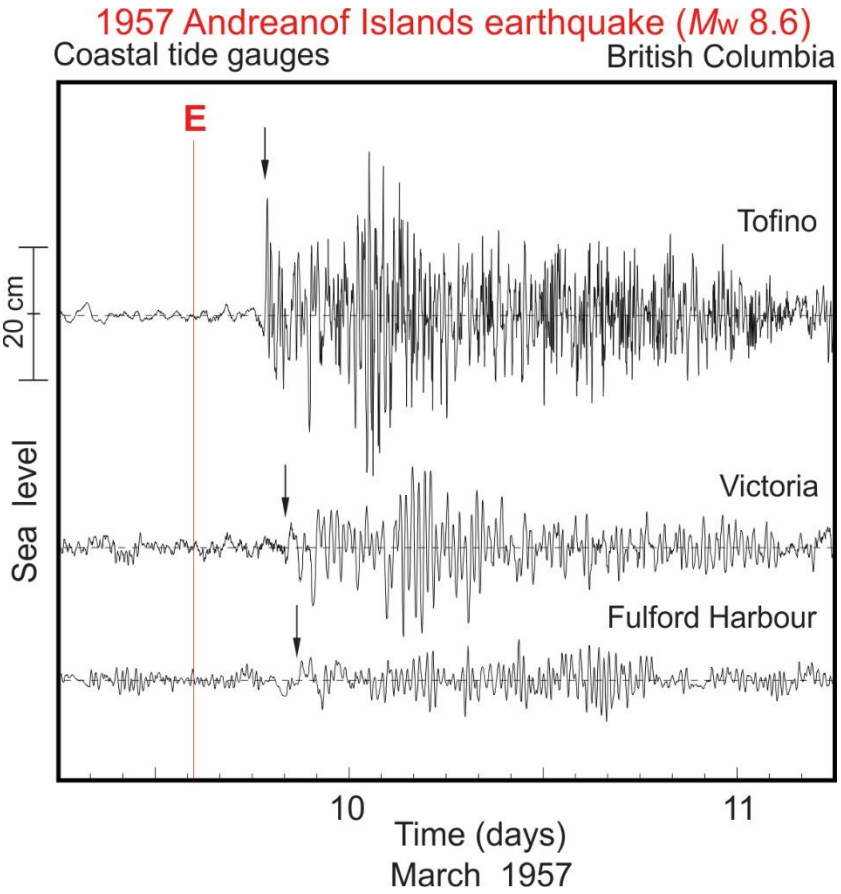

Figure 8. The 9 March 1957 Andreanof Islands tsunami recorded at Tofino, Victoria and Fulford Harbour on the coast of British Columbia. The solid vertical red line labelled "E" denotes the time of the earthquake; the arrows indicate the tsunami arrival.

3.5. The Chilean Tsunami of 22 May 1960

The Chilean tsunami of 22 May 1960 was generated by the $M_w = 9.5$ Great Chilean (Valdivia) Earthquake, also known as "the 1960 Valdivia earthquake", the strongest earthquake ever instrumentally recorded in the World Ocean. The main shock of the earthquake occurred at 19:11 UTC; the earthquake lasted for about 10 min and the rupture length was approximately 900 km [*Satake and Atwater,* 2007]. The tsunami from this event was the largest of the 20th century. In southern Chile, about 1,655 people were killed, 3,000 injured and two million displaced; 61 people lost their lives on the coasts of the Hawaiian Islands, 142 in Japan, 32 in the Philippines and 2 on the west coast of the USA [*Kong et al.*, 2015]. The high degree of destruction and loss of life in a number of the Pacific countries located far from the source area was the impetus for international cooperation in tsunami research and mitigation, and resulted in the establishment of the International Tsunami Warning System in the Pacific (ITSU) and the Pacific Tsunami Warning Center (PTWC) in Honolulu, Hawaii, based on the former Seismic Sea Wave Warning System (SSWWS) [*Kong et al.*, 2015].

The tsunami was recorded by an unprecedented number of about 250 tide gauges including far-field sites at the Aleutian Islands and in the Sea of Okhotsk, located 16-18 thousand kilometers from the source area [*Berkman and Symons*, 1960; *Takahashi and Hatori,* 1961 *Miller et al.,* 1962]. The maximum observed far-field wave heights were 10.5 m on the Hawaiian Islands, 6-9 m on other Pacific Islands and in Japan, and 4-6 m in Russia. Strong oscillations with trough-to-crest wave heights of more than 3-5 m were recorded at a number of stations on the coast of Alaska [*Lander,* 1996].

Altogether, there were 21 CHS tide gauges in operation on the coast of British Columbia in May 1960. Of the 7 permanent and 14 temporary gauges, 17 of them (6 permanent and 11 temporary) recorded the 1960 Chilean tsunami [*Wigen,* 1960]. There were also numerous eye-witness reports of strong oscillations along the BC coast. From an observational perspective, the entire situation with the 1960 tsunami tide gauge measurements was completely different from that for the 1946, 1952 and 1957 events. While tsunami waves for the previous events had been recorded at only a few BC stations, the 1960 tsunami was observed at 17 stations, many of them located in regions where tsunami waves had never been observed before. Moreover, the 1960 tsunami was much stronger than any of the previous events recorded on the BC. All 17 existing

records were examined by *Wigen* [1960] using the original paper records, in which tsunami oscillations were superimposed on tides.

All available tide gauge records for this event were carefully digitized and de-tided by *Rabinovich et al.* [2019]. The residual 1-minute records made it possible to examine this event along the British Columbia coast and, in particular in the area of Victoria, with much higher precision than was possible using paper records [*Wigen*, 1960; *Stephenson et al.*, 2007] and to accurately estimate the main characteristics of the observed tsunami waves. The results of these analyses for Tofino, Victoria, Fulford Harbour and Caulfield (Point Atkinson) are presented in Table 3 and Figure 9.

Table 3. Parameters of the Great Chile tsunami of 22 May 1960 recorded by CHS analogue tide gauges on the coast of southern British Columbia (Main shock, M_w = 9.5 at 19:11 UTC)

Station	First wave			Maximum wave			Visible period (min)
	Arrival time (UTC)	Travel time (hh:mm)	Amplitude (cm) Sign	Amplitude (cm)	Time (UTC) of max amplitude	Height (cm)	
Tofino	12:23	17:12	+35	60	19:48	132	22
Victoria	12:57	17:46	+40	41	19:48	73	22
Fulford Hbr.	13:31	18:20	+12	17	22:56	34	30
Caulfield	14:02	18:51	+12	12	15:47	20	180

Comments:

(1) Parameters of the tsunami waves were estimated based on digitized analogue tide gauge records re-sampled to 1-min.

(2) At most stations, the first (frontal) wave appears in the record as an extensive (~2 hours) "hump" followed by higher frequency oscillations.

The tsunami arrived at Victoria at 12:57 UTC on 23 May 1960, or 17 hours 46 minutes after the main earthquake shock and 34 minutes later than at Tofino (12:23 UTC) on the west coast of Vancouver Island. The wave propagated into the Strait in Georgia and, at 13:31 UTC, it reached Fulford Harbour and then, at 14:02, reached Caulfield in West Vancouver (Figure 9). The tsunami observed at Victoria, Fulford and Caulfield consisted of very long-period waves with periods T ~ 150-160 minutes. However, after reflection within Victoria Harbour, waves with shorter periods

were induced (T ~ 55 minutes). The effect of wave dispersion is clearly present in the tsunami record for Victoria; roughly four hours after the first wave arrival, a train of prominent waves with much shorter periods (T ~22 minutes) arrived; the maximum trough-to-crest tsunami wave of 73 cm was associated with this wave train. The maximum wave occurred at 21:41 UTC, more than 8.5 hours after the leading wave arrival. In general, the records at all stations were characterized by very long ringing (> 3 days) and slow energy decay.

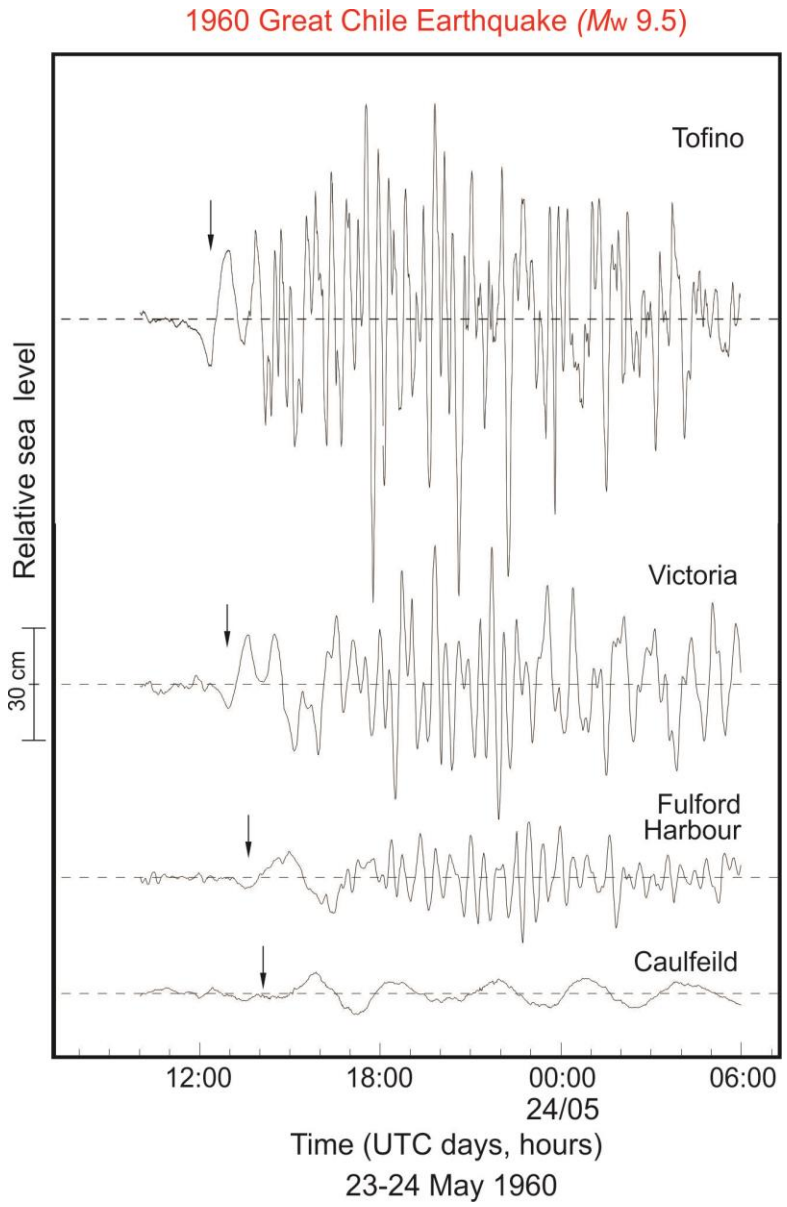

Figure 9. The 22 May 1960 Chile tsunami recorded at Tofino, Victoria, Fulford (Salt Spring Island) and Caulfield (Point Atkinson). The arrows indicate the tsunami arrival time.

The 1960 Chilean tsunami was the first event that was clearly recorded in the Strait of Georgia. Similar to the 1957 tsunami, the 1960 tsunami at Fulford Harbour had a maximum wave height (34 cm) of roughly one half that recorded at Victoria. At Point Atkinson, the recorded waves were even weaker (maximum was only 20 cm). Also, while at other stations (Tofino, Victoria and Fulford Harbour) the dominant periods of the observed periods were relatively short (22-30 min), the recorded waves at Point Atkinson had very long periods (T~3 hours).

3.6. The Alaska Tsunami of 28 March 1964

The Alaska earthquake of 28 March 1964 with magnitude M_w = 9.2 produced a catastrophic tsunami, the second strongest in the 20th century (after the 1960 Chilean tsunami). The maximum water rise was 20 m at the source. The earthquake also initiated a great number of landslides and submarine landslides that generated local tsunamis with a runup up to 70 m [*Lander,* 1996]. The earthquake, which was the strongest instrumentally recorded earthquake in the North Pacific Ocean and one of the strongest earthquakes ever recorded, occurred in the region of Prince William Sound, leading to widely used name of the "Prince William Sound Earthquake" [*Spaeth and Berkman*, 1967; *Johnson et al.,* 1996]. Because of the date (28 March 1964), this earthquake and associated tsunami are also called the "Good Friday Earthquake and Tsunami". This event generated the strongest tsunami response ever recorded on the coast of British Columbia.

The 1964 earthquake occurred within the Alaska-Aleutian megathrust zone, where the Pacific Plate subducts under the North American Plate (Figure 10). This zone has the greatest potential to generate destructive tsunamis and is one of the most seismically active fault zones in the North Pacific. The 1964 megathrust Alaska earthquake caused the most destructive tsunami in Alaskan history and, further south, strongly impacted the west coasts of the USA and Canada [*Johnson et al*., 1996; *Suleimani et al*., 2013; *Fine et al.,* 2018]. In addition to the major tectonically-generated tsunami, the earthquake triggered several landslides in the coastal fjords of Alaska, resulting in more than 20 local tsunamis. Of 132 fatalities associated with the 1964 earthquake, 122 were caused by tsunamis [*Lander*, 1996]. The tsunami spread over the entire Pacific Ocean and was recorded by a number of coastal tide gauges.

The tsunami swept southward from the source area in Prince William Sound along the British Columbia coast, causing about $10 million in damage (1964-dollar values). If such an earthquake and tsunami were to occur today, the cost of the damage would be a factor of 10 to 100 times greater. The 1964 tsunami was the strongest tsunami ever observed on the Pacific coast of Canada. According to [*Spaeth and Berkman*, 1967], the tsunami struck the coast of British Columbia near the time of high tide (see also [*Stephenson et al.*, 2007; *Rabinovich et al.*, 2019]). The earliest recorded arrival was at 05:33 UTC at Tasu Sound on the west coast of Haida Gwaii. The highest wave reported in Canada was at Shields Bay on the west coast of Graham Island where the crest wave was ~5.5 m above the spring high water; the wave damaged a logging camp located in this region. The main damage occurred at the twin towns of Alberni and Port Alberni, with the maximum tsunami run-up at Port Alberni reaching more than 8 m [*Stephenson et al.*, 2007; *Rabinovich et al.*, 2019].

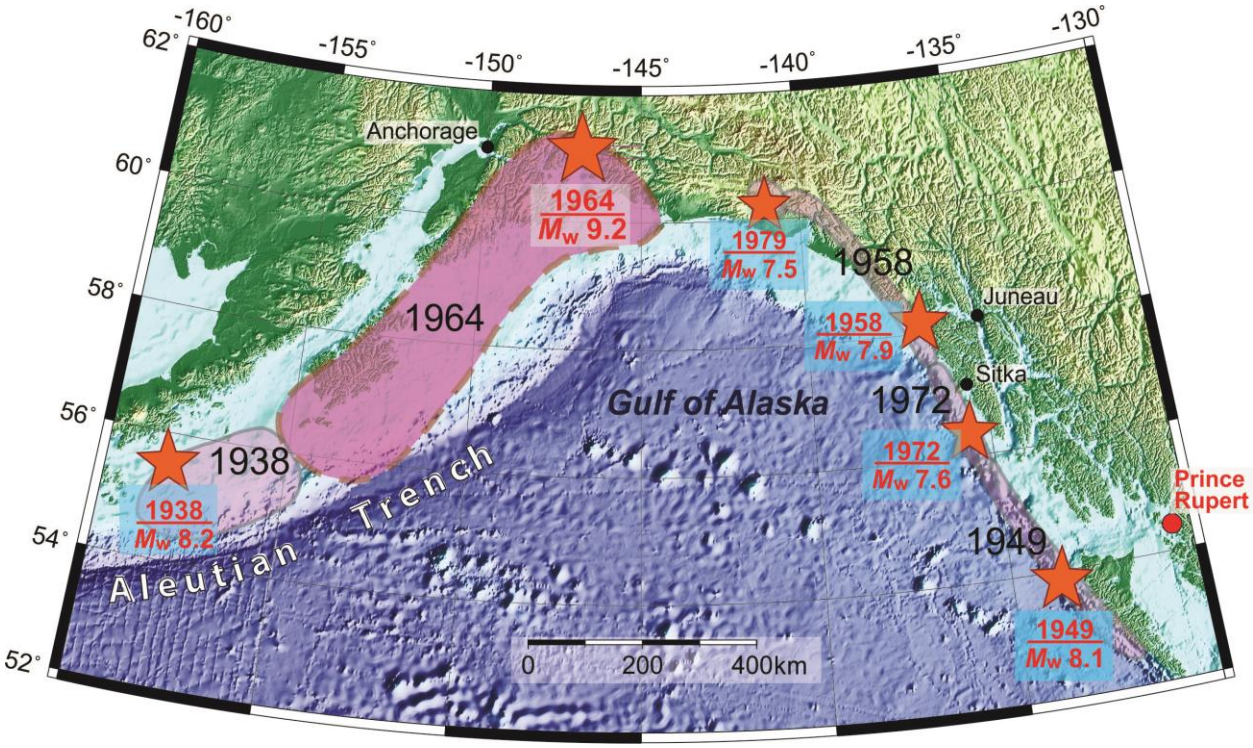

Figure 10. Map of south-central and southeastern Alaska with the rupture zones of six major historical earthquakes (shaded); the rupture zone of the 1964 Alaska earthquake is contoured by a thick brown dashed line. Red stars indicate epicenters of the earthquakes; the sizes of the stars are proportional to the earthquake magnitudes (modified from *Suleimani et al.* [2013]). Tide gauges at Sitka, Juneau and Anchorage are indicated by solid black circles; the red circle denotes the tide gauge at Prince Rupert.

The de-tided (but unfiltered) tsunami records from nine tide gauges located in southern British Columbia are shown in Figure 11. Three of the tsunami records in Figure 11a are for Tofino (outer coast of Vancouver Island), Victoria (Juan de Fuca Strait) and Fulford Harbour (the southern coast of Salt Spring Island, the southern Strait of Georgia). These records show that the tsunami waves propagated from the source area (Prince William Sound, Alaska; see Figure 10) in a southeast direction along the outer coast of Haida Gwaii and then along the outer coast of Vancouver Island. The leading wave arrived at Tofino at 07:01 UTC on 28 March and then propagated through Juan de Fuca Strait, arriving at Victoria at 08:08 UTC (4 hours 32 minutes after the main shock). The waves then entered the Strait of Georgia and propagated into narrow inlets on the mainland coast and into the Fraser River delta. Waves were observed not only at Fulford Harbour, but also Point Atkinson, Vancouver, Stevenson, the North Arm of the Fraser River, New Westminster and even Pitt Lake (Figure 11b).

A prominent feature of the 1964 Alaska tsunami at Tofino and Victoria is that the leading wave was the highest (Figure 11a). The wave arrived as a pronounced wave crest of 70 cm, followed by an abrupt trough of 77 cm; the period of this wave was about 100 minutes. Although the same wave is evident in the Fulford Harbour record (Figure 11a), the highest wave was the third wave, not the first, apparently a result of wave amplification by local harbour resonant effects and reflections from other islands. In contrast to other major tsunamis (1946, 1960, 2010 and 2011), the 1964 tsunami at Victoria and Fulford, as well as at other stations of the British Columbia coast (see Figures 8 and 9), decayed relatively quickly. The reason for this decay appears to be the closeness of the 1964 source region to the observation area. As shown by *Rabinovich et al.* [2011] for the global 2004 Sumatra tsunami, near-field tsunami oscillations decay much faster than more distant far-field oscillations.

After it entered the Strait of Georgia, the 1964 tsunami reached Point Atkinson (formerly Caulfield) at 9:14 UTC on 28 March and then propagated into the numerous narrow inlets on the mainland coast and into the Fraser River. Although the tsunami oscillations are barely recognizable in the original tidal records for these areas, the waves are clearly evident in the residuals (de-tided) (Figure 11b). The character of these oscillations is significantly different from those observed in other regions of the BC coast in that the wave oscillations at all six stations were very similar and

much more regular than at other stations. Short-period oscillations were not observed at these stations, while long-period oscillations were very consistent among the records, with a predominant period $T \sim 2$ hrs. The maximum tsunami wave heights at all stations (ignoring Pitt Lake) ranged from 22 cm at Vancouver to 50 cm in the North Arm of the Fraser River (Table 4) [*Rabinovich et al.*, 2019].

A unique feature of the 1964 event were tsunami oscillations recorded at Pitt Lake. Pitt Lake has a tidal range of ~ 1 m and is one of the few tidal lakes on the BC coast. The water gauge is located at the southern tip of the lake, about 18 km from the confluence of the Pitt and Fraser rivers, which, in turn, is about 46 km from the Strait of Georgia. To reach the Pitt Lake gauge from the strait, the 1964 tsunami had to propagate ~64 km upstream. The first wave arrived at the lake at 11:49 UTC, 2 hrs 35 min later than at Point Atkinson and 1 hr 20 min later than New Westminster (Table 4). Despite the small wave height of 9 cm, the tsunami is clearly detectable in the Pitt Lake record (Figure 11b).

Table 4. Parameters of the Alaska (Prince William Sound) tsunami of 28 March 1964 recorded by CHS analogue tide gauges on the coast of British Columbia (Main shock, $M_w = 9.2$ at 03:36 UTC)

Station	First wave			Maximum wave			Visible period (min)
	Arrival time (UTC)	Travel time (hh:mm)	Amplitude (cm) & Sign	Amplitude (cm)	Time (UTC) of max amplitude	Height (cm)	
Tofino	07:01	3:25	+99	99	07:15	237	25
Victoria	08:08	4:32	+70	70	08:20	147	25, 90
Fulford Harbour	08:35	4:59	+24	42	12:41	83	30, 110
Pt. Atkinson	09:14	5:38	+11	12	09:45	28	120
Vancouver	09:23	5:47	+6	11	09:52	22	120
Steveston	09:36	6:00	+7	13	13:48	32	120
North Arm	09:49	6:13	+13	22	14:11	50	120
New Westminster	10:29	6:53	+10	16	12:38	34	120
Pitt Lake	11:49	8:13	+1	5	13:33	9	120

Comment: Parameters of the tsunami waves were estimated using digitized analogue tide gauge records that had been re-sampled to 1-min.

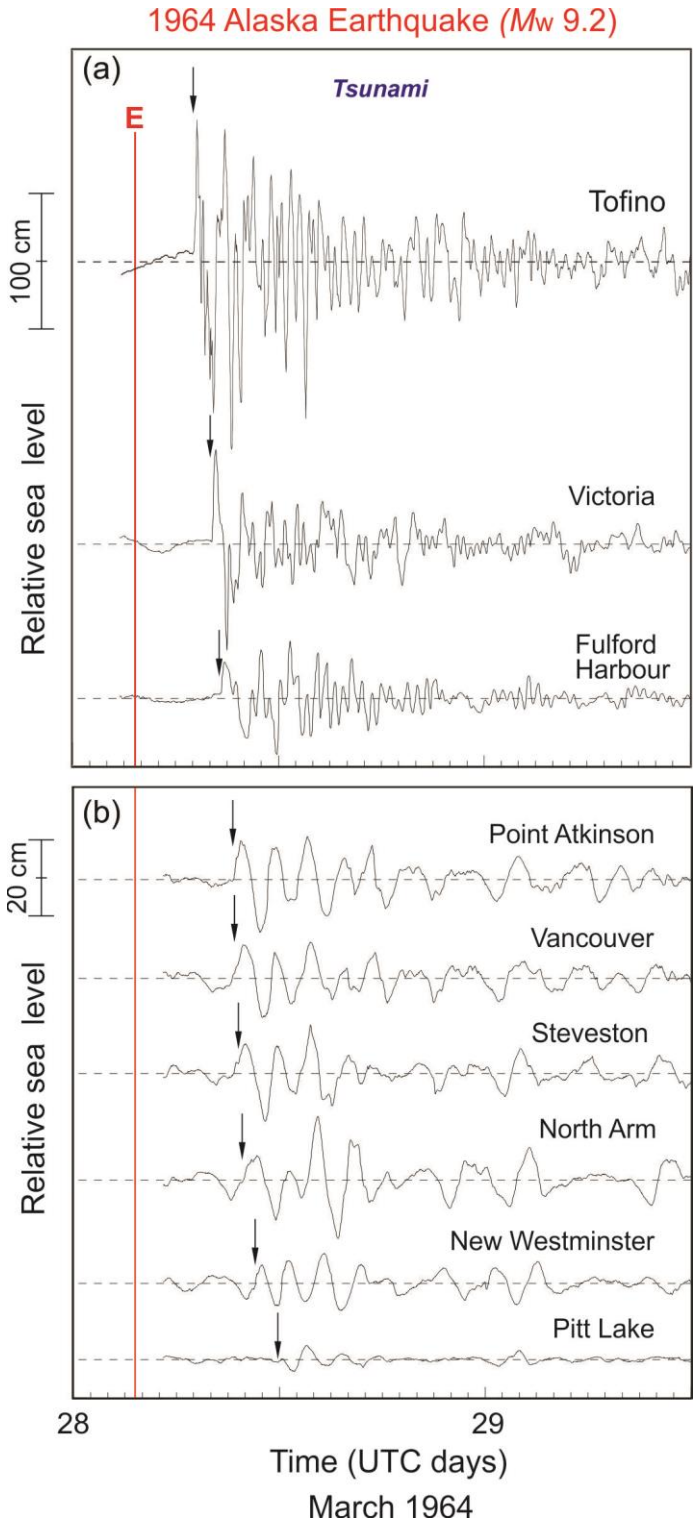

Figure 11. The 28 March 1964 Alaska tsunami recorded at (a) Tofino, Victoria and Fulford Harbour (Salt Spring Island) and (b) at six stations in the area of Burrard Inlet and the Fraser River. The solid vertical red line labelled "E" denotes the time of the earthquake; the arrows indicate the tsunami arrival time.

As was mentioned above, the 1964 Alaska tsunami was the strongest tsunami recorded on the coast of British Columbia and it was the strongest observed in the Strait of Georgia. Below is a comparison of the maximum recorded wave heights for three stations:

Year	Victoria	Fulford	Pt. Atkinson
1957	26	11	-
1960	73	34	20
1964`	147	83	28

Thus, the 1960 tsunami in this region was roughly three times larger than the 1957 tsunami and the 1964 was two times larger than the 1960 tsunami. During these three events there were no sea level measurements at either Patricia Bay or Nanaimo. However, tsunami observations at these three stations give us an idea about possible tsunami wave heights in the SoG during these events. The 1964 tsunami estimates in this region are supported by the results of numerical modelling [*Fine et al.*, 2018a].

3.7. The 2010 Chilean (Maule) Tsunami of 27 February 2010

During the 46 years following the 1964 Alaska earthquake, the Pacific region was relatively quiet. However, on 27 February 2010, a magnitude M_w = 8.8 thrust-fault earthquake occurred near the coast of Central Chile, offshore of the Maule region. The source area of the 2010 Chilean earthquake, which was about 550 km long and more than 100 km wide, was located immediately to the north of the rupture zone of the M_w = 9.5 Great Chilean Earthquake of 22 May 1960. The 2010 earthquake was one of the most powerful earthquakes in recent human history and the largest in the Southern Hemisphere since 1960. The 2010 Chilean earthquake generated a trans-oceanic tsunami that caused major damage and loss of life along 800 km of the Central Chilean coastline. Tsunami alerts (Warnings and Advisories) were declared in 54 Pacific countries, including Canada, the United States, Russia, and Japan. Although tsunami waves were observed throughout the entire Pacific Ocean, the only noticeable damage and casualties, except Chile, were reported for California. The 2010 tsunami was recorded by more than 200 high-precision digital coastal tide gauges and by a large number of Deep-ocean Assessment and Reporting of Tsunamis (DART) bottom pressure stations operated by NOAA.

The 2010 Chilean tsunami was clearly recorded by many tide gauges along the British Columbia coast. Detailed analysis of these data is provided by *Rabinovich et al.* [2013]. The tsunami waveforms for three southern stations are shown in Figure 12 and the respective tsunami parameters in Table 5. The tsunami arrived at Victoria at 23:48 UTC on 27 February, roughly 17 hours 14 minutes after the earthquake. The maximum wave height of 23 cm was associated with the second train of waves that came to the site approximately four hours after the first train (Figure 12). The oscillations at Victoria and at other British Columbia stations were characterized by long ringing and slow energy decay.

The 2010 Chilean tsunami was very similar to the 1960 Chilean tsunami but was approximately 3.5 times weaker (Compare Tables 3 and 5). There was no tide gauge in Fulford during the 2010 event, but based on information from Tofino and Victoria we can expect the tsunami wave height at this station should be about 10 cm.

Table 5. Parameters of the Chile (Maule) tsunami generated by a M_w = 8.8 of 27 February 2010 at 06:34 UTC as recorded on the coast of British Columbia

Station	First wave			Maximum wave			Visible period (min)
	Arrival time (UTC)	Travel time (hh:mm)	Amplitude (cm) & Sign	Amplitude (cm)	Time (UTC) of max amplitude	Height (cm)	
Tofino	23:15	16:41	+20.3	20.3	23:42	36.6	20-30
Bamfield	23:19	16:45	+17.2	19.6	02:30*	39.4	150
Victoria	23:48	17:14	+16.2	16.2	00:34*	23.2	25

Comments: * 28 February 2010.
In their estimation of parameters for the 2010 tsunami on the coast of British Columbia, *Rabinovich et al.* [2013] erroneously considered the frontal trough ("negative phase") as the tsunami arrival. Later Watada et al. (2014) demonstrated that this negative phase is mainly related to the elasticity of the Earth (see also *Eblé et al.* [2015]). These parameters for the 2010 tsunami waves for Tofino, Bamfield and Victoria have been corrected for this study.

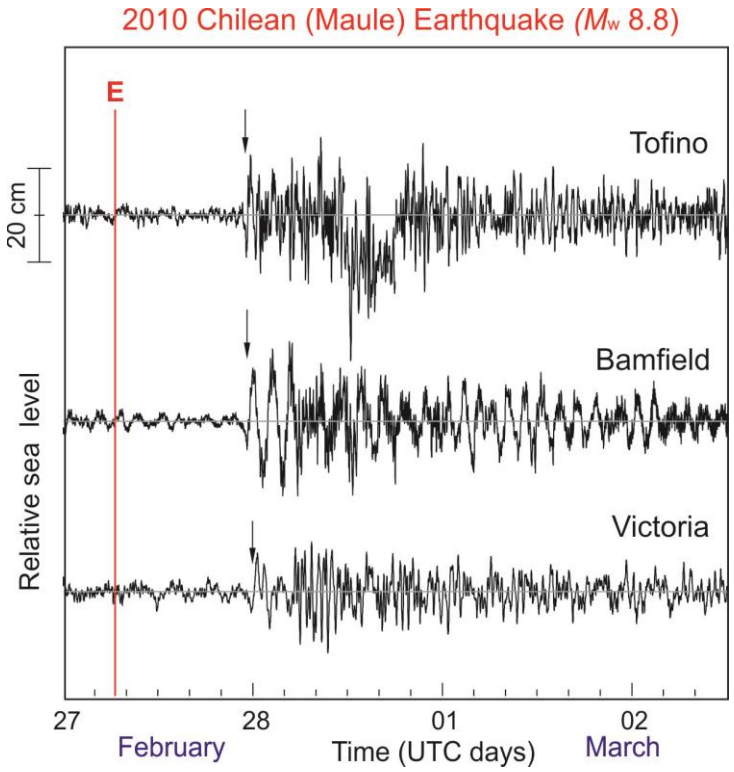

Figure 12. The 27 February 2010 Chilean tsunami recorded at Victoria. The solid vertical red line labelled "E" denotes the time of the earthquake; the arrow indicates the tsunami arrival time.

3.8. The Tohoku (East Japan) Tsunami of 11 March 2011

At 05:46 UTC on 11 March 2011, a giant thrust fault earthquake of magnitude M_w = 9.0 occurred off the coast of the Tohoku District, northeastern Honshu Island, Japan. The earthquake was the strongest in Japan's history and one of the strongest ever instrumentally recorded. Waves from the tsunami reached run-up heights of up to 41 m along the coast of Japan. The tsunami was responsible for almost 20,000 deaths and caused enormous structural damage, including the serious accident at the Fukushima Dai-ichi nuclear power station. The 2011 tsunami was recorded by approximately 250 coastal tide gauges throughout the Pacific Ocean and by numerous bottom pressure gauges at autonomous and cabled observatories.

The 2011 Tohoku tsunami waves were recorded by 15 CHS permanent tide gauges along the coast of British Columbia and by several temporary tide gauges, including five gauges in Victoria

Harbour and adjacent waterways. It was also measured by multiple NEPTUNE-Canada and VENUS bottom observatories, in particular by those located in the southern part of the Strait of Georgia and in Saanich Inlet/Patricia Bay. In the Strait of Georgia, the tsunami was measured by five CHS permanent tide gauges: Patricia Bay, Point Atkinson, West Vancouver, Vancouver and Campbell River and by four ONC VENUS instruments in the Strait of Georgia and Saanich Inlet. The de-tided and high-pass filtered records from four gauges on the outer coast of Vancouver Island (Tofino, Port Alberni, Bamfield and Victoria) and the five gauges in the Strait of Georgia are shown in Figure 13; four bottom pressure VENUS instruments are shown in Figure 14. All these instruments were high-resolution digital gauges with 1-min sampling, which enabled us to estimate principal parameters of the observed tsunami waves with high precision (Tables 6 and 7).

The maximum wave height on the BC coast of 136 cm was recorded at Port Alberni. At Tofino the wave had a similar height, 125 cm. This "beacon" station was the first that recorded the arriving wave: at 15:23 UTC; i.e. 9 hrs and 37 min after the main earthquake shock. The wave then propagated through Juan de Fuca Strait and at 16:17 UTC entered Victoria. In the Inner Harbour of Victoria, the maximum wave height was 52 cm. The tsunami waves then entered the Gorge Waterway and amplified to up to 67 cm at Selkirk Water and 94 cm at Aaron Point. Associated currents were very strong, reaching several knots. A typical feature of the Victoria record, as well as all other 2011 tsunami records on the British Columbia coast, is the very long ringing (4 to 5 days) and very slow energy decay.

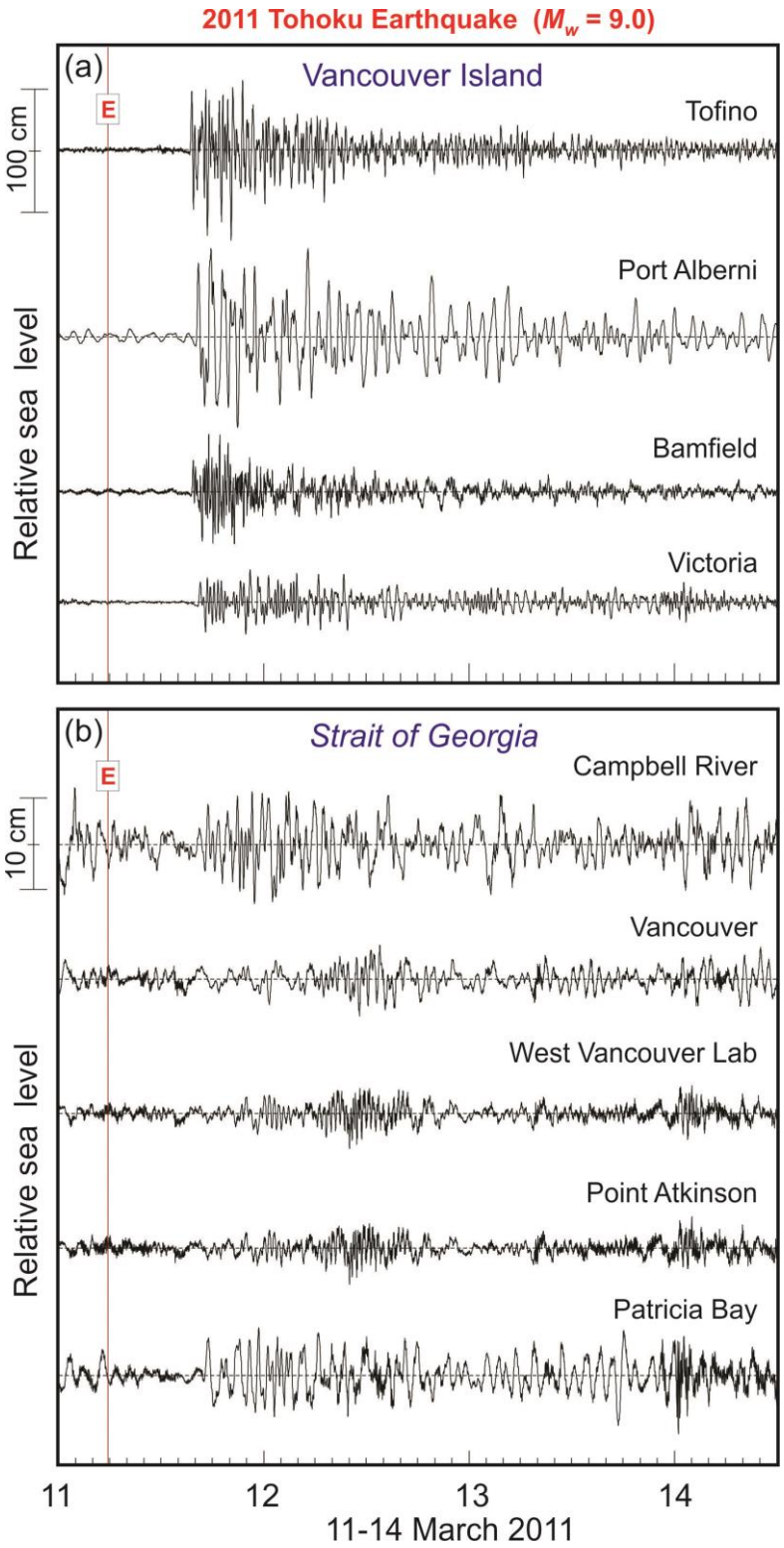

Figure 13. The 11 March 2011 Tohoku (East Japan) tsunami recorded at (a) four stations on the outer coast of Vancouver Island and (b) five stations in the Strait of Georgia. The solid vertical red line labelled "E" denotes the time of the earthquake.

Table 6. Parameters of the Tohoku (East Japan) tsunami of 11 March 2011 recorded by tide gauges on the coast of British Columbia (Main shock, M_w = 9.0 at 05:46 UTC)

Station	First wave			Max wave			Period (min)
	Arrival (UTC)	Travel time (hh:mm)	Amplitude (cm) & Sign	Amplitude (cm)	Time (UTC) of max amplitude.	Wave height (cm)	
Tofino	15:23	09:37	+51.0	56.3	21:31	124.5	20
Port Alberni	16:05	10:19	+64.6	71.5	17:50	135.7	85
Bamfield	15:35	09:49	+27.3	46.7	17:34	79.5	18
Victoria	16:17	10:31	+20.0	26.3	22:24	52.0	24
Patricia Bay	17:04	11:18	+3.7	5.3	23:23	9.5	33, 70
Campbell River	16:08	10:22	+3.2	5.9	22:35	12.5	25, 35
Vancouver	Unclear	-	-	3.8	13:32*	7.2	30
West Vancouver Lab	Unclear	-	-	2.8	12:19*	6.0	33
Point Atkinson	Unclear	-	-	2.8	12:20*	5.8	33

* 12 March 2011

Table 7. Parameters of the Tohoku (East Japan) tsunami of 11 March 2011 recorded by the VENUS stations inside the Strait of Georgia and Saanich Inlet. The parameters estimated for tide gauge Patricia Bay within Saanich Inlet are given for comparison.

Station	First wave			Max wave			Period (min)
	Arrival (UTC)	Travel time (hh:mm)	Amplitude (cm) & Sign	Amplitude (cm)	Time (UTC) of max amplitude.	Wave height (cm)	
Patricia Bay TG	17:04	11:18	+3.7	5.3	23:23	9.5	33, 70
DSF-11, CM-887 (Saanich Inlet)	17:03	11:17	+3.4	5.2	23:21	8.6	33, 70
DSF-11, CTD-4996 (Saanich Inlet)	17:05	11:19	+4.1	5.2	23:23	9.0	33, 70
VIP-12, CTD-6536 (Saanich Inlet)	17:01	11:15	+4.2	5.3	23:21	8.9	33, 70
VIP-05, CTD-4686 (Strait of Georgia)	Unclear	-	-	1.8	12:18*	4.1	25

* 12 March 2011

The 2011 Tohoku tsunami occurred in the "instrumental era" and was the first event that was measured by a number of precise instruments in the Strait of Georgia and in neighbouring basins. In particular, this was the first and, so far, the only tsunami to be recorded by tide gauges at Patricia Bay and Campbell River. The corresponding records are quite clear (Figure 13b). The maximum wave height at Patricia Bay was 9.5 cm, at Campbell River 12.5 cm (Table 5). The wave arrived at these instruments 44-48 min after it arrived at Victoria.

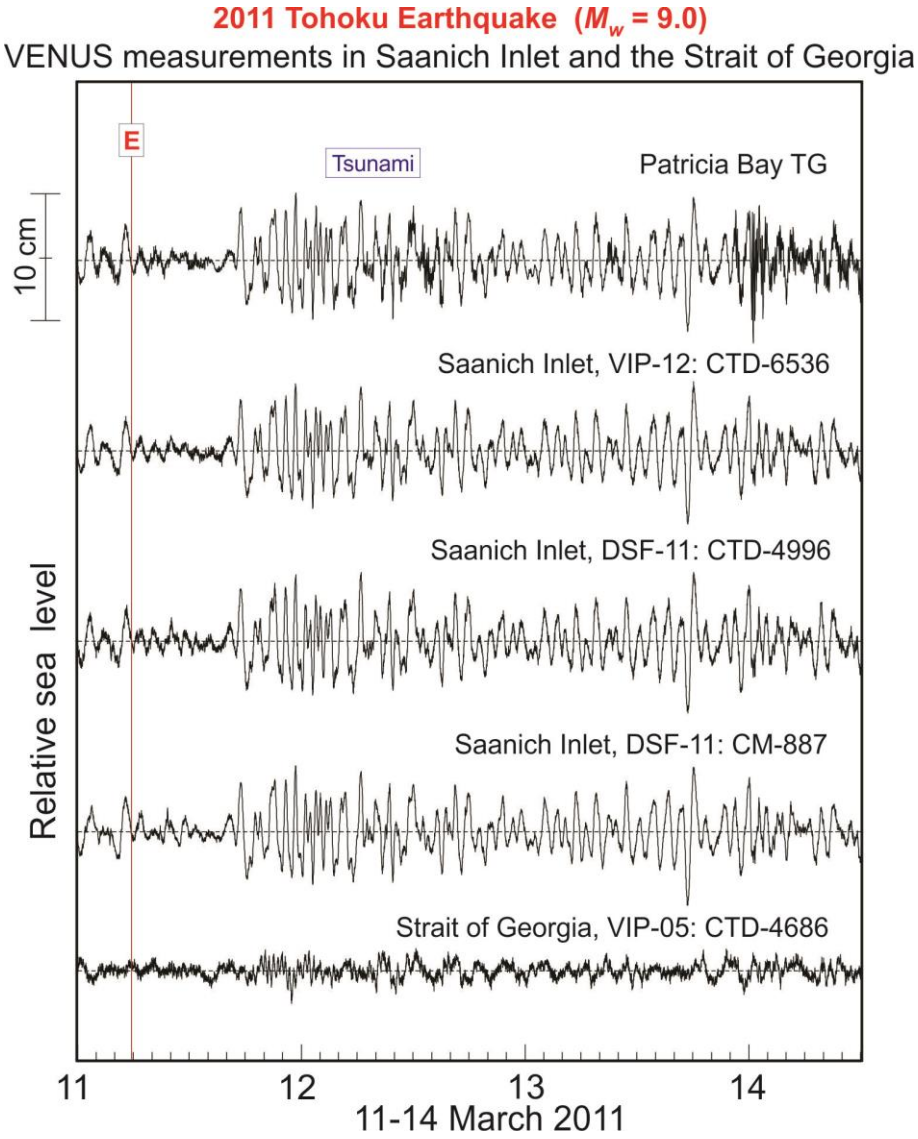

Figure 14. The 11 March 2011 Tohoku (East Japan) tsunami recorded by the VENUS stations inside the Strait of Georgia and Saanich Inlet. The record of the tide gauge Patricia Bay within Saanich Inlet is given for comparison. The solid vertical red line labelled "E" denotes the time of the earthquake.

What is also important, the 2011 Tohoku tsunami was recorded by four ONC VENUS BPRs; three of them were located in Saanich Inlet, only a couple of kilometers from the Patricia Bay CHS tide gauge. This means that there were four independent measurements of this tsunami in Patricia Bay. All these measurements are in very good agreement with each other (Figure 14, Table 7). The maximum recorded wave height was from 8.9 to 9.5 cm.

The 2011 Tohoku tsunami was measured at three mainland coast tide gauges: Point Atkinson, West Vancouver Lab and Vancouver. The recorded waves at all three instruments were relatively weak: 5.8-7.2 cm (Figure 13b, Table 6). The wave recorded by the VENUS BPR in the middle of the Strait of Georgia was even weaker: only about 4 cm. There were no measurements at Nanaimo at the time of the event, but it evident that the maximum 2011 wave that could reach this site was not higher than 10 cm.

3.9. Summary of trans-oceanic tsunami observations

We examined seven major trans-oceanic tsunamis observed on the coast of British Columbia. Three of them were of particular interest: the 1960 Chile, 1964 Alaska and 2011 Tohoku (East Japan). The importance of these events is not only they were the strongest, but also that they can be considered as "*worst case scenarios*" for three regions within the Pacific Rim of Fire that have the maximum tsunamigenic potential: (1) Chile, (2) Alaska-Aleutian Islands, and (3) Japan-Kuril Islands-Kamchatka.

- *The 1960 Chilean tsunami* was generated by a M_w 9.5 earthquake, the strongest ever instrumentally recorded. This tsunami created catastrophic effects on the coasts of the Philippines, Hawaiian Islands and Japan. However, no damage was reported on the coast of British Columbia. The maximum 1960 wave height of 132 cm was measured at Tofino. The waves penetrated into the Strait of Georgia and were recorded at Fulford Harbour (34 cm) and Point Atkinson (20 cm). Based on these observations we can conclude that the strongest trans-oceanic tsunamis initiated by Chilean earthquakes barely exceed **50 cm** in the Strait of Georgia and, in particular, in the area of Pat Bay and Nanaimo.

- *The 1964 Alaska tsunami* was induced by a M_w 9.2 earthquake in the Alaska-Aleutian Subduction Zone. This was the strongest tsunami ever observed on the coast of British Columbia. Severe damage was reported at Prince Rupert, Port Alberni and at several sites along the oceanic coast of Vancouver Island (*Rabinovich et al.*, 2019). Maximum wave heights in Shields Bay (Haida Gwaii) and Alberni Inlet were up to 800 cm, at Tofino the recorded wave was 237 cm and at Victoria 147 cm. The waves entered the Strait of Georgia and were measured at Fulford Harbour (83 cm) and at a number of mainland stations in the region of Vancouver and the Fraser River delta (22-50 cm). Based on these results, we conclude that in Patricia Bay and at Nanaimo the maximum 1964 wave heights were up to **50-100 cm**. The 1964 Alaska tsunami was an extreme event with a recurrence period of ~1000 years. Therefore, these estimates for Patricia Bay and Nanaimo may be considered as maximum possible values for the Alaska events.
- *The 2011 Tohoku tsunami* was induced by a M_w 9.0 earthquake offshore of Honshu Island, Japan. The tsunami was precisely recorded on the coast of British Columbia, and had a maximum height of 154 cm measured at Winter Harbour; at Tofino it was 125 cm and at Victoria 52 cm. The tsunami propagated through Juan de Fuca and Haro straits, penetrating into the Strait of Georgia and was directly recorded at Patricia Bay at **9.5 cm** (the only existing tsunami record in this bay). This means that, in comparison to Tofino, the wave in Patricia Bay was attenuated 13 times and relative to Victoria 5.5 times. The 2011 tsunami was also recorded at Campbell River (12.5 cm) and at several mainland stations waves in the area of Vancouver/Fraser River delta (6-7 cm). Based on this information, the 2011 tsunami wave at Nanaimo was estimated to be about **10-15 cm**. The 2011 earthquake is an extreme event; the last time an earthquake with similar magnitude occurred off Japan was approximately 1150-1200 years ago.

Based on our analysis of these seven major events, we conclude that **trans-oceanic tsunamis do not constitute a major threat to either Patricia Bay or to Nanaimo**. These tsunamis can penetrate into this region but will have a height of only a few tens of centimeters. Even in the case of a great Alaska tsunami, comparable to the 1964 event, expected maximum tsunami trough-to-crest wave heights in the southern Strait of Georgia will be up to 50-100 cm; in the vicinity of Patricia Bay and Nanaimo they will be even less.

These conclusions are in good agreement with the official Provincial Emergency Preparedness tsunami planning levels (Figure 15). The inner coast of the island and the entire Strait of Georgia are indicated as regions of low tsunami risk with expected tsunami wave heights of 0.5-1.0 m.

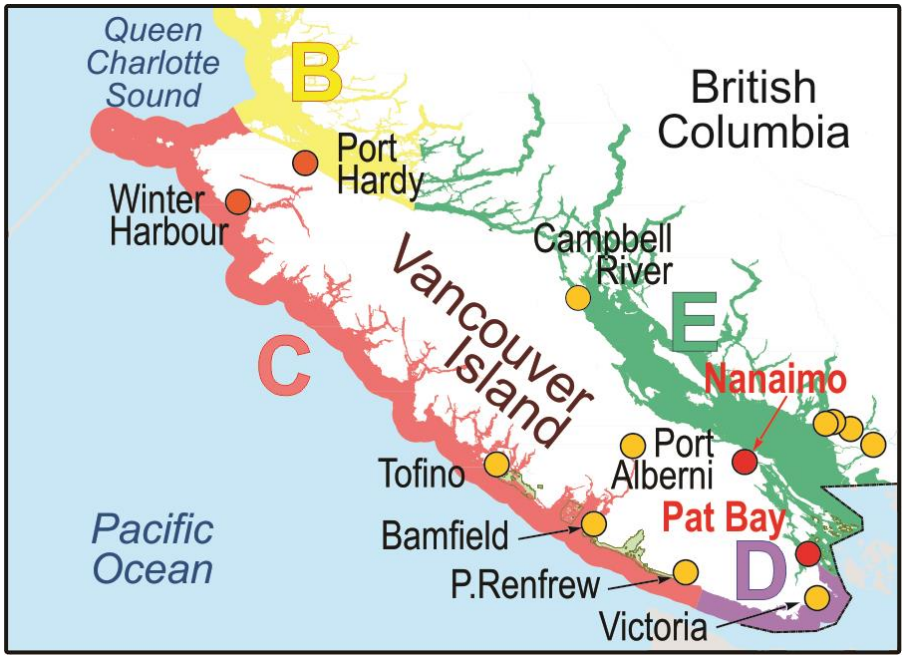

Figure 15. Vancouver Island tsunami zone map (Provincial Emergency Preparedness, 2019). Map shows recommended tsunami planning levels for the coast of British Columbia: "B" = Central coast, 2-4 m (*yellow*); "C" = West Vancouver coast, 3-6 m (*red*); "D" = Juan de Fuca Strait, 1.3-2.7 m (*purple*); and "E" = the Strait of Georgia, 0.5-1.0 m (*green*).

Our analysis of the seven major tsunamis allows us to establish empirical relationships between Tofino, Victoria and SoG stations. The time-of arrival difference (advance time) for tsunami waves arriving at Tofino and then Victoria is between 35 min (for Chilean tsunamis) and 80 min (for Alaska tsunamis); between Victoria and Fulford the corresponding differences are between 30 and 45 min, between Victoria and Patricia Bay about 45 min. The tsunami wave heights at Tofino are approximately twice those at Victoria, four times those at Fulford and thirteen times larger than those at in Patricia Bay. These relationships enable us to use tsunami measurements at Tofino and Victoria to predict tsunami parameters in the Strait of Georgia.

Of primary concern is a major tsunami generated by a great M_w earthquake in the Cascadia Subduction Zone (CSZ). The only known event of this type occurred on 27 January 1700

(reconstructed based on paleotsunami field surveys on the coasts of British Columbia, Washington and Oregon and Japanese chronicles) [*Satake et al.*, 1996; *Atwater et al.*, 2005]. There were no observations or witness reports during the event and no signatures of the 1700 tsunami have been found so far on the coasts of the Strait of Georgia. Nevertheless, estimated of the risk for this region from CSZ tsunamis was provided by *Ng et al.* [1991] based on preliminary numerical modelling of a CSZ tsunami for the coast of British Columbia: "*Inside the Strait of Georgia, the wave heights are significant enough to receive closer attention, especially in low-lying areas*", *Ng et al.* [1991] used a sufficiently coarse grid of 2-km that was available at that time. Still, their conclusions are important. According to their results, "…*After the tsunami propagates into the Strait of Georgia, the wave amplitude is greatly attenuated partly because the wave energy continues to be dispersed over a greater area along the path of propagation and, additionally, because energy is lost to friction which becomes important in shallow waters, notably in the complex Gulf Island system. Such a decrease in amplitude is seen in the sequence of <simulated> time-series from Victoria to Vancouver, where the wave is attenuated by a factor of two. The tsunami action near Vancouver, though small, is still noticeable, with an amplitude of about 60 cm. As the oscillations continue for many hours, a tsunami would be superimposed upon a high-tide and might pose some danger to low-lying areas of the Fraser River delta. In general, elevations in the Strait of Georgia are below a metre…*".

It is obvious that all these results and conclusions for the Strait of Georgia have to be verified based on high-resolution **numerical modelling**, similar way to what was done for Juan de Fuca Strait [*Cherniawsky et al.*, 2007; *Cheung et al.*, 2011; *Fine et al.*, 2018b] and Puget Sound [*Eungard et al*., 2018].

4. LOCAL TSUNAMIS IN THE STRAIT OF GEORGIA

The strongest tsunamigenic earthquakes in the Pacific region occur in major subduction zones bordering the Pacific Ocean that form the *Fire Rim*. All eight principal trans-oceanic tsunamis discussed in Section 3 were generated by great M_w 8.6-9.5 earthquakes with source areas located in these zones. However, as was shown, the Strait of Georgia is strongly sheltered from incoming oceanic tsunamis by the San Juan and Gulf islands. That is why we need to consider the threat for this region from *local tsunamis*, i.e. from tsunamis generated by earthquakes directly in the Strait of Georgia.

4.1. Seismicity of the Strait of Georgia

The distribution of earthquakes in and around Vancouver Island, over the past 5-year (2005-2010) period is shown in Figure 16. Vancouver Island's earthquake activity is mainly attributed to subduction of the Juan de Fuca plate beneath the North America plate in what is called the Cascadia Subduction Zone (see Figure 4). According to *Seemann et al.* [2011], the seismic zone in this region includes three types of earthquakes: (1) shallow crustal earthquakes in the North America plate; (2) deeper sub-crustal earthquakes in the subducting Juan de Fuca plate; and (3) very large subduction interface earthquakes at the interface of the two plates.

Most of the crustal earthquakes beneath Vancouver Island occur within approximately 20–30 km of the surface. These crustal events and their associated aftershocks are usually less than M7.5 and have a typical duration of less than a minute [*Rogers*, 1998]. Owing to the fact that these earthquakes are relatively shallow events, their potential proximity to built-up urban areas poses a significant threat to Vancouver Island communities; a map of earthquake shake hazard for Vancouver Island and neighbouring mainland coast is presented in Figure 17. Crustal seismicity on Vancouver Island area has been characterized by numerous, small events (Figure 16), which do not exhibit distinct patterns that would indicate the locations of active faulting The strongest damaging crustal earthquake in the region was the **M_w 7.3 1946 event on eastern Vancouver Island.**

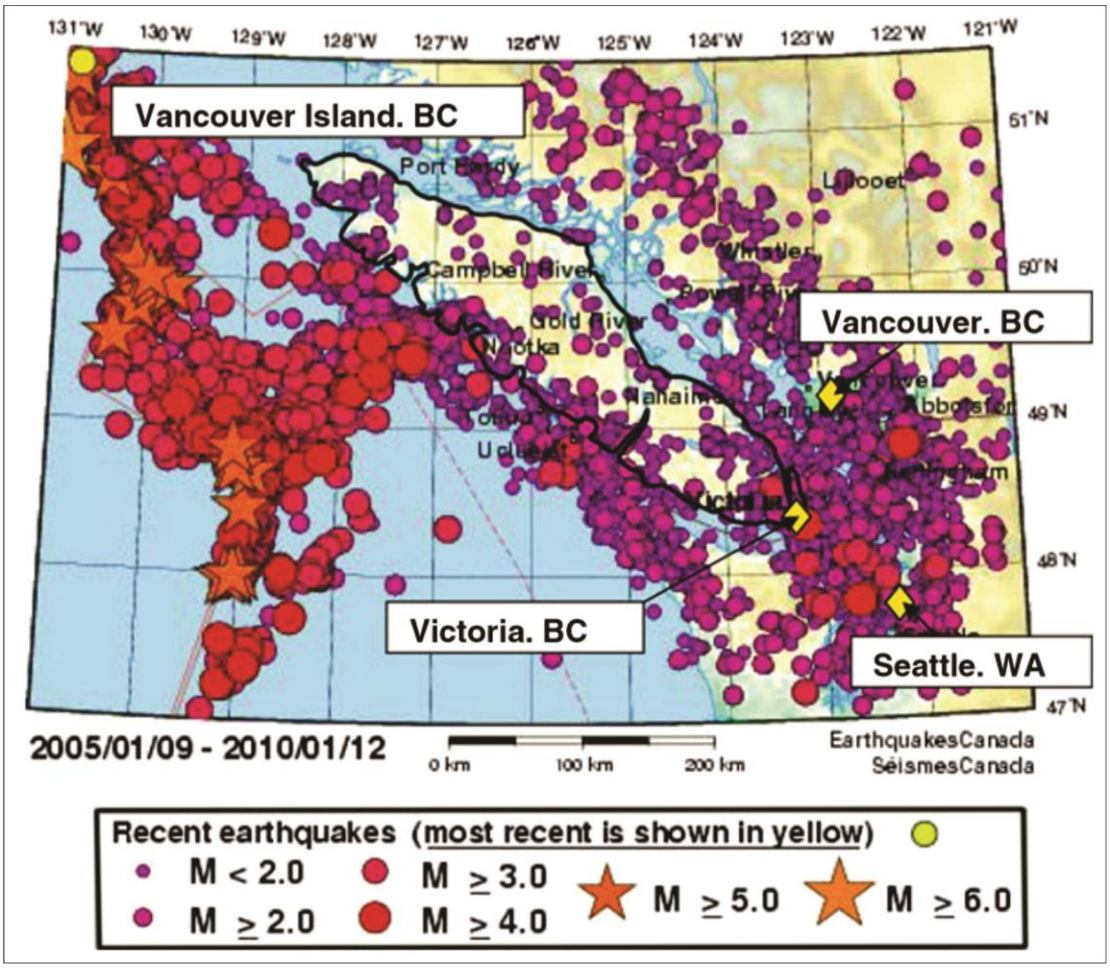

Figure 16. Recent seismicity (2005-2010) in the Vancouver Island region (Natural Resources of Canada).

Deeper sub-crustal earthquakes and their associated aftershocks typically occur between 30 and 45 km depth under Vancouver Island and deeper beneath the Strait of Georgia and Puget Sound to the east [*Seemann et al.*, 2011]. Like the crustal earthquakes, these earthquakes are generally less than M_w=7.5. Because they are sub-crustal earthquakes, these events may affect a larger area than similar sized crustal events. A concentration of sub-crustal earthquakes has been recorded beneath the Strait of Georgia and Puget Sound, and these events have the potential to affect major urban areas in the region [*Rogers*, 1998]. The most damaging recent sub-crustal earthquake in the region was the 2001 M_w 6.8 Nisqually, WA event.

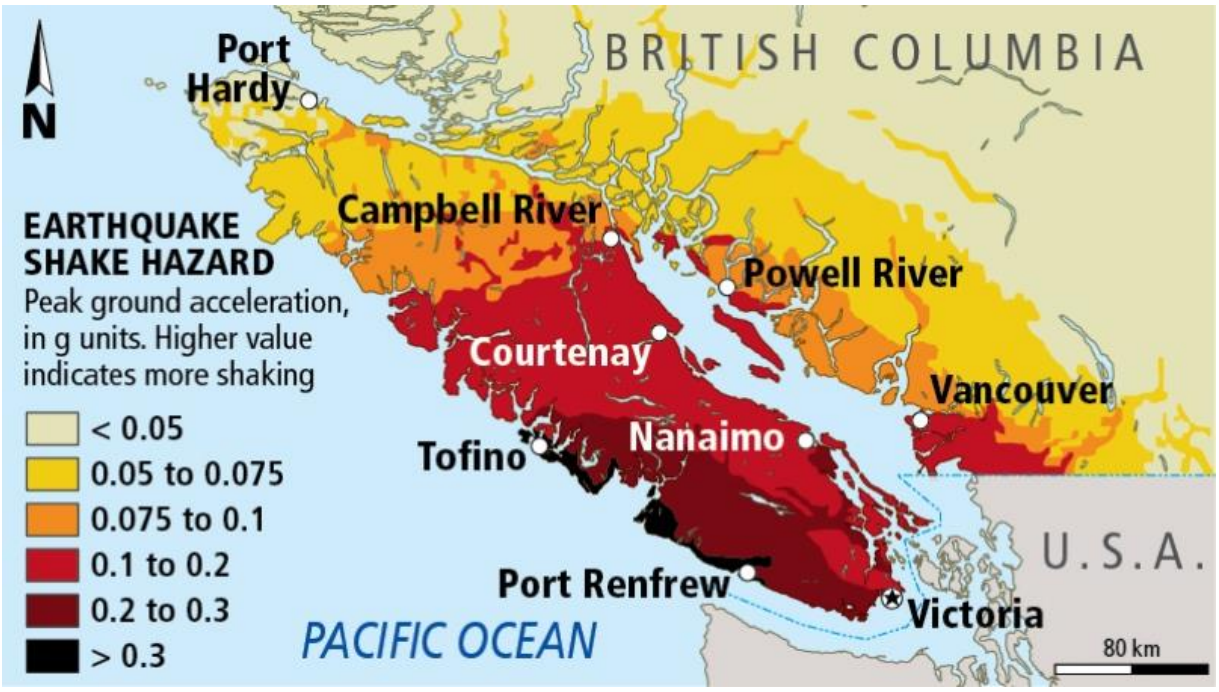

Figure 17. Map of earthquake shake hazard for Vancouver Island and neighbouring mainland coast (courtesy of the Pacific Geoscience Centre). Colours indicate peak ground acceleration in *g* units.

Significant earthquakes in the Victoria/Vancouver areas are shown in Figure 18. Most of the prominent earthquakes in this region occurred along the Seattle Fault that crosses Puget Sound. That is why, to estimate the tsunami risk for Seattle and other cities located on the coast of Puget Sound, the PMEL/NOAA and the University of Washington tsunami scientists considered earthquake sources related to this fault [*Walsh et al.*, 2003; 2014]. However, the San Juan and Gulf islands shelter the Strait of Georgia from tsunamis generated in this region.

Major earthquakes in Strait of Georgia are very rare. The strongest was the 1946 earthquake (Figure 18) that a created a local tsunami [*Stephenson et al.*, 2007]. This event is discussed in the following section.

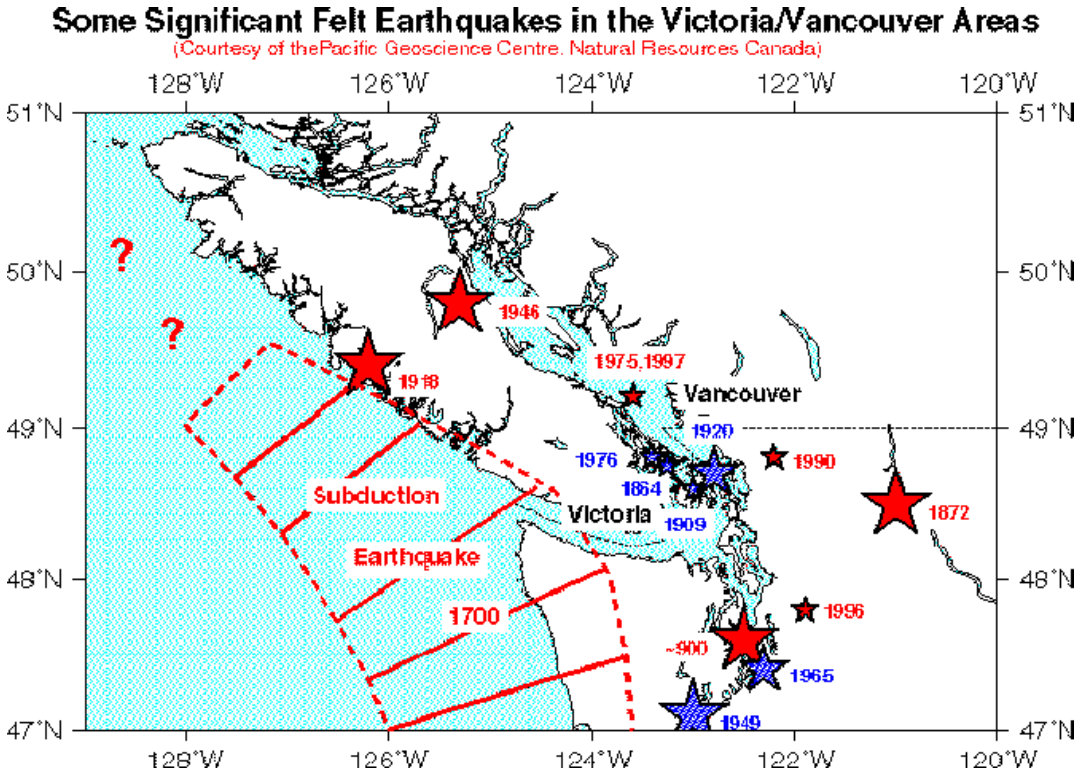

Figure 18. Map of significant earthquakes in the Victoria/Vancouver areas. *Red stars* denote indicate epicenters of earthquakes in the crust of the North America Plate; *blue stars* indicate earthquakes within the subducting Juan de Fuca Plate. The "belt" of epicenters located in bottom right part of the figure (900, 1949, 1965, 1996, etc.) are related to the Seattle Fault (Modified from *Rogers* [1998])

4.2. The Vancouver Island Tsunami of 23 June 1946

On 23 June 23, 1946 at 17:13 UTC an earthquake with a magnitude of about 7.3 occurred on Vancouver Island, British Columbia, Canada. It was felt as far south as Portland, Oregon, and north as Ocean Falls, while the point farthest east reporting the shock was Kelowna in the Okanagan Valley [*Hodgson*, 1946]. This earthquake was Vancouver Island's largest historic earthquake (and Canada's largest historic onshore earthquake). It was located at 49.76°N, 125.34°W [*Rogers and Hasegawa*, 1978], about 16 km SSW from Campbell River [*Murty and Crean*, 1986]. According to *Rogers and Hasegawa* [1978], the earthquake caused a vertical displacement in the land and water depth of up to 3 m [*Murty and Crean*, 1986]. The earthquake knocked down 75% of the chimneys in the closest communities, Cumberland, Union Bay and

Courtenay, and did considerable damage in Comox, Port Alberni and Powell River (on the eastern side of Georgia Strait). A number of chimneys were shaken down in Victoria and people in Victoria and Vancouver were frightened - many running into the streets. Two deaths resulted from this earthquake, one due to **drowning when a small boat capsized in an earthquake-generated tsunami wave**, and the other from a heart attack in Seattle. The tsunami caused also some local damage. It was observed at several locations along the coastline; the location and shape of the earthquake source is given in Figure 19 [*Soloviev and Go,* 1975; *Murty and Crean*, 1986].

According to *Rogers and Hasegawa* [1978], this earthquake did not produce a major tsunami. However, due to local landslides and slumping triggered by the earthquake, some minor water level disturbances occurred in coastal areas. The only casualty, mentioned above, was associated specifically with one of these waves. The earthquake hypocenter depth was near 30 km, making surface rupture a distinct possibility [*Rogers and Hasegawa*, 1978]. The earthquake was generally preceded and accompanied by a heavy subterranean roar. At several places, however, competent observers indicate that there was absolutely no sound until the heavy shock occurred [*Hodgson*, 1946].

In addition to broken chimneys, damaged goods, broken crockery and glassware, and windows, there were marked changes in the land, particularly at Maple Guard Spit, which flanks Deep Bay, at Goose Spit near Drew Harbour on the east side of Quadra Island and near Burdwood Bay on the east coast of the south promontory of Read Island. Cracks several metres deep and up to 0.45 m wide opened up for lengths of up to a few hundred metres on the sand spits. On Read Island an area of level, cultivated fields, fifteen to twenty acres in extent, was down-dropped. Some of the faces of these drops were as much as 6 to 9 m in depth [*Hodgson*, 1946].

At many places along the coast from Deep Bay to north of Campbell River, waterspouts were seen, which were described in some cases as 9 m in height. These left permanent records on the sand spits, in the form of craters or “sand blows", which varied from several centimetres across to craters 1.5 m in diameter and 0.9 m deep, even after several weeks of exposure to rain. At the time of the earthquake some of these “could not be bottomed with a twelve-foot pole” [*Hodgson*, 1946]. In many sites the coastal waters were found to have increased in depth just offshore by up to 30 m. A beach disappeared at the west end of Comox Lake, leaving a measured water depth of 10 m where, previously there had been a beach. No report indicates any place

where a rise in the ground occurred, or where water depth decreased, except for a long welt which appeared on the beach at Westview, on the mainland south of Powell River [*Hodgson*, 1946].

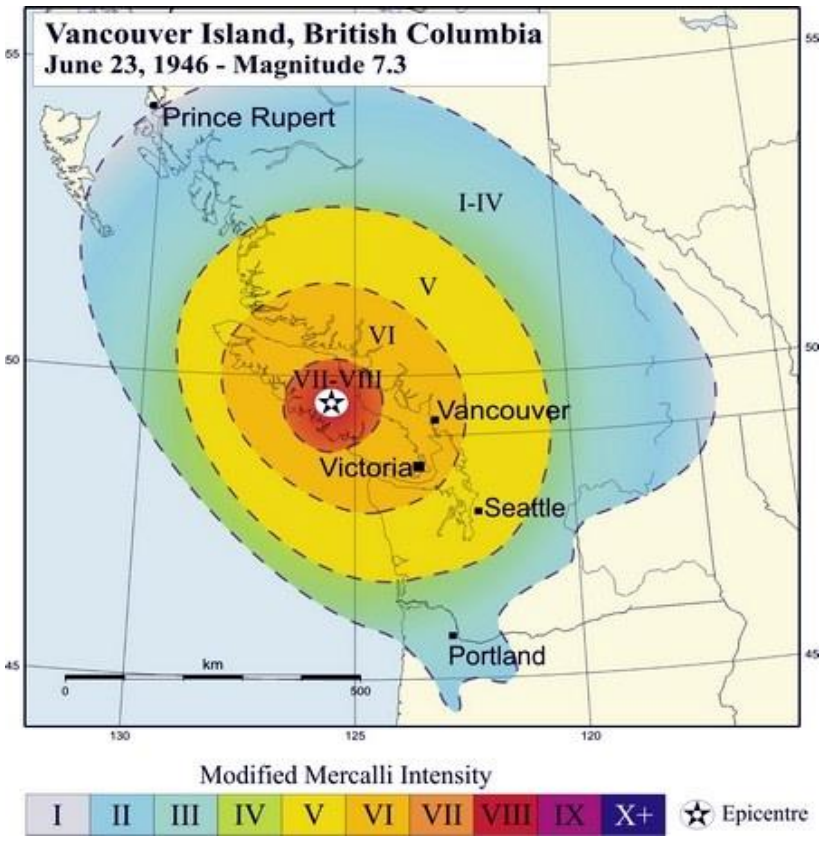

Figure 19. The epicenter of the Vancouver Island M_w 7.3 earthquake of 23 June 1946 and distribution of the Mercalli intensity.

Rogers and Hasegava [1978] note that the presence or absence of a general wave in the Strait of Georgia is important in determining if there was vertical movement under the strait. A special search was made through newspapers and correspondence sent to Hodgson in 1946 to see if reports of a wave, even a small one, could have been missed. This seems unlikely, but the tide was at mid-height at the time of the earthquake, opening the remote possibility that a small wave could have occurred leaving no trace. However, it was a clear day and most of the

communities affected by the earthquake border on the water and there was *no noticeable wave reported*. Yet, there were numerous reports of waterspouts and sand boils near the water's edge and some detailed descriptions of waves due to slumping indicating that there were people observing the water at the time of the earthquake. With one exception, all of the lighthouse keepers around *Vancouver Island* reported no wave activity. The single exception [*Hodgson*, 1946] was at *Sisters Rock Lighthouse* (south of the centre of Texada Island and east of the southern tip of Denman Island). The report reads: "*One tidal wave came at 10.22 A.M., seven minutes after the earthquake. The wave was 7 to 8 feet (2.1-2.4 m) high. A second wave, 100 feet (30 m) from the first was 4 to 5 feet (1.2-1.5 m) high. The speed was 10 knots (18.5 km/h*)." This would seem to indicate (roughly) that the wave was generated around *Deep Bay* or *Union Bay*. From the description of the wave given by the lighthouse keeper, including an estimate of its speed and arrival time, it seems very likely that this was *the same wave* that *caused the death of a man* due to the swamping of a small boat at *Deep Bay*, the only death that can be attributed to the earthquake. Both newspaper reports and the police report on the incident indicate that the end of a sandy spit slumped off during the earthquake, causing the wave.

There were waves observed in most of the lakes in the region either due to local landslides or generated seiches. The wave at the southern end of Comox Lake seems to have been the most severe and it may be significant that *Hodgson* [1946] thought the cause of the wave seemed "to have been a tectonic drop". The Beaufort Range fault runs under the lake at this point, and if it were active during the earthquake, a down-drop under the lake would have been the result. The disturbance on this lake was at the end farthest from Cumberland – the southwest end. Here, on the north shore, was situated the camp of the Comox Logging and Lumber Co. Across the narrow end of the lake an old shack stood on a gently sloping beach with a stretch of sand, variously estimated as from a few tens of centimetres to 100 m in width, leading down to the water which is, of course, non-tidal. At the time of the earthquake, this beach disappeared. *The water rushed into the void, receding from the camp on the other side of the lake, so that the raft "bumped on the bottom", then it came back as a high wave.* A man on the wharf, seeing it coming, ran for higher ground and only just got away, the water surging about his legs. *The wave washed inland about 90 m,* as shown by debris on the roadway. Mooring piles in the harbour were popped out and washed ashore in every case but two. A twenty-foot motor boat was carried inland fourteen metres and lodged in the bushes. A heavy donkey engine on the wharf was thrown into the lake.

It is stated that the new piles, being driven prior to the event, were 24 m long, to give the same above-water stand as was given previously by 9-metre piles [*Hodgson*, 1946].

At Goose Spit, those who were in the immediate vicinity of a subsidence or of a landslide report "*tidal waves" of which the estimated heights range from 6 to 40 feet (1.8-12 m).* Undoubtedly, these waves were generated in various localities, but there seems to be no evidence of any large "tidal" waves anywhere on the coast or on the lakes. On Goose Spit *there is some evidence that there was a wave, and it was not very large* [*Hodgson*, 1946]. Many landslides occurred in different lakes - Nitinat, Cowichan, Great Central, Sproat, Buttle, etc. [*Hodgson*, 1946].

4.3. Numerical Modelling of Local Tsunamis

Local seismically generated tsunamis have never been considered a major threat for the Strait of Georgia. For this reason, very few studies have been focused on this subject. *Murty and Crean* [1986] numerically simulated the 1946 Vancouver Island tsunami in the Strait of Georgia and adjacent parts of Johnstone and Juan de Fuca straits using the seismic motion diagram of *Rogers and Hasegawa* [1978] that showed a vertical ground uplift of up to 3 m. The indicated displacement was mostly on land, but part was in the Strait of Georgia. Clearly, a subsidence of up to 3 m in a water body would likely generate a tsunami, even if it does not spread far and wide. The grid size of the numerical model in both directions was 2.62 km and the total computational domain included 91 grid points in the *x*-direction and 36 grid points in the *y*-direction. Such a model is too coarse to resolve local topographic features and estimate possible resonant effects of numerous bays, inlets and narrow channels, typical for this region. but it shows the general character of the tsunami.

According to the numerical simulations, there was no major Strait of Georgia-wide tsunami, but the water level disturbances were large enough to be noticeable. The computed tsunami wave heights at various locations along the west and east shores of the Strait of Georgia, including some islands, were from 0.4 to 2.7 m. In particular, at Nanaimo the tsunami range was from -0.9 to +0.9 m, at Campbell River from -0.9 to +0.9 m, at Parksville from -0.2 to +0.3 m and at Vancouver (Burrard Inlet) from -0.8 to +0.7 m. Areas farther from the initial source area had greater tsunami ranges than in closer areas; this was mainly due to attenuation of the tsunami waves in shallow

areas and their amplification in some inlets and bays. In particular, even though Parksville is closer to the epicenter than Nanaimo, the modeled tsunami amplitude at Parksville is somewhat smaller because the extensive shallows and tidal flats at Parksville damped the tsunami waves significantly.

Murty and Hebenstreit [1989] developed a numerical model for the system consisting of the Strait of Georgia, Juan de Fuca Strait, and Puget Sound (GFP model). The GFP model was used for two purposes: (1) to simulate tsunamis propagating from the Pacific Ocean into the GFP region through the mouth of Juan de Fuca Strait; and (2) to simulate tsunamis due to earthquakes in the GFP itself.

It is generally believed that the probability of major tsunamigenic earthquakes inside the GFP system is small. Nevertheless, *Murty and Hebenstreit* [1989] considered hypothetical earthquakes to occur off Victoria (in Juan de Fuca Strait), off Vancouver (in the Strait of Georgia), and off Seattle (in Puget Sound). The bottom motion used in these simulations approximated the corresponding sources for the 1946 event model taken from *Rogers and Hasegawa* [1978]. As expected, earthquakes occurring off the three cites produced greatest tsunami heights within their immediate source areas. Little wave energy passes through to locations in the Strait of Georgia from the Victoria area earthquake simulation, although some effects can be felt farther along Juan de Fuca Strait and in Puget Sound. The Vancouver area earthquake simulation produced the most moderate effects of the three simulations. The computed heights tended to be smaller at Little River even though it is closer to the earthquake source than Campbell River, indicating that shallow water attenuates the waves at the former location. The Gulf and San Juan islands effectively block entry into Juan de Fuca Strait and Puget Sound. The simulated earthquake off Seattle has little impact anywhere but in the Puget Sound. However, *Murty and Hebenstreit* [1989] noted that, unlikely as it might be, if a major earthquake (Richter magnitude greater than 8.0) were to occur in the GFP system, it could result in a major tsunami (with amplitudes of almost 3 m) in the vicinity of the source area. Also, submarine slides, whether occurring independently or in association with earthquakes, could generate tsunamis that could be locally significant.

5. LANDSLIDE-GENERATED TSUNAMIS IN THE STRAIT OF GEORGIA

Submarine landslides, slumps, rock-falls, and avalanches can generate significant tsunami waves in coastal areas of the World Ocean. Although landslide-generated tsunamis are much more localized than seismically generated tsunamis, they can produce destructive coastal run-up and cause severe damage, especially where the wave energy is trapped by the confines of inlets or semi-enclosed embayments [*Jiang and LeBlond*, 1992]. The best known example of catastrophic landslide-generated tsunami is the Lituya Bay (Southeast Alaska) event of 10 July 1958, when an earthquake associated rockslide at the head of the bay caused a giant tsunami that impacted the sides of the inlet to a height of 525 m [cf. *Murty*, 1977; *Lander*, 1996; *Fritz et al*., 2009].

5.1. General Properties

The catastrophic event of 3 November 1994 in Skagway Harbor, Southeast Alaska triggered active investigation of landslide generated tsunamis. The event began with the collapse of the Pacific and Arctic Railway and Navigation Company (PARN) Dock and led to a series of large amplitude waves estimated by eyewitnesses to have heights of 5-6 m in the harbour and 9-11 m at the shoreline [*Cornforth and Lowell*, 1996; *Lander*, 1996; *Kulikov et al*., 1996]. The landslide and associated tsunami claimed the life of one worker and caused an estimated $21 million damage [*Thomson et al*., 2001]. This event initiated intensive scientific discussion and eventually led to greater understanding of slide/wave interaction and to substantial improvement in the numerical modelling of landslide generated tsunamis (see *Thomson et al*. [2001] for a detailed description of this case and associated discussion). One of the lessons from the Skagway event was the necessity for a thorough examination and modelling of possible submarine sliding/slumping and slide-generated tsunamis in areas of new construction, especially those located in regions of moderate to large tidal ranges and in the vicinity of unstable sediment accumulations [*Bornhold and Thomson*, 2012].

Coastal and submarine landslides typically have horizontal scales ranging from a few hundred to a few thousand meters. Because of their localized nature, landslides and associated tsunamis may go undetected [*Lander*, 1996; *Evans*, 2001]. At the same time, it is common for landslides to occur regularly at specific sites, in particular, Lituya Bay, Yakutat, Russell Fjord, Skagway Harbor (all located in Southeast Alaska), Kitimat Inlet (mainland BC coast), Puget Sound

(Washington State) [*Rabinovich et al.*, 2003]. Underwater slopes in fjords and inlets commonly attain a delicate equilibrium with the long-term ambient marine conditions associated with wave, current and tidal regimes, and the rate and character of sedimentation. This stability can be disrupted, leading to failure, by events or conditions that depart significantly from ambient conditions.

Landslides, slumps and rock falls are often the secondary effects of earthquakes. The 1958 Lituya Bay rockslide and tsunami, as well as a similar event in 1899, were triggered by strong earthquakes [*Lander*, 1996]. Submarine landslides that accompanied the 1964 Alaska earthquake generated wave amplitudes of several tens of meters in certain locations on the Alaska coast [*Lander*, 1996]. The Vancouver Island Earthquake of 23 June 1946 (M_w 7.3) produced many hundreds of local landslides and slumps along the coast of Vancouver Island and most of them generated tsunami waves (see Section 4.2). The only death associated this event was caused when a slump-generated tsunami wave overturned a small boat [*Rogers*, 1980]. However, in many cases, damaging submarine landslides are produced by local processes in the absence of seismic events (*Evans*, 2001). In particular, the 1854, 1874, and 1936 Lituya Bay tsunamis and the 1952-1975 Kitimat slides and tsunamis occurred during seismically quiet periods. The 1975 Kitimat Arm failure and tsunami occurred at an extreme low tide and were coincident with coastal construction activity [*Prior et al.*, 1984; *Johns et al.*, 1985; *Kulikov et al.*, 1998]. Similarly, the 1966 and 1994 Skagway Harbor events coincided with anomalously low tides (*Cornforth and Lowell*, 1996; *Kulikov et al.*, 1998; *Thomson et al*., 2001]. The same situation existed for the destructive 1894 Tacoma landslide and slide-generated tsunami (*H. Mofjeld*, Pers. Comm., 1999). Sudden deposition of large sediment loads, especially in deltaic areas during flooding, erosion of the base of the slope, or construction-related loads and activity, as well as meteorological factors such as rainfall, strong winds, and atmospheric pressure change, are common triggers of subaerial slope failures in coastal zones [cf. *Ren et a*l., 1996].

5.2. Landslides and Slide-Generated Tsunamis in the Strait of Georgia

Landslide-induced tsunamis have been observed all over the world [cf. *Rabinovich et al.*, 2003], however, it is in the inlets and narrow straits of the Pacific coast of North America (e.g. Lituya Bay, Yakutat, Russel Fjord, Skagway Harbor, Kitimat Arm, Tacoma) that landslide-generated tsunamis occur most frequently and are accompanied by the largest runup [*Soloviev and*

Go, 1975; *Lander*, 1996; *Evans*, 2001]. For example, in August 1905, a large landslide took place on the right bank of the Thompson River at Spences Bridge in southwestern British Columbia. The landslide also generated a displacement wave in the river that ran up the opposite valley wall to a height of 22.5 m, destroyed many buildings in the settlement and killed 15 people [*Evans*, 2001]. On December 4, 2007, a three million cubic meters landslide impacted Chehalis Lake, 80 km east of Vancouver, British Columbia. The failed mass rushed into the lake, forcing a tsunami that ran up 38 m on the opposite shore, destroyed trees, roads and campsite facilities [*Brideau et al*., 2012; *Wang et al.*, 2015]. Other locations in British Columbia where landslides have been reported include Howe Sound [*Terzaghi*, 1956] and the Fraser River delta region [*Hamilton and Wigen*, 1987; *McKenna and Luternauer*, 1987*; McKenna et al*., 1992].

In general, studies in the coastal areas of Alaska, British Columbia, Washington, Oregon, and California indicate high instability of deltaic and nearshore sediments (*Prior et al.*, 1981, 1984; *Johns et al*., 1986). Large accumulations of unstable sediments deposited in deltas of North American rivers, such as the Fraser, Skeena, and Nisqually, are particularly dangerous [*F. Stephenson and M. Blackford*, Pers. Comm., 2000]. Construction sites, buildings, and submarine cables in these areas are at significant risk to direct damage from subaerial and submarine landslides. In these areas, tsunamis generated by the failure events probably pose an even greater threat in terms of damage and loss of life than tsunamis generated by earthquakes. In this respect, it is important to define areas of high landslide risk (especially in new construction zones) and to provide appropriate computations of possible landslide motions and associated tsunamis.

There are two specific areas having especially high potential risk of possible underwater slope failures: (a) Malaspina Strait, separating the mainland coast from Texada Island; and (b) Roberts Bank on the southern Fraser River delta, southern Strait of Georgia (Figure 20). Three factors sparked interest in these areas: (1) The large volumes of unconsolidated sediments accumulated in the regions; (2) the possible risk of instability under earthquake loading; and (3) the presence of significant coastal infrastructure, including ferry terminals, port facilities, and electrical transmission cables.

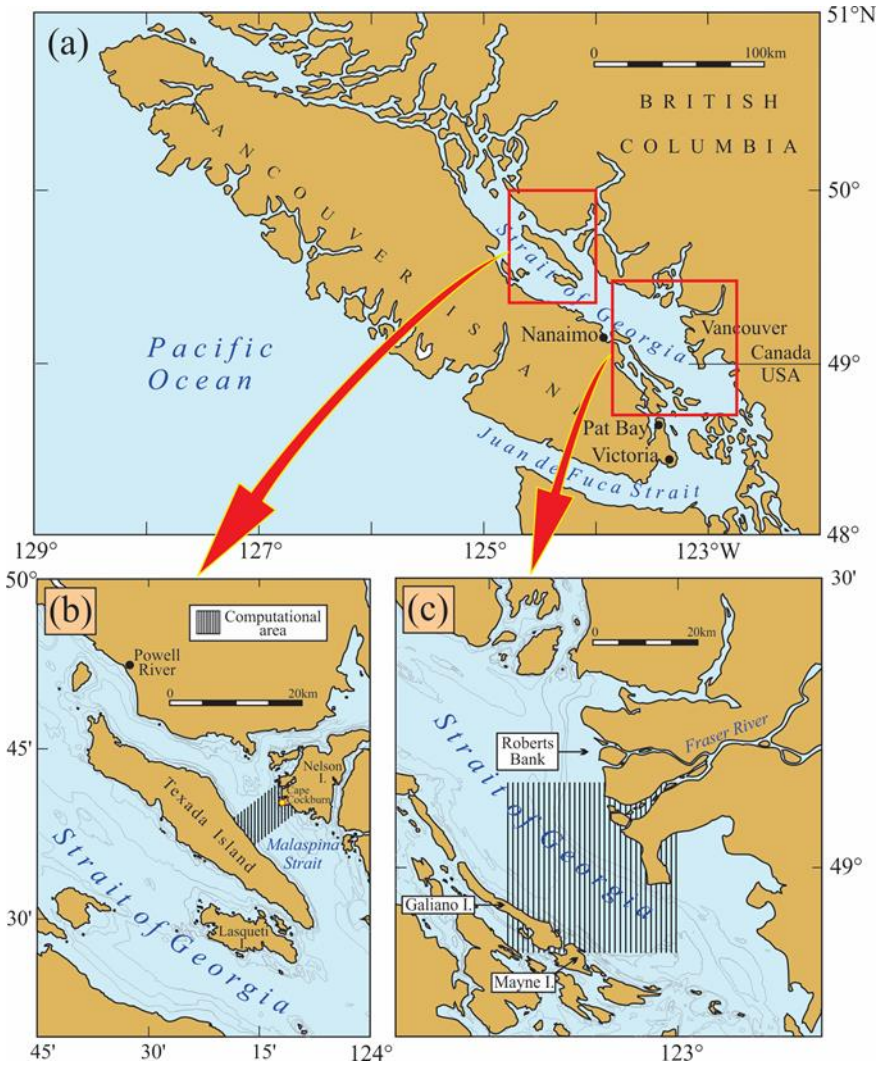

Figure 20. (a) Map of southern British Columbia showing the computational domains (shaded) for (b) Malaspina Strait, and (c) the southern Strait of Georgia (modified after *Rabinovich et al.* [2003]).

The Strait of Georgia is a long (222 km) and narrow (28 km) channel separating Vancouver Island from the mainland of British Columbia with an average depth of about 155 m. Freshwater discharge into the strait comes mainly from the Fraser River; the mouth of the Fraser River adjoins the Strait of Georgia along a 37-km delta front from Point Grey to Point Roberts Peninsula (Figure 21). The delta has been adding sediments at high rate and forms deposits 100-200 m thick over glacial deposits. Roberts Bank is the main area of accumulated alluvial deposits. It is located at the entrance of the South Arm of the delta between Sand Heads in the north and Point Roberts

Peninsula in the south [*Thomson,* 1981]. The large unstable sediment mass (109 m^3) identified on the Roberts Bank slope [*Christian et al.*, 1997a,b] could potentially result in significant submarine landslides and associated tsunamis and would likely produce severe damage.

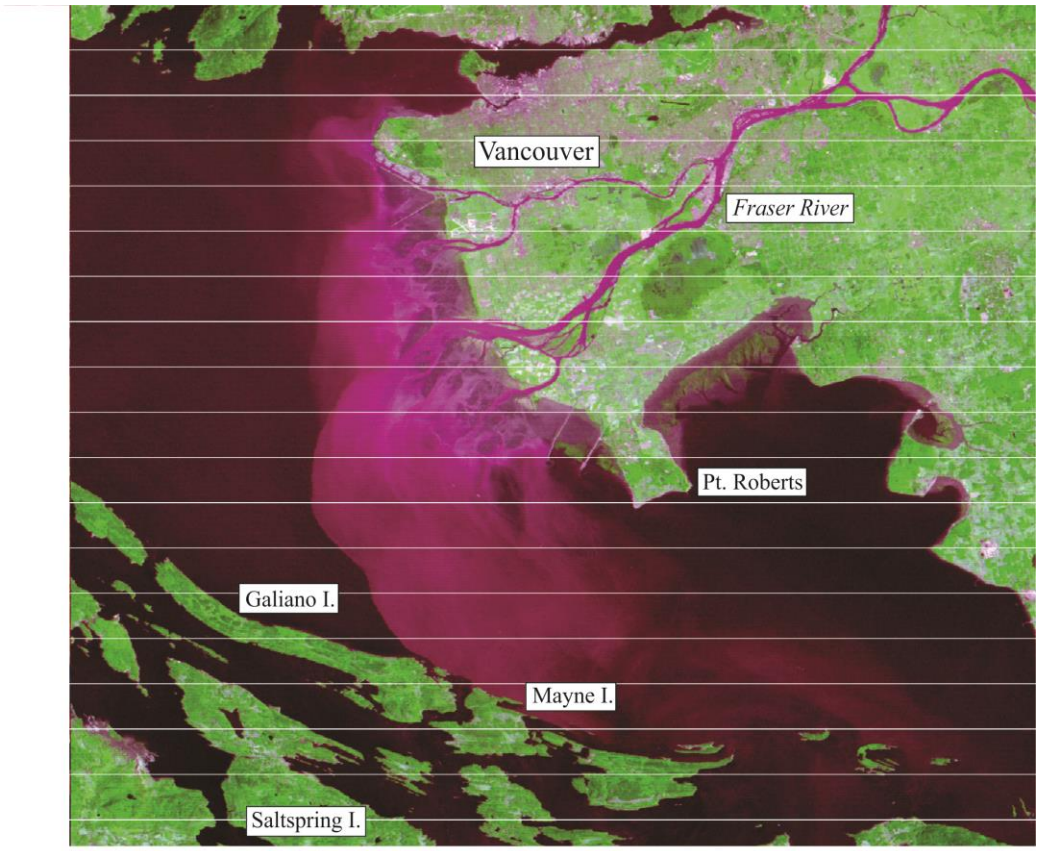

Figure 21. ERTS-1 satellite image of the Fraser River delta and plume on August 12, 1973. Spatial resolution is about 80 m. The colours are from infrared composite images showing vegetation as green, clear water as dark blue, and muddy water as red. The tide was low, exposing mud flats and eel grass (courtesy of Jim Gower, IOS).

The southern Strait of Georgia has been identified as a region of potentially high risk to submarine landslides [cf. *Terzaghi*, 1956; *Tiffin et al.*, 1971; *Christian et al.*, 1997a,b; *Chillarige et al.*, 1997b]. The Fraser River discharges up to 10,000 m^3/s of silt-laden waters into the strait (see Figure 21) with an annual sediment load of ~17.3 million tonnes [*Currie and Mosher*, 1996]. Unconsolidated sediments deposited off Roberts Bank produce an unstable delta front. The instability of the foreslope on the Fraser River delta has long been known [cf. *Terzaghi*, 1956;

Mathews and Shepard, 1962; *Hamilton and Luternauer*, 1983]. Two very general types of failure may occur in this region: (1) Shallow, retrogressive flow slide failures, and (2) deep-seated large-scale rotational failures [*Tiffin et al*., 1971; *Hamilton and Wigen,* 1987]. Five known flow slides occurred in the Fraser River delta between 1970 and 1985 [*McKenna et al.,* 1992; *Chillarige et al.* 1997a,b]. A failure in July 1985 was documented by *McKenna* and *Luternauer* [1987] and *McKenna et al.,* [1992] who assumed that the failure was a "*slow retrogressive flow over a period of hours*" so that no tsunamis were generated. However, according to *Hamilton and Wigen* [1987] and *Dunbar and Harper* [1993], more rapid (second-type failures) may generate significant tsunamis with amplitudes exceeding several meters. Tsunamis, in combination with high tide and storm surge, could cause coastal flooding in this area of the Strait of Georgia, with possible loss of life. As noted by *Hamilton and Wigen* [1987] "*Such a disturbance radiating from Sand Heads in the central Strait of Georgia would easily propagate both up the Strait (NW) to affect urban centres like Nanaimo, Parksville, Comox, Powell River and Campbell River, by reflection into Burrard Inlet and down the Strait (SE) to affect the American San Juan Islands and Puget Sound*".

An intensive collaborative effort was begun in 1992 to determine the geological and geotechnical properties of the offshore portion of the Fraser River delta, to identify seabed instability processes and to map their characteristics [*Christian et al.,* 1997a,b]. Roberts Bank is one of the main areas of alluvial sediment instability. Much has been written about the potential for submarine slope failures on Roberts Bank, driven by concerns for the security of infrastructure in the area. The western edge of the modern Fraser Delta consists of a broad tidal flat extending about 6 km to the top of the delta front slope at about 9 m depth. The upper delta front is characterized by slopes of up to 23°, diminishing to 1 to 2° at 300 m depth in the adjacent Strait of Georgia basin. Approximately 100 to 110 m of Holocene silts and sands have accumulated at the edge of the delta platform. These sediments overlie stiff, Pleistocene diamictons and coarse outwash deposits [*Christian et al.,* 1997a,b]. The thickness of the sediments over the top of the Pleistocene deposits is only about 9 m at the landward end of the BC Ferry Terminal Causeway; Pleistocene deposits make up Point Roberts.

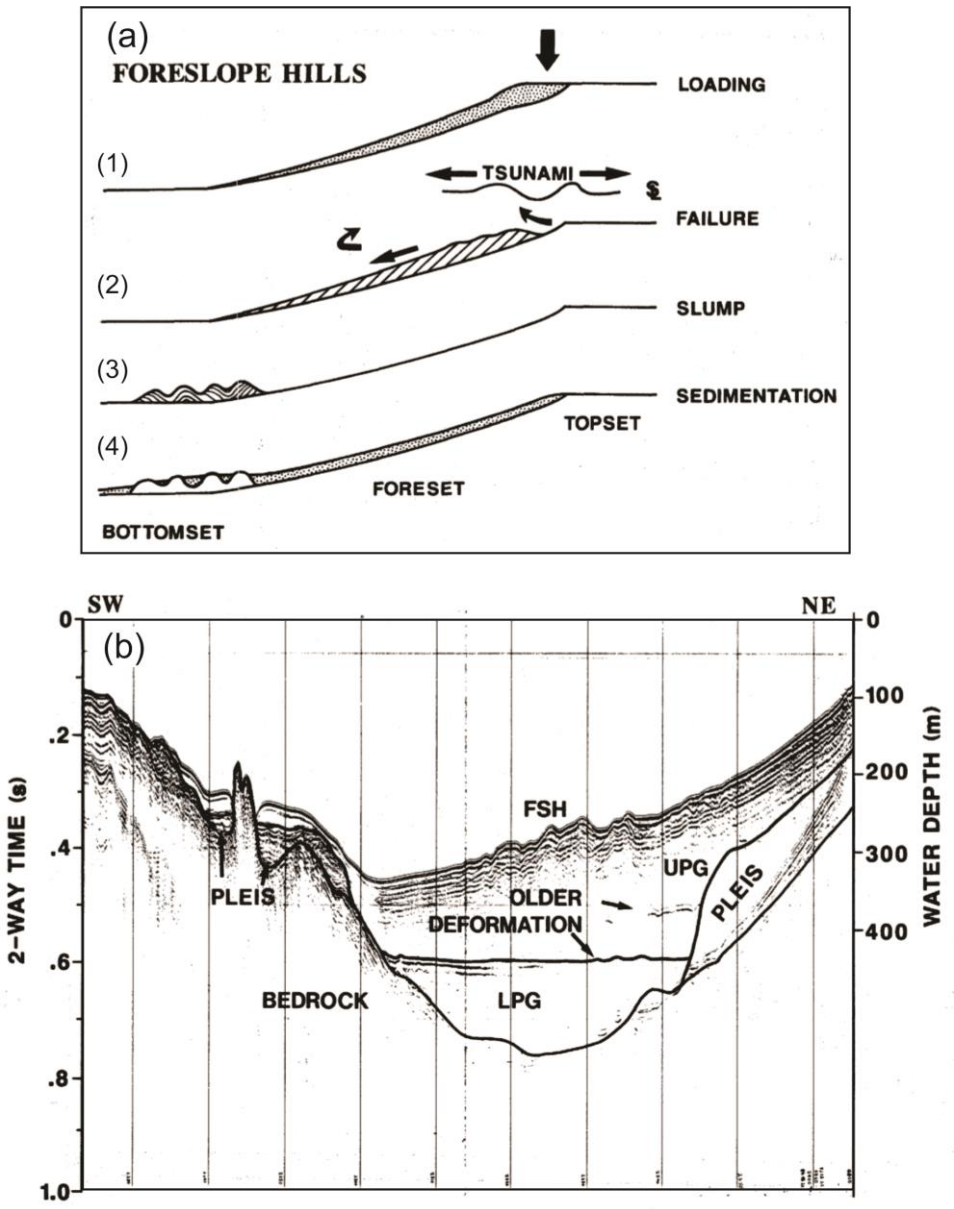

Figure 22. (a) A mechanism for the formation and evolution of the Foreslope Hills in stages. (b) Single channel airgun, continuous seismic profile 84 across the Foreslope Hills (FSH), showing the Quaternary stratigraphy and subsurface structure. Vertical exaggeration approximately 21x. Bedrock comprise Tertiary and Cretaceous Sedimentary rocks of the Whatcom and Nanaimo basins. Pleis (Pleistocene) denotes dense unconsolidated sediments of Glacial age and origin. LPG (Lower Post Glacial) denotes accumulations of horizontally bedded unconsolidated sediments confined to the deepest portions of the Pleistocene erosional basins. UPG (Upper Post Glacial) refers to the youngest unconsolidated sediments, here, these are dominantly deltaic facies of the foreslope and foredeep (From *Hamilton and Wigen* [1987]).

Hamilton and Wigen [1987] were probably the first to discuss the possibility (and probable historical precedents) for tsunamis in the southern part of the Strait of Georgia generated by the Foreslope Hills (FSH) failure in the area of the Fraser River delta (Figure 22). The origin of the FSH is explained by a four-stage model involving loading, failure, slump and sedimentation (Figure 22a). In areas like deltas with high sedimentation rates, sediment accumulation is too rapid to permit steady state compaction, dewatering, degassification and dissipation of high pore pressures (approaching geostatic). On the Fraser delta, where most of the sediment load arrives in one annual pulse associated with the spring freshet, it is easy to visualize a loading-induced failure. External causes all relate to increased shearing stress with possible contributions from seismic accelerational loading (shaking), sediment loading (burden of spring freshet, dredging/dumping/landfill), water loading (high runoff and large tidal ranges) and cyclic wave loading occurring in shallow water during intense storms. All of these potential triggering mechanisms are present, at least intermittently, in the region of the Fraser delta.

According to the model, the transfer of energy and momentum from the moving sediments to the overlying water column could generate a tsunami. Such a disturbance radiating from the vicinity of Sand Heads in the central Strait of Georgia would easily propagate both up the strait (NW) to affect urban centres like Nanaimo, Parksville, Comox, Powell River and Campbell River and down the strait (SE) to affect the American San Juan Islands and Puget Sound [*Hamilton and Wigen*, 1987].

The Foreslope Hills were then thoroughly examined by *Mosher and Thomson* [2002]. The FSH are composed of clay, silt and fine sand. Previous authors have interpreted them as: (1) a single mass-slide deposit, (2) mud diapirs, (3) in situ rotational failures, and (4) creep deformation features, but collaborative evidence for these interpretations was lacking. Seafloor surface morphological renders derived from recent multibeam sonar bathymetry data show linear, evenly spaced symmetrical ridges with ridge bifurcation, resembling wave ripples but on a much larger scale (Figure 23). The authors suggested that the Foreslope Hills should be re-interpreted as shoreward-advancing, current-induced sediment waves. A recent study of six-month duration current velocity data from bottom-mounted Acoustic Doppler Current Profilers (ADCPs) by *Thomson and Spear* [2020; under review] finds that the hills are formed and maintained by strong currents associated with internal bores and waves ("solibores") propagating shoreward over the bottom from the central axis of the strait.

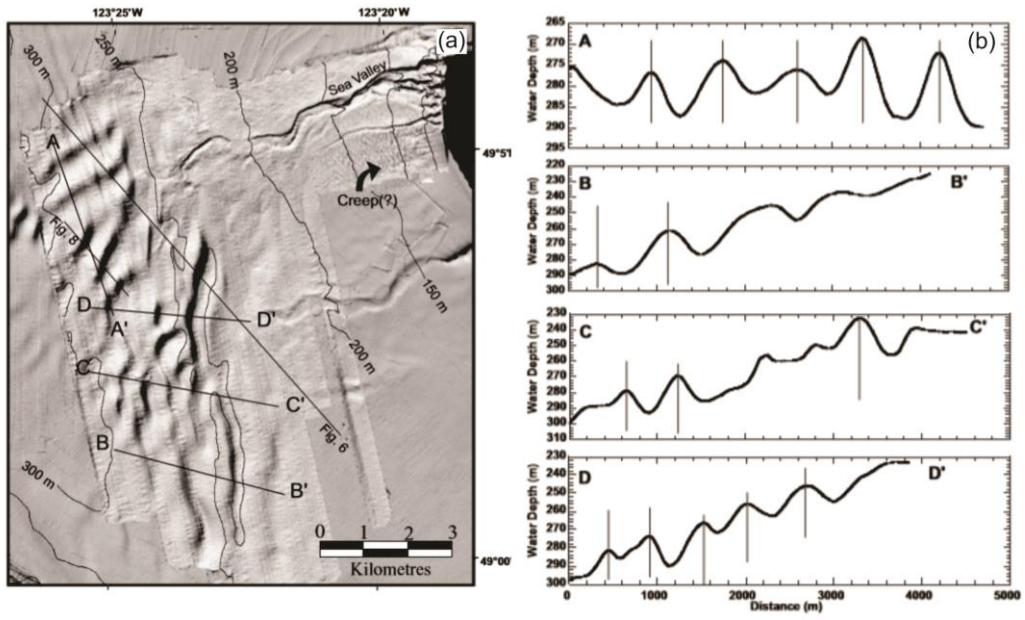

Figure 23. (a) Sun-shaded relief image of the Foreslope Hills and the Sand Heads sea valley, generated with multibeam sonar bathymetric data. The image is a composite of the 1994 data overlying the 2000 and 2001 data. The artificial sun angle is at an altitude of 50° from horizontal with an azimuth of 320°. (b) Depth profiles across the Foreslope Hills. The letters on the profiles are keyed to their locations shown in (a). The mean wave height is 12 m (maximum 20 m) and wavelength is about 700 m. Vertical lines are placed through the waveforms to assist in observation of the symmetry of most of the ridges. (From *Mosher and Thomson* [2002]).

5.3. Numerical Modelling of Slide-Generated Tsunamis in the Strait of Georgia

Long-term prediction of landslide-generated tsunamis has a number of specific features:

(1) Numerical simulation of earthquake-generated tsunamis normally is based on historical seismic parameters (source characteristics) or on parameters of hypothetical earthquakes. For constructing a model of slide-generated tsunamis, it is possible to use actual parameters of the unstable sediment body estimated by geotechnical or geophysical methods.

(2) Based on present capabilities, it is not possible to release the accumulated energy of a pending earthquake in order to prevent associated catastrophic tsunamis. Ignoring the liability

issue, it may be possible in specific cases to incrementally trigger subaerial or submarine sediment slides (in the same manner as for avalanches) to prevent sediment from accumulating in dangerous amounts and generating significant tsunamis. Using numerical modelling, it is straightforward to consider various scenarios and define the corresponding "triggering" strategy.

(3) Seismically-generated ("classic") tsunamis are natural phenomena which occur independently of human activity. In contrast, landslide-generated tsunamis are often the direct result of construction activity in coastal areas (see described examples and discussion of this question in *Thomson et al.* [2001] and *Rabinovich et al.* [2003]; *Bornhold and Thomson* [2012]).

Dunbar and Harper [1993] (herein DH93), using a relatively coarse (2 km) grid, undertook a preliminary simulation of tsunamis in the southern Strait of Georgia assuming a large delta front slide (from 2.5 to 7.5 km^3) as the source. The DH93 numerical model represented the slide volume as a number of independent slabs acting under the influence of gravitational acceleration and friction. Their study showed that such slides may induce tsunamis with heights from 1 to 4 m. *Rabinovich et al.* [2003] for the same region used much smaller volumes (from 0.23 to 0.75 km^3), but applied a more realistic numerical model of a viscous slide (VS2003 model) [cf. *Fine et al.*, 1998; *Thomson et al.*, 2001]. The authors emphasized that there are no specific geotechnical data that would suggest that, under anticipated earthquake loading, failure would actually occur; they simply assumed that failure would occur and then estimated possible tsunami waves that could be produced by such a failure. Because of the many uncertainties with respect to sediment physical properties in these areas, the results presented in that paper should be viewed as very preliminary estimations of actual tsunami magnitudes. *Rabinovich et al.* [2003] assumed a single rotational or translational failure of the entire sediment mass, i.e. the "*worst case scenario*". A retrogressive failure would result in lower tsunami amplitudes and a more complex resultant tsunami wave field.

Guided by available qualitative information about the region (Section 5.2), *Rabinovich et al.* [2003] postulated two failure scenarios for the edge of Roberts Bank: (a) A large (0.75 km^3) failure occurring at a depth of about 100 m (the zone of postulated sensitive clays), extending 7 km along the delta front between Canoe Passage and the BC Ferry Terminal with a swath width of 3 km; and (b) a smaller (0.23 km^3) failure, also occurring at a depth of 100 m, extending 4 km from Westshore Terminals to the BC Ferry Terminal with a width of 2.6 km (Figures 20c and 24).

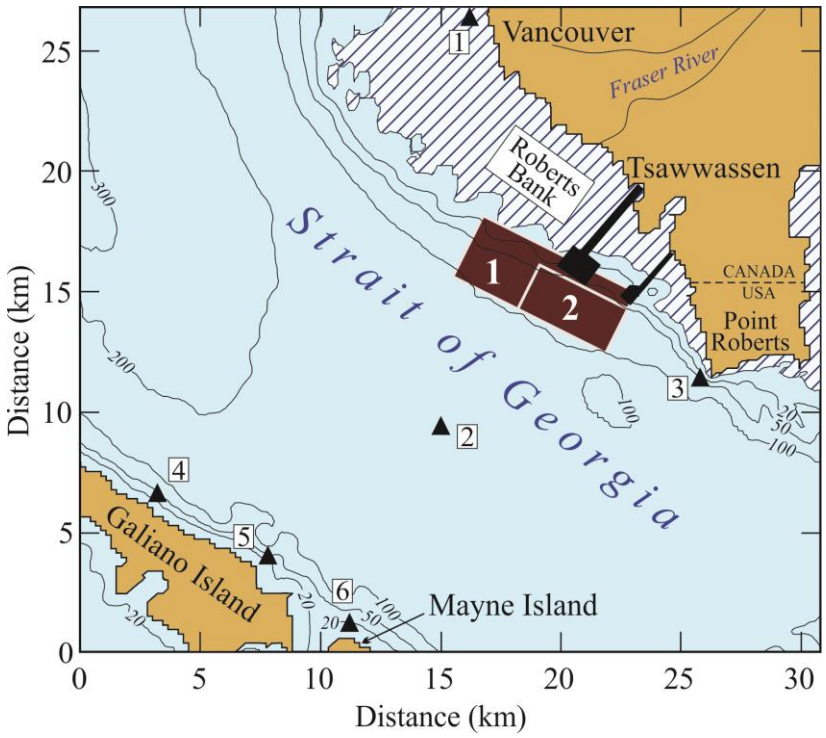

Figure 24. The computational domain used for the southern Strait of Georgia models. The dashed region denotes the area assumed to dry at low tide. Bold numbers refer to the modelled slide-body source areas for Cases 1 and 2. Specific computational sites 1 to 6 are marked. (Modified from *Rabinovich e et al.* [2003]).

Bathymetric data, including multibeam echo-sounding, were used to define the morphology of the basin. These data were important in determining both the character of the resultant tsunami waves and the extent of the flow slides on the basin floor. The Roberts Bank slide was assumed to have a rectangular bottom boundary at an angle of 28º relative to the computational grid (see Figure 24), but the thickness of the slide was taken from the actual geomorphic measurements above the uniform slope. The computational area (Figure 24) had grid dimensions 309×269 with length steps of 100 m. The Strait of Georgia is characterized by large tides with tidal amplitudes up to 3 m. These tides significantly change the geometry of the coastal area in the vicinity of the Fraser River delta. As a consequence, the computations had been made for two different grid areas, corresponding to extreme high water (3 m above sea level) and extreme low water (3 m below mean sea level). The main difference between these areas occurs in the vicinity of Roberts Bank. During high water, the area is under water, during low water, the area is fully drained (Figure 24).

Figure 25 presents snapshots of the slide body and tsunami wave patterns for Case 1 at high tide for times t = 1, 3, 6, and 10 min for the VS2003 model. The advancing submarine slide and intensification of the southwestward propagating wave crest are clearly evident. The waves cross the strait in about 7 min, reflect from the coasts of Galiano and Mayne islands, and then spread into the open strait. After multiple reflections from both coasts, and scattering from shore irregularities, the waves form a "chaotic" pattern of standing and propagating oscillations (Figure 25b, at t = 10 min). Figure 25 also shows the large extent of the flow slide run-out.

An important aspect of the modelled tsunami wave field is that Roberts Bank efficiently reflects the waves and protects the mainland coast (see Figure 25b). Therefore, maximum waves are observed opposite the source area, rather than on the northeastern coast of the strait near the initial failure zone (Figure 26). A similar result was obtained for low tide.

As indicated by Figure 25b, the maximum wave heights are associated with the leading tsunami waves produced by the hypothetical Fraser Delta failures. In this respect, these results differ from the modelling results of *Dunbar and Harper* [1993] (DH93 model), who found that the maximum waves occur more than 3 hours after the beginning of the failure in some locations. In addition, computed wave heights were much smaller in the DH93 model (from 1 to 4 m) than in the VS2003 model, despite the fact that total slide volume used in the DH93 model was about ten times larger (from 2.5 to 7.5 km^3). There are three main reasons for these differences: (1) Use in the VS2003 model of a single body slide instead of a number of retrogressive slides; (2) locating the slide source area in the shallower water compared to the DH93 model; and (3) use of a much more detailed computational grid area (spatial step of 0.1 km) compared with 2.0 km for DH93.

The wave parameters for computed waves for the six sites in Figure 24 are presented in Table 8 for Case 1 (large slide) and high tide (+3 m relative to MSL). There are marked variations in wave heights from one site to another, indicating the strong influence of local topography on the formation of tsunami waves. The maximum trough and crest amplitudes along the southwestern and northeastern coasts of the strait for Case 1 (high tide) are shown in Figure 26.

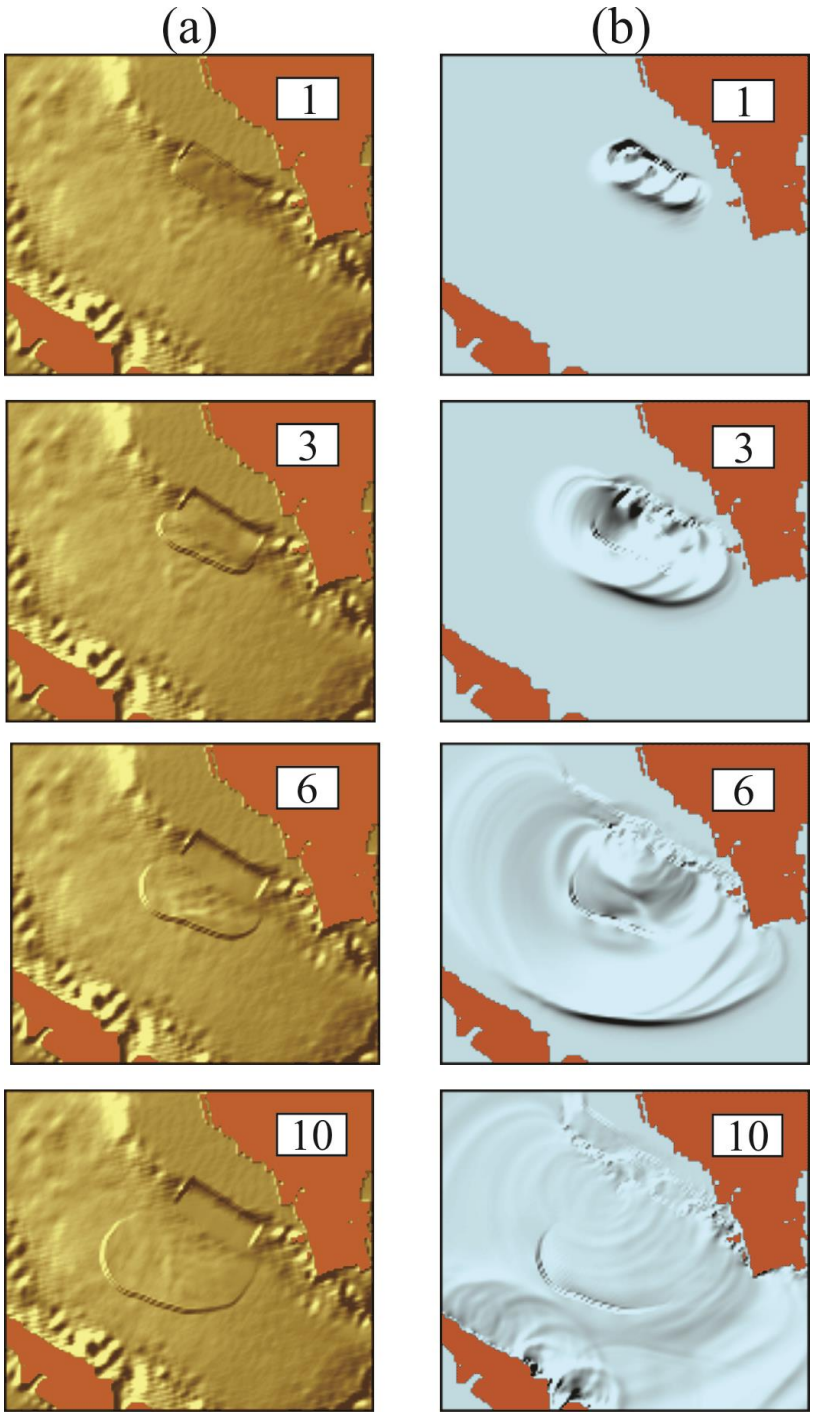

Figure 25. Snapshots of the simulated slide and tsunami fields at 1, 3, 6, and 10 min after the hypothetical slide failure in the vicinity of Roberts Bank for Case 1 at the time of high tide. (a) Movement of the slide body; and (b) propagation of the tsunami waves. (From *Rabinovich e et al.* [2003]).

Table 8. Timing and amplitude values for simulated landslide-generated tsunamis for sites in the southern Strait of Georgia for Case 1 (large slide with horizontal dimensions 7 km × 3 km) computed for high tide (3 m above mean sea, MSL) and low tide (3 m below MSL) (in brackets). Times for all waves, except the first wave, are the times between successive waves. NA = not applicable (from *Rabinovich et al.* [2003]).

Parameters	Site					
	1	2	3	4	5	6
Leading wave arrival time (min)	19.0 (NA)	2.8 (2.8)	3.4 (3.5)	6.3 (6.5)	6.2 (6.3)	7.0 (7.2)
	Maximum crest (positive wave)					
Arrival time (min)	30.0 (NA)	3.8 (3.9)	11.3 (17.1)	8.1 (8.2)	7.2 (7.3)	7.7 (7.9)
Amplitude (m)	2.1 (NA)	11.1 (11.9)	2.0 (2.6)	6.9 (7.5)	8.1 (8.8)	12.2 (12.9)
	Maximum trough (negative wave)					
Arrival time (min)	28.5 (NA)	8.9 (8.9)	9.3 (9.2)	10.4 (10.6)	9.9 (10.4)	10.3 (10.6)
Amplitude (m)	-0.4 (NA)	-10.1 (-11.2)	-3.1 (-2.5)	-5.6 (-5.0)	-7.3 (-5.3)	-6.4 (-10.4)

The main features of these computations are as follows:

1. Hypothetical tsunami waves generated by the VS2003 model along the southwestern coast of the strait (Galiano and Mayne islands) are much larger than along the northeastern coast (Tsawwassen); maximum crests are from +4 to +18 m and maximum troughs from –3 to –12 m for the southwestern coast compared to +1.5 to + 5 m and –0.2 to –5 m for the northeastern coast.

2. For both the southwestern and northeastern coasts of the strait, there is a tendency for a north-to-south increase in wave amplitudes, with minimum computed amplitudes at the northernmost end of Galiano Island and the coast north of Tsawwassen; maximum amplitudes occur on the coasts of Mayne Island and Point Roberts.

3. For both coasts, crest amplitudes are significantly larger than trough amplitudes, the exception being the coast of Point Roberts where they are approximately equal (4 to 5 m).

4. Complicated coastal geometry and seafloor topography cause significant variability in tsunami wave heights. For example, the maximum computed wave amplitude at Site 6 (northern coast of Mayne Island) was 12.2 m whereas the maximum height at a nearby station a few kilometers to the south was 18.0 m.

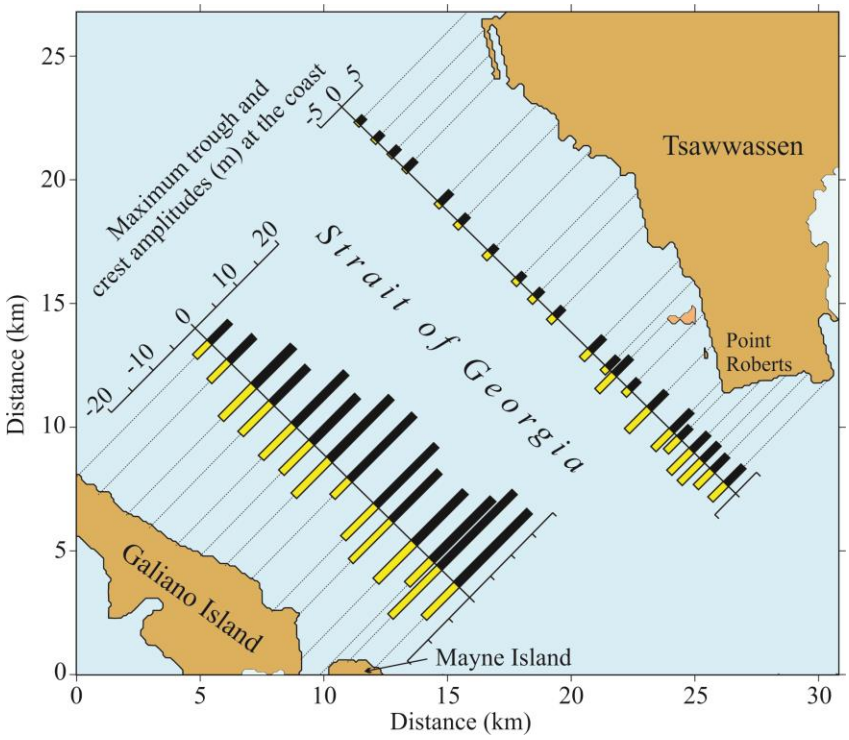

Figure 26. Maximum negative (trough) and positive (crest) wave amplitudes computed along the western and eastern coasts of the southern Strait of Georgia for Case 1 at high tide. (Modified from *Rabinovich et al.* [2003]).

The alluvial materials brought by the Fraser River, which form Roberts Bank, is the main source of unstable sediment deposits in the Strait of Georgia. From this point of view, the VS2003 model developed by *Rabinovich et al.* [2003] is the "**worst case scenario**" for this region. Extreme wave crests of 2 to 18 m are generated by the large (Case 1) delta failure, with maximum simulated wave amplitudes occurring on the southwest side of the strait, opposite the source area, with amplitudes of 14 to 15 m on the coast of Galiano Island and 18 m on the coast of Mayne Island. Amplitudes on the eastern side of the strait near the Tsawwassen Ferry Terminal and Fraser River delta are much smaller (1 to 4 and 0.2 to 2 m, respectively) because of the efficient wave reflection at the outer edge of Roberts Bank. The leading semi-wave from the landslides consists of a positive wave propagating into the deep portion of the basin toward the southwest. The first trough, which would normally propagate onshore, is immediately reflected back into the strait by Roberts Bank.

These waves can penetrate into shallow water and inundate the mainland coast; significant non-linear effects can be expected in this case. The slide body moving downslope on the Fraser Delta could reach speeds of about 20 m/s. Comparison of "low tide" and "high tide" numerical simulations indicates that simulated waves are 5-10% higher at low tide, apparently because the slide body is located closer to the sea surface. However, because water levels are 6 m higher at high tide than low tide, the destructive capacity of the tsunami waves at the coast is greater during high tide.

Rabinovich et al. [2003] did not estimate possible wave heights produced by the Roberts Bank slide failure for either Saanich Inlet/Patricia Bay or the Nanaimo area. Nevertheless, the results of their modelling simulation enable us to roughly estimate possible tsunami heights for these two regions. It is well known that landslide-generated tsunamis are typically *local events*. Even the largest known tsunami of 525 m in Lituya Bay, SE Alaska, was insignificant beyond the bay [*Lander*, 1996; *Fritz et al.*, 2009]. The main reason is that, compared to the seismic source, the slide source extension is too small. The Case 1 "large Roberts Bank source" is 7 km × 3 km, while the lengths of the 1960 Chile and 2004 Sumatra tsunami source regions were approximately 1000 km and widths of ~200 km. Therefore, landslide-generated tsunamis are *locally destructive* but attenuate quickly in the off-source directions. This tendency is evident in Figure 26. Extrapolating the computed tsunami amplitudes to the area of Nanaimo, we obtain a positive tsunami wave amplitude of ~0.5-1.0 m. Similarly, the wave propagating in the direction of Saanich Inlet would also strongly attenuate. In addition, the Gulf Islands effectively shelter the inlet from tsunamis in the Strait of Georgia. As a consequence, any wave that reaches Saanich Inlet would have an amplitude < 0.5 m.

5.4. Numerical Modelling of Slide-Generated Tsunamis in Malaspina Strait

Malaspina Strait is a narrow (5-10 km), 50 km long channel separating Texada Island in the central Strait of Georgia from the mainland of British Columbia (Figure 20b). Mid-channel depths throughout the channel range from about 300 to 375 m. The central part of the strait is underlain by a thick (~100 m) sequence of sediments, mostly derived from the Fraser Delta [*Currie and Mosher*, 1996]. This region is located relatively close to Nanaimo (Figure 20b); that is why it is

important to consider the possible effects of landslide-generated tsunami produced by a Malaspina slide.

Geophysical investigations carried out by the Geological Survey of Canada identified a perched sediment mass, divided into two lobes, located along the slope between approximately 30 and 120 m water depth (Figure 27a). This unit was identified in initial investigations (high-resolution seismic profiling and sidescan sonar) and was subsequently studied using a remotely operated vehicle (ROV). Extensive video coverage in 1996 of the downslope edge of the unit revealed large (up to several metres) blocks of cohesive sediment, which had collapsed from the front of the unit resulting in a vertical-to-undercut slope in many localities. The lower eroding edge of the unit is everywhere very steep along a scarp-like feature between the 110-120 m isobaths. The failed material has remained just below the scarp on the lower slope (Figure 27b) as angular blocks of cohesive mud. The northern lobe is up to 38 m thick and displays internal seaward dips averaging 7.5° (Figure 27b). The unit rests on an underlying slope of approximately 16°, assumed to be bedrock, and extends about 400 m along the slope with a width of approximately 300 m (Figure 27a). The entire sediment body is an overconsolidated Pleistocene glaciomarine mud underlying the Quadra Sand unit found throughout the Strait of Georgia.

The landslide tsunami modelling presented by *Rabinovich et al.* [2003] considered failure of the northern lobe only. The hypothesized scenario was that of a severe earthquake causing the entire sediment unit to fail along its steeply dipping basal slope (Figure 27b). The numerical model for the Malaspina Strait region had grid dimensions of 365×197 with length steps $\Delta x = \Delta y = 25$ m (Figure 20b). The initial slide area was rectangular in plan with parabolic cross-sections along both axes (as recommended by *Jiang and LeBlond* [1992]) and has the following properties: volume = 1,250,000 m^3; width = 200 m; mean thickness = 30 m; slide centre coordinates = 49 º37.94' N, 124º 16.80' W; mean depth = 80 m; sediment density (ρ_2) = 2.0 $g \cdot cm^{-3}$; and kinematic viscosity (ν) = 0.01 $m^2 \cdot s^{-1}$.

Figure 28 presents snapshots of the slide body movement and surface wave propagation. The slide movement is mainly directed normal to the shoreline (Figure 28a), spreading cylindrical surface waves ahead of the moving slide (Figure 28b). A positive wave (crest) propagates in front of the submarine slide eastward across the strait toward the mainland coast, while a negative wave (trough) moves in the opposite direction (westward) toward Texada Island (Figure 28b). The

leading wave transits Malaspina Strait and arrives at Cape Cockburn on Nelson Island just over 2 minutes (about 132 s) after the inception of the slide. Following refraction on the shelf of Nelson Island and reflection from the coastline, the tsunami waves form a complicated structure of standing oscillations in the strait. Radiation through the open strait boundaries results in rapid decay of these oscillations.

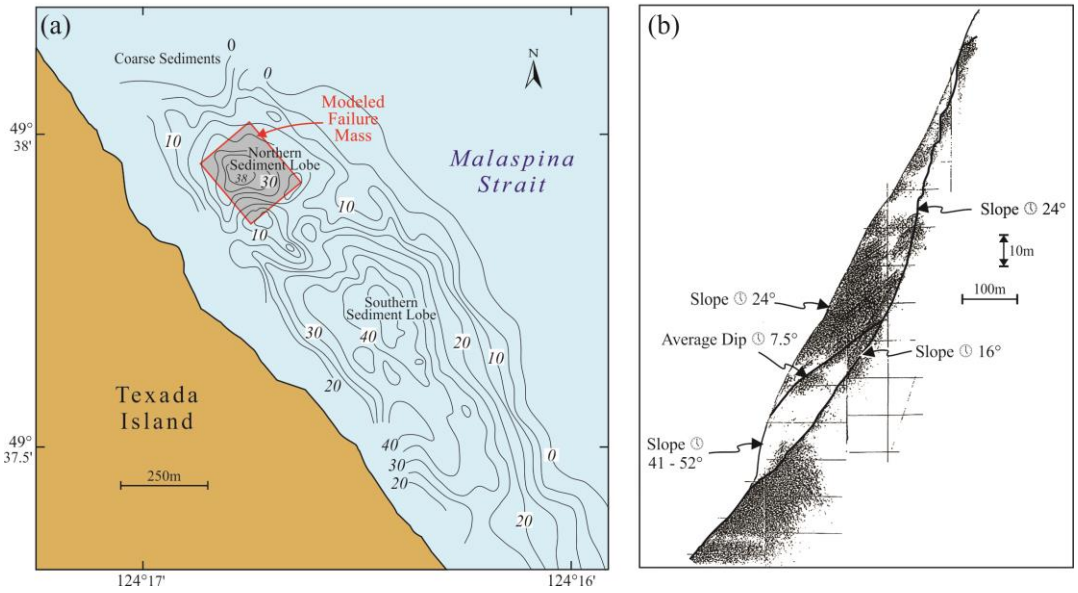

Figure 27. (a) Map of the area off eastern Texada Island showing the distribution of the perched surficial sediment lobes and their thickness on the upper slope. Depth contours are in 5-m increments. (b) High-resolution seismic profile through the northern sediment lobe, assumed to fail in the numerical investigation, on the eastern slope of Texada Island. Profile reveals the internal structure of the lobe and the steep underlying surface on which the sediment rests (Modified from *Rabinovich et al.* [2003]).

Table 9 gives the derived wave characteristics at sites A, B, and C (positions of the sites are shown in the upper plot of Figure 28b). Maximum wave heights are observed at Site A, close to the generating area, while minimum heights occur at Site B in the middle of the channel. The first wave is negative at site A and positive at sites B and C. This means that the wave crest precedes the slide in an eastward direction. Wave oscillations attenuate rapidly at sites A and B, apparently because of strong outward radiation of wave energy. In contrast, the oscillations at site C decay slowly, probably due to a trapping effect in this area and the formation of standing oscillations over the shelf. The periods of the simulated wave oscillations shorten with time from 80 to 40 s.

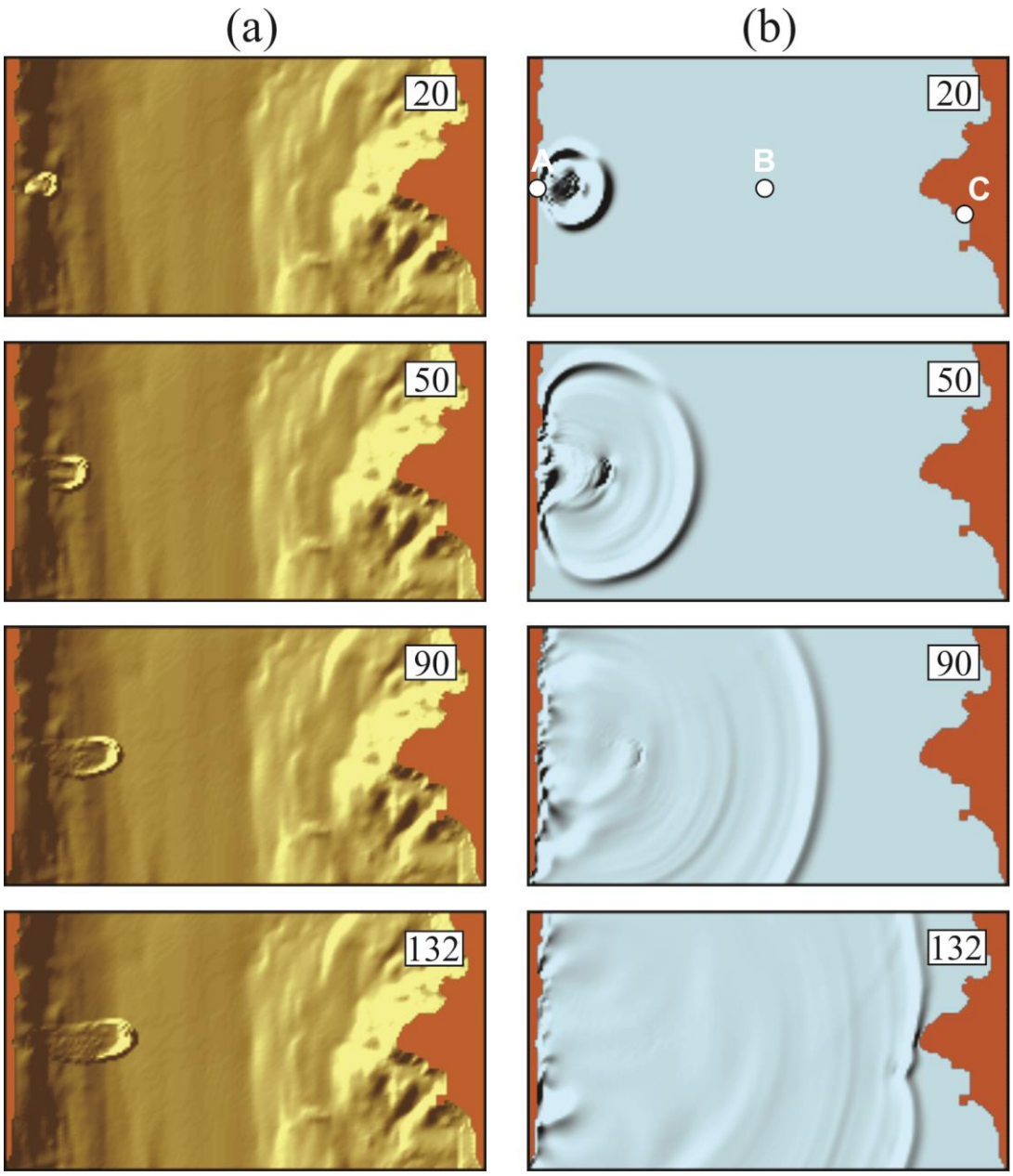

Figure 28. Snapshots of the slide and associated tsunami waves from numerical simulations for times 20, 50, 90, and 132 s after the initial hypothetical slide failure in Malaspina Strait. (a) Viscous slide body; and (b) tsunami.

Table 9. Wave heights and arrival times for slide-generated tsunamis for various sites in Malaspina Strait.

1. Parameters	Site		
	A	B	C
Leading wave arrival time from start of landslide (s)	6	64	163
	Maximum crest		
Arrival time (s)	50	71	176
Height (m)	1.9	0.5	0.7
	Maximum trough		
Arrival time (s)	24	90	195
Height (m)	-4.8	-0.2	-0.5

Using the viscous slide model, *Rabinovich et al.* [2003] estimated maximum trough and crest heights along the western and eastern coasts of the strait (Figure 29). Results indicate that maximum wave troughs (up to –5 m) would be observed in the vicinity of the source area. Northward and southward from this area, the trough amplitudes decay rapidly. Maximum wave crests would also be observed along the western coast, though smaller than troughs (up to +2.7 m) and distributed in a more irregular way. On the opposite (eastern) coast, both trough and crest amplitudes would be much smaller (about ±1 m) and less spatially consistent. The much greater variability in wave height along the eastern (Nelson Island) coast, in comparison with the western (Texada Island) coast, appears to be related to local topographic irregularities of the western coastline.

The results of numerical modelling demonstrate that maximum waves would be observed on the same coast, close to the source area, rather than on the opposite coast of the strait. From this point of view, these results are in contrast with those obtained for the southern Strait of Georgia (Section 5.3), where maximum amplitudes of the simulated tsunami waves were observed on the opposite (southwestern) coast. Also, the computed wave heights for Malaspina Strait were much weaker than those in the southern SoG, mainly because the Malaspina slide body was much smaller than the Roberts Bank potential slide (0.00125 and 0.75 km^3, respectively).

Figure 29 shows very fast decay in wave amplitudes in the southward direction (i.e., in the direction of Nanaimo). It is evident that in the vicinity of Nanaimo the corresponding waves will be negligible (<0.2 m).

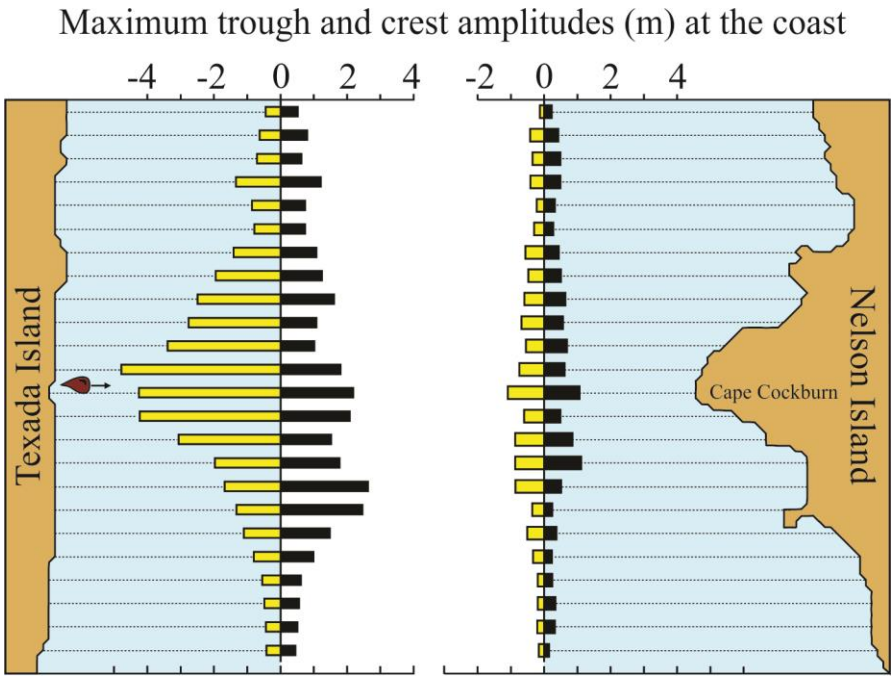

Figure 29. Maximum negative (trough) and positive (crest) amplitudes computed along the western and eastern coasts of Malaspina Strait. (Modified from *Rabinovich et al.* [2003]).

.

5.5. Summary of Landslide Generated Tsunamis in the Strait of Georgia

In the present section, we have discussed possible effects of landslide generated tsunami waves within the Strait of Georgia. The results of a literature overview indicate that the waves can be strong, even destructive in some areas of the strait and adjacent Puget Sound; the maximum wave heights can reach several meters and even tens of meters. However, the effects are **local.** Tsunami amplitudes associated with submarine landslides decay quickly with distance from the source area.

Following the numerical study of *Rabinovich et al.* [2003], we examined two specific regions of high risk of submarine slides: (1) Roberts Bank formed by alluvial sediment materials from the Fraser River delta; and (2) Malaspina Strait separating Texada Island from the mainland BC coast. The first (Roberts Bank) slide, with an assumed volume of 0.75 km^3, can produce significant tsunami runup on the southeastern coasts of the Gulf Islands. However, the estimated amplitudes

for the areas of Patricia Bay and Nanaimo would be <0.5 m. The second study, based on a failure in Malaspina Strait, yielded 4-m waves on the SE coast of Texada Island but waves would be negligible at Nanaimo and not measurable at Patricia Bay.

In general, the risk from landslide-generated tsunamis for the regions of Patricia Bay and Nanaimo is low.

6. EXTREME SEA LEVEL OBSERVATIONS IN PATRICIA BAY AND NANAIMO

As indicated in Section 2, there are CHS tide gauges in Patricia Bay and Nanaimo Harbour located near the Institute of Ocean Sciences (IOS) and the Pacific Biological Station (PBS), respectively. The Patricia Bay tide gauge has been working continuously since its installation in June 1976, first as an analogue (pen-and-paper) instrument and since July 1997 as a high-resolution digital gauge. Regular sea level measurements from Nanaimo are from January 1997 to October 2003 and then from July 2014 to the present. The sea level data from these two stations have been used to estimate the extreme statistical characteristics and maximum observed sea levels at these two sites.

6.1. Extreme Sea Level Oscillations in Patricia Bay

From June 1976 until 1997, the Patricia Bay tide gauge provided analogue data that were digitized and stored with 1-hour sampling. However, for extreme events, the CHS estimated the exact sea level heights and the corresponding timings from paper records. Since July 1997, the same characteristics were estimated directly from digital 1-min records. Thus, the total length of the data series is ~43.5 years. The monthly extrema for this period, both for the original records (with tides) and residual (de-tided), were tabulated. These data were used to construct Table 10 and Figures 30a and 31a.

Table 10 includes events with residual heights of more than 0.7 m relative to the Patricia Bay mean sea level. Altogether, there were 14 such events from June 1976 to December 2019. The maximum height of 1.04 m occurred on 16 December 1982. There were four other events when the extreme heights were >0.8 m: on 5 December 1981, 22 November 1988, 27 January 1983 and 10 March 2016. From these five events, two occurred during the El Niño period of 1982-1983. It

appears that all 14 events listed in Table 10 were produced by storm surges initiated by cyclones passing over southern Vancouver Island. It should be emphasized that the typical "high amplitude phase" of a surge lasts for a few hours. This means that this phase can coincide with high tide, in particular even with "king" (spring) tide, being especially dangerous, but can also occur during low tides and remain unnoticed. This is the reason why the actual (original) observed sea levels (Column 3 in Table 10) vary so widely. For example, the difference in the residual (surge) heights is 33 cm for the events of 16 December 1982 and 15 December 1977, while the difference in the recorded (tidal) height is 89 cm. Figure 30a shows the "observed" (i.e., total) sea level heights, while Figure 31a the residual (storm surge) heights.

Table 10. Extreme monthly sea levels observed at Patricia Bay, British Columbia, for the period of June 1976 – December 2019 for 14 events when residual sea levels were more than 0.7 m. The events are tabulated in decreasing order.

Date	Time (hh:mm)	Observed sea level with tides (m)	Residual non-tidal sea level (m)	Comment
16 December 1982	07:31	4.38	1.04	El Niño
5 December 1981	12:05	4.07	0.86	
22 November 1988	14:23	4.03	0.86	
27 January 1983	05:29	4.29	0.85	El Niño
10 March 2016	05:58	4.19	0.822	
20 December 2018	13:46	4.14	0.788	
3 December 2007	12:09	4.14	0.784	
4 February 2006	09:05	4.29	0.741	
18 November 1982	08:13	3.99	0.74	El Niño
14 November 1981	07:51	4.09	0.73	
1 January 1997	10:12	4.14	0.728	
19 December 1994	07:25	4.01	0.72	
15 December 1977	09:26	3.49	0.71	
21 November 1992	13:32	3.86	0.71	

Comment: Two decimal digits in columns 3 and 4 are given for analogue records; three digits are given for digital high-precision records with 1-min sampling.

The list of the strongest events presented in Table 10 cannot be considered as totally complete, because only one (the strongest) event per month is considered. Other events during the same month, even quite strong, are ignored. Nevertheless, they enable us to estimate the strength and approximate probability of the observed extreme events.

One of the evident properties of the estimated extreme values are their marked seasonal variations. All 14 strongest events presented in Table 10 occur during the winter season, specifically between 14 November and 10 March. The seasonal variations of extreme values, both original (with tides) and residual (de-tided) are clearly evident in Figures 30a and 31a.

To better examine this question, we constructed plots of seasonal changes of extreme values at Patricia Bay, both original and residual, and estimated the corresponding mean values. The results are shown in Figures 32a and 33s, respectively. The minimum values are associated with six “summer” months (April - September) and enlarged values with six “winter” months (October – March); the highest values are observed in December – January.

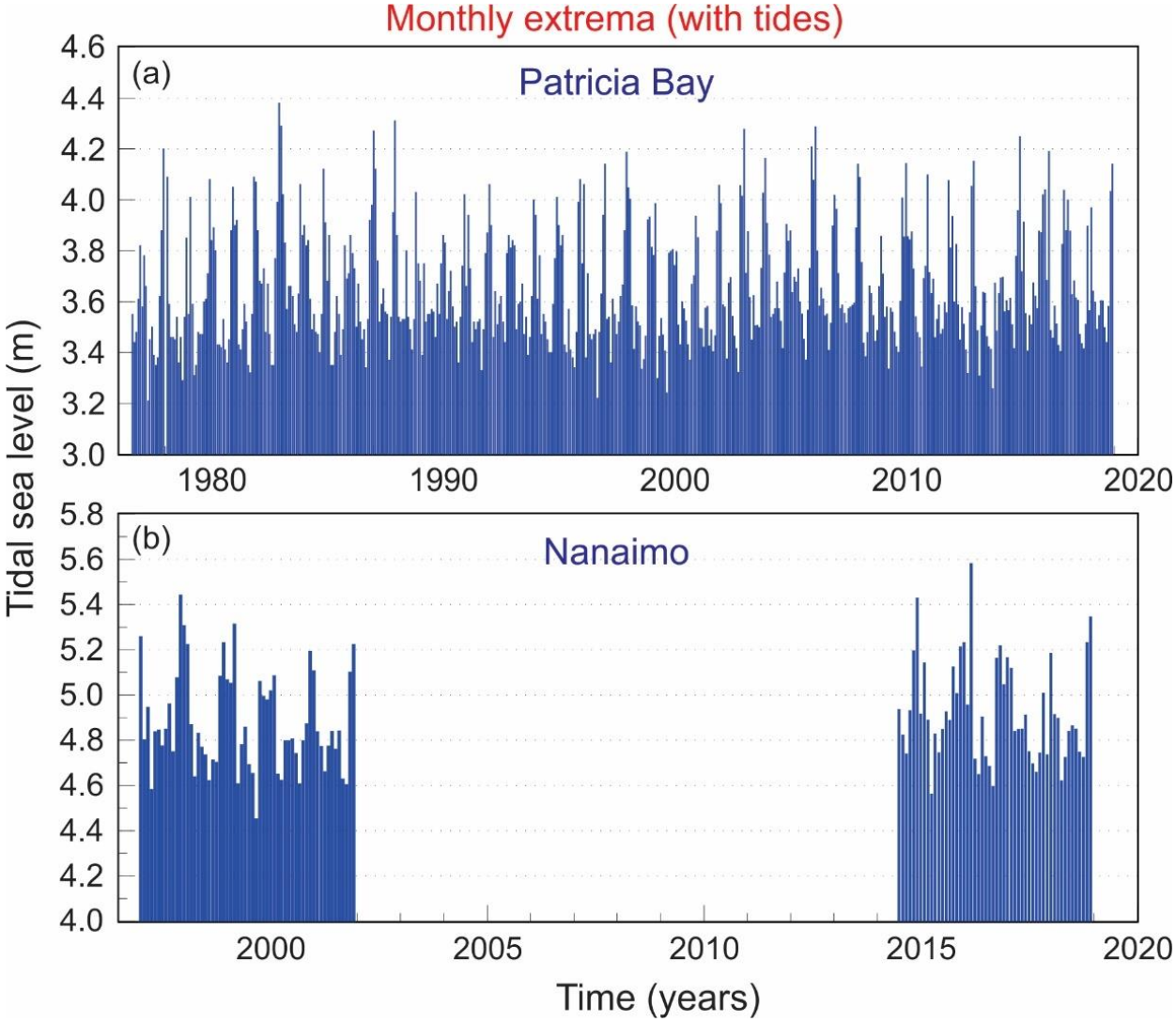

Figure 30. Extreme observed (original with tides) monthly sea levels observed (a) at Patricia Bay, British Columbia, for the period of June 1976 – December 2019 and (b) at Nanaimo for the periods of January 1997 - October 2003 and July 2014 – December 2019.

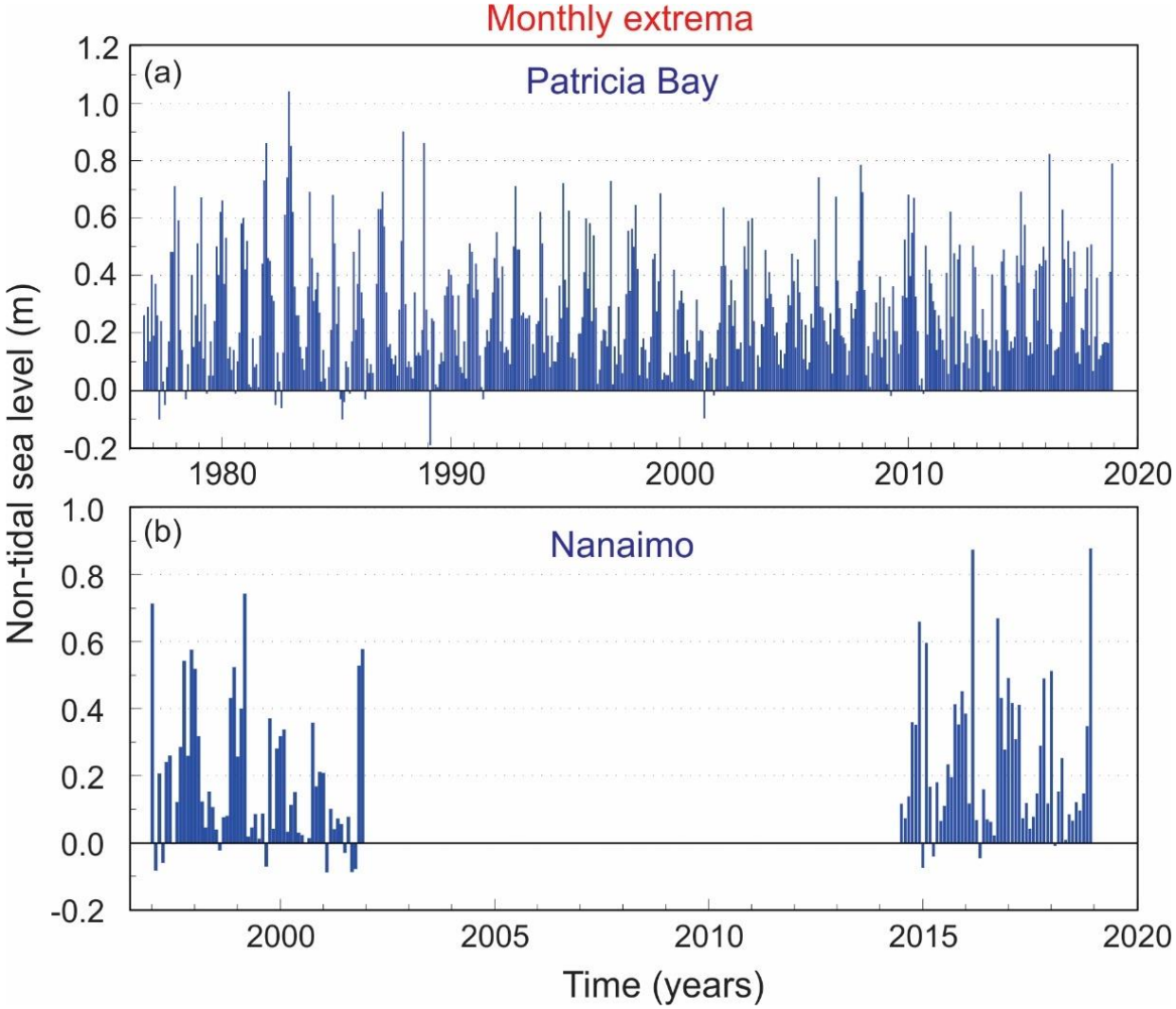

Figure 31. Residual (de-tided) extreme monthly sea levels observed (a) at Patricia Bay, British Columbia, for the period of June 1976 – December 2019 and (b) at Nanaimo for the periods of January 1997 - October 2003 and July 2014 – December 2019.

6.2. Extreme Sea Level Oscillations at Nanaimo

Extreme monthly sea levels at Nanaimo have been examined in the same way as for Patricia Bay. However, the available time series at Nanaimo were much shorter than at Pat Bay, covering only about 12 years (January 1997 - October 2003 and July 2014 to the present) in comparison with 43.5 years at the latter station. Consequently, the statistics at Nanaimo are limited.

Nevertheless, the 12-year series of sea level observations allow us to provide some preliminary conclusions about possible extreme sea level heights at this station.

Figure 30b and 31b present all available monthly extremes at Nanaimo (original/tidal and residual, respectively); parameters of the strongest events are shown in Table 11. Taking into account the limited number of strong events recorded at this station, we included into this table all events with observed heights >0.6 m. Altogether, there were six such events, with the strongest ones of 0.877 m and 0.873 m observed on 20 December 2018 and 10 March 2016, respectively.

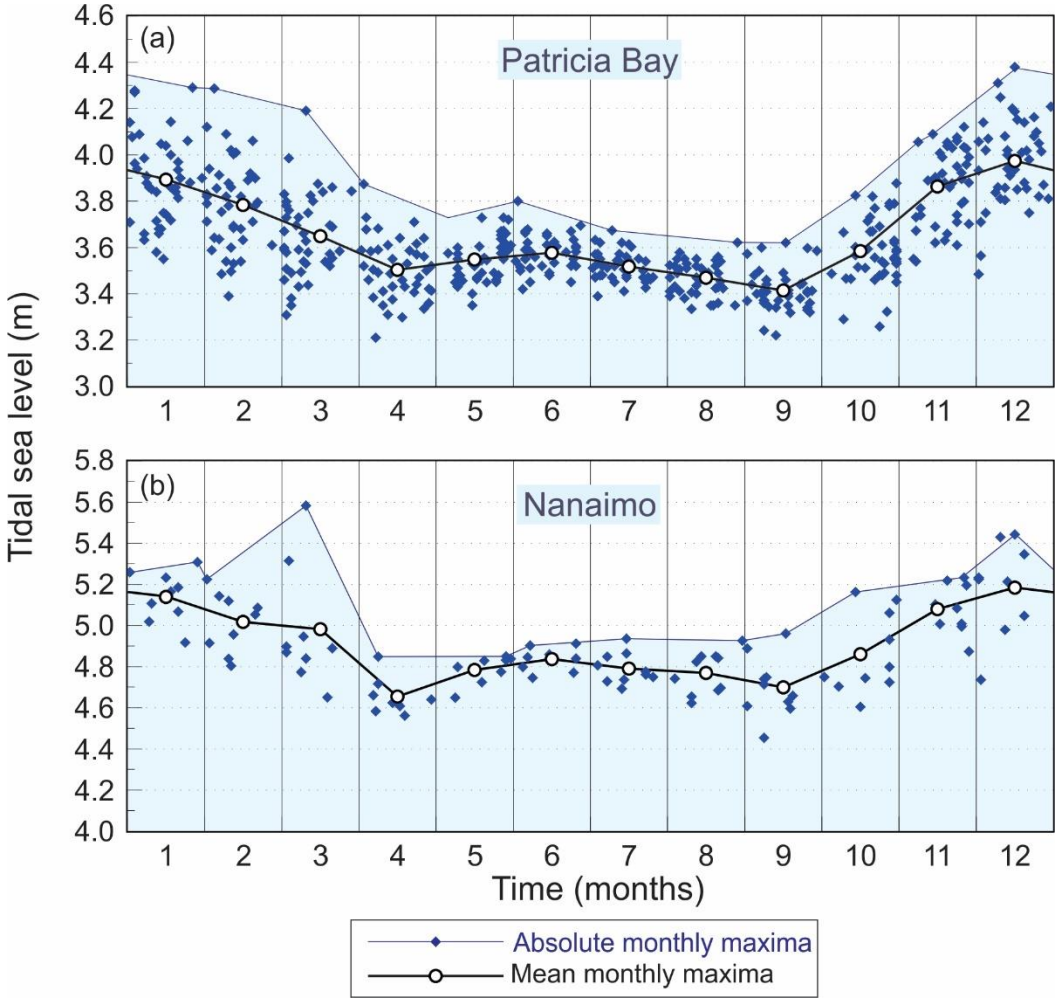

Figure 32. Seasonal changes of extreme observed (original with tides) monthly sea levels observed (a) at Patricia Bay, British Columbia, for the period of June 1976 – December 2019 and (b) at Nanaimo for the periods of January 1997 - October 2003 and July 2014 – December 2019.

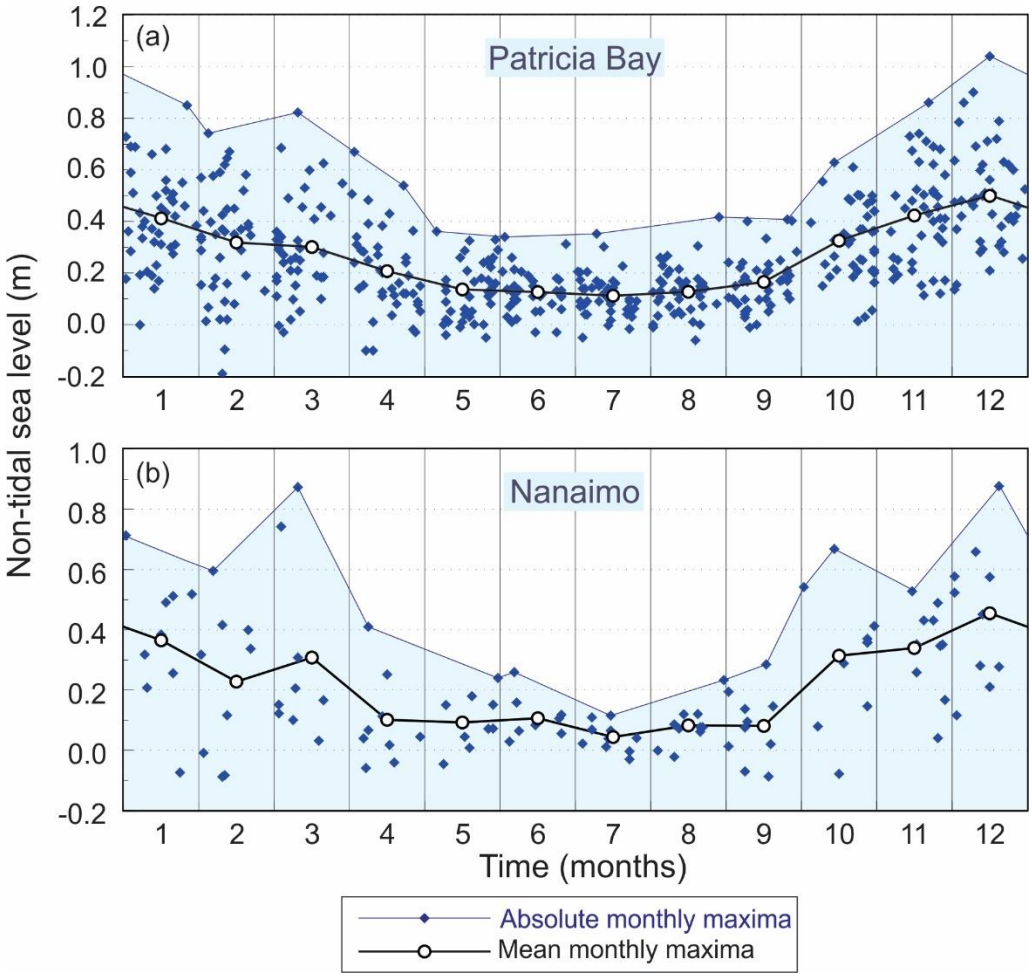

Figure 33. Seasonal changes of residual (de-tided) extreme monthly sea levels observed (a) at Patricia Bay, British Columbia, for the period of June 1976 – December 2019 and (b) at Nanaimo for the periods of January 1997 - October 2003 and July 2014 – December 2019.

All six extreme events recorded at Nanaimo were also recorded at Patricia Bay (Table 11). The correlation coefficient between the corresponding wave heights is quite high: $R^2 = 0.86$. This enables us to estimate empirical relationship between sea level heights at Nanaimo (H_{Nan}) and Patricia Bay (H_{PB}):

$$H_{\mathrm{Nan}} = (1.07 \pm 0.02) H_{\mathrm{PB}}. \quad (1)$$

This means that maximum wave heights at Nanaimo for the same events are approximately 7% higher than at Patricia Bay. For example, if the highest storm surge recorded at Patricia Bay was 1.04 m (on 16 December 1982, when there were no instrumental sea level measurements at Nanaimo), at Nanaimo it would have been ~1.11 m.

Table 11. Extreme monthly sea levels observed at Nanaimo, British Columbia, for the periods of January 1997 - October 2003 and July 2014 – December 2019 for 6 events when residual sea levels were more than 0.7 m. The events are tabulated in decreasing order.

Date	Time (hh:mm)	Observed sea level with tides (m)	Residual non-tidal sea level (m)	Residual at PB (m)	Ratio Nan/PB
20 December 2018	14:36	5.346	0.877	0.788	1.11
10 March 2016	06:19	5.582	0.873	0.822	1.06
3 March 1999	06:55	5.315	0.742	0.685	1.08
1 January 1997	10:05	5.259	0.713	0.728	0.98
14 October 2016	16:04	5.163	0.668	0.628	1.06
6 February 2015	05:43	5.143	0.659	0.576	1.14

Comment: Two decimal digits in columns 3 and 4 are given for analogue records; three digits are given for digital high-precision records with 3-min and 1-min samplings.

Figures 30b and 31b demonstrate the same character of seasonal variations of monthly extreme values at Nanaimo as at Patricia Bay (Figures 30a and 31a); additional details are shown in Figures 32b and 33b. Similar to Patricia Bay, maximum values are observed in winter time, minimum at summer.

6.3. Summary of Extreme Sea Level Observations at Patricia Bay and Nanaimo

Residual variations of sea level are mainly associated with atmospheric activity. Strong cyclones propagating over Vancouver Island in wintertime produce the largest positive sea level changes, i.e., *storm surges.* The monthly extrema at Patricia Bay and Nanaimo, presented in Tables 10 and 11, are related to storm surges. As indicated by *Crawford* [1980], long-period atmospherically induced sea level variations are commonly uniform along the British Columbia

coast. An inverted barometer effect, i.e. the adjustment of sea level to air pressure changes, is the most important factor driving these variations [*Crawford*, 1980]. According to this effect, a pressure fall of 30 hPa (that is typical for strong cyclones) produces a sea raise of 30 cm. However, during some extreme storm events, air pressure can fall by 40 and even by 50 hPa. It is these extreme events that are responsible for the maximum observed sea levels (Tables 10 and 11). Strong onshore winds are an additional factor that significantly amplify storm surge.

There are two main causes of seasonal variations in extreme sea level:

(1) *Seasonal variations in atmospheric activity*. In winter, atmospheric processes are much more active and energetic than in summer; almost all strong storms over the coast of British Columbia occur in winter [*Thomson*, 1981].

(2) *Seasonal changes in sea level*. The seasonal sea level maximum is observed in January, the minimum in May-July [*Crawford*, 1980]. A typical amplitude for the annual tidal harmonic, Sa, is ~12 cm [*Crawford*, 1980; *Thomson*, 1981]. This means that relative to mean sea level, in January the sea level is 12 cm higher than mean value and in July it is 12 cm lower; the difference is significant.

The spatial uniformity of long-period sea level changes in the Strait of Georgia enables us to generalize our estimates. For example, the difference in extreme sea level anomalies between Nanaimo and Patricia Bay is only 7%. The highest sea level recorded at Patricia Bay during 43.5 years of observations was 1.04 m. If we allow for a "safety factor" of 1.5, we find that the maximum possible sea level rise associated with meteorological forcing for these two stations is **1.6-1.7 m**.

These estimates can be verified using the 106 years of sea level observations at Point Atkinson (Caulfield), which has the longest water level record for the Strait of Georgia. Extreme sea level statistics for this station can be effectively used to estimate possible extreme sea level heights at Patricia Bay and Nanaimo. This can be a subject of an independent study.

Possible extreme sea level heights at Patricia Bay and Nanaimo caused by atmospheric forcing are substantially larger than those related to trans-oceanic and local tsunamis [cf. *Rabinovich et al.*, 2021, 2023]. Our preliminary analysis of available data indicates that storm surge for this region (the Strait of Georgia) is more of a hazard than tsunami waves.

7. DISCUSSION AND CONCLUSIONS

Large segments of the British Columbia coast are susceptible to floods produced by a variety of marine hazards, including trans-oceanic tsunamis, local tsunamis, landslide-generated tsunamis, storm surges and meteotsunamis. For different coastal regions, different hazards are the major threats. As a consequence, comprehensive research is needed to know in advance the sources of major risk and to plan for damage mitigation.

The main focus of the present study was the southern part of the Strait of Georgia, more specifically the Saanich Inlet/Pat Bay and Nanaimo regions, where the Institute of Ocean Sciences and Pacific Biological Station are located. We consequently examined various types of marine hazards and their risk for the two regions specified.

We examined seven major trans-oceanic tsunamis observed on the coast of British Columbia during the years 1946, 1952, 1957, 1960, 1964, 2010 and 2011. Three of these events were of particular interest - the 1960 Chile, 1964 Alaska and 2011 Tohoku (East Japan) tsunamis – and can be considered as "*worst case scenarios*" for three regions within the Pacific Rim of Fire that have maximum tsunamigenic potential: (1) Chile, (2) the Alaska-Aleutian Islands, and (3) Japan-Kuril Islands-Kamchatka. From these three, *the 1964 Alaska tsunami* induced by a M_w 9.2 earthquake in the Alaska-Aleutian Subduction Zone, was the most destructive. This was the strongest tsunami ever observed on the coast of British Columbia and it created the severest damage at Port Alberni and at other sites along the oceanic coast of Vancouver Island (*Rabinovich et al.*, 2019). The tsunami penetrated into the southern Strait of Georgia generating estimated maximum wave heights in Patricia Bay and at Nanaimo of up to **50-100 cm**. As the 1964 Alaska tsunami was an extreme event, with a recurrence period of ~1000 years, our estimates for Patricia Bay and Nanaimo can be considered as maximum possible values for Alaska tsunamis. Therefore, based on our analysis of these seven major events, we conclude that **trans-oceanic tsunamis present a significant, but not major, threat to the Institute of Ocean Sciences in Patricia Bay or to the Pacific Biological Station in Nanaimo**. These conclusions are in good agreement with the official Provincial Emergency Preparedness tsunami planning levels that indicate the inner coasts of the Strait of Georgia as regions of low tsunami risk with expected tsunami wave heights of 0.5-1.0 m.

The primary concern is a major tsunami generated by a great earthquake in the Cascadia Subduction Zone (CSZ). As was indicated by *Ng et al.* [1991], "*Inside the Strait of Georgia, the*

wave heights are significant enough to receive closer attention, especially in low-lying areas". It is clear from this statement and from the findings of existing numerical results for a CSZ event for the Strait of Georgia [*Cherniawsky et al.*, 2007; *Cheung et al.*, 2011; *Fine et al.*, 2018b] that further high-resolution **numerical modelling** is needed for the Institute of Ocean Sciences and Pacific Biological Station locations to confirm the limited risk to wave inundation proposed for these facilities.

The probability of major tsunamigenic earthquakes inside the Strait of Georgia is small. The strongest crustal earthquake in the region was the $\boldsymbol{M_w}$ **7.3 1946 event on eastern Vancouver Island.** *Murty and Hebenstreit* [1989] simulated this event based on the 1946 event model taken from *Rogers and Hasegawa* [1978] and found that the earthquake produced moderate effects in the vicinity of Nanaimo and negligible effects in Saanich Inlet.

Submarine landslides, rock falls, slumps and avalanches can produce significant tsunamis along the coast of British Columbia [cf. *Evans*, 2001; *Rabinovich et al*., 2003]. Large accumulations of unstable sediments deposited in river deltas and, primarily, in the deltaic regions of the Fraser River, are particularly dangerous. These sediments form a huge body of unstable alluvial deposits at the entrance to the river and could, potentially, produce a destructive tsunami in the southern part of the Strait of Georgia that might impact Patricia Bay and Nanaimo. In terms of damage and loss of life, such events are more threatening than tsunamis generated by distant earthquakes. However, the effects are **local**: tsunami amplitudes associated with submarine landslides decay quickly with distance from the source area.

Following the numerical study of *Rabinovich et al.* [2003], we examined two specific regions of high risk of submarine slides: (1) Roberts Bank formed by alluvial sediment materials from the Fraser River delta; and (2) Malaspina Strait separating Texada Island from the mainland BC coast. The Roberts Bank slide was found to produce significant tsunami runup on the southeastern coasts of the Gulf Islands, but the estimated amplitudes for the areas of Patricia Bay and Nanaimo would be <0.5 m. A failure in Malaspina Strait yielded 4-m waves on the SE coast of Texada Island but waves would be negligible at Nanaimo and not detectable at Patricia Bay. In general, the risk from landslide-generated tsunamis for the regions of Patricia Bay and Nanaimo is low.

There is considerable risk to the east coast of Vancouver Island associated with sea level oscillations caused by atmospheric processes. Several storm-initiated floods have been measured in the past in the southern part of the Strait of Georgia. The Saanich Inlet/Pat Bay and Nanaimo

regions are susceptible to anomalously highwater levels during major southeasterly storms at the time of "King Tides". As part of the present study, we examined the monthly extrema in water levels at Patricia Bay and Nanaimo, both original and residual (de-tided) records. Residual positive sea level changes (storm surges) are mainly associated with strong cyclones propagating over Vancouver Island in wintertime. These changes are caused by an inverted barometer effect, i.e. the adjustment of sea level to air pressure changes, and to strong onshore winds.

Two main causes determine seasonal variations in extreme sea level and their amplification in winter: (1) Seasonal variations in atmospheric activity; in winter, atmospheric processes are much more active and energetic than in summer; and (2) seasonal sea level changes; in January, the sea level is 12 cm higher than the mean sea level value and in July it is 12 cm lower.

The spatial uniformity of long-period sea level changes in the Strait of Georgia enables us to generalize our estimates. In particular, the difference in extreme sea level anomalies between Nanaimo and Patricia Bay is only 7%. The highest sea level recorded at Patricia Bay during 43.5 years of observations was 1.04 m. If we allow for a "safety factor" of 1.5, we find that the maximum possible sea level rise associated with meteorological forcing for these two stations is **1.6-1.7 m**. **Based on existing data, we find that possible extreme sea level heights at Patricia Bay and Nanaimo caused by atmospheric forcing are substantially higher than those arising from trans-oceanic and local tsunamis. Our preliminary analysis of available data indicates that storm surge for this region (the Strait of Georgia) is more of a hazard than tsunami waves.**

Additional risk for the east coast of Vancouver Island is associated with *meteorological tsunamis (meteotsunamis)* – high-frequency sea level oscillations with typical periods from a few minutes to a couple of hours generated by atmospheric pressure jumps, internal atmospheric gravity waves, squall lines or frontal passages [*Monserrat et al.*, 2006; *Rabinovich*, 2020]. This question requires an independent study. However, preliminary estimates based on results of *Thomson et al.* [2009] and *Rabinovich et al.* [2021, 2023] demonstrate that meteotsunamis regularly occur in the southern Strait of Georgia, but their positive amplitudes are typically <15-20 cm. This means that they themselves cannot create significant floods in this region but combined with storm surges they can amplify the negative effect of surge.

There is also another important factor that should be taken into consideration: the speed of currents that accompany sea level oscillations. As current speeds arising from wave-like motions

are inversely proportional to the wave period, the typical period of meteotsunamis of ~15 min is approximately 50 times smaller than the predominant 12.5-hour semidiurnal tidal period. Current speeds are directly proportional to wave height; with typical amplitudes of tides (~1.5 m) approximately ten times larger than typical amplitudes of meteotsunamis (~15 cm). However, because meteotsunami periods are ~50 times shorter than tidal, currents caused by a 15-cm meteotsunami will be five times stronger than tidal currents associated with 1.5 m tide. For example, if tidal currents on the shelf or in a narrows are 30-50 cm/s, then the meteotsunami currents can be 1.5-2.5 m/s (3-5 knots). Such currents can cause damage to yachts, boats, port infrastructure, including those in Nanaimo and Patricia Bay harbours. Strong currents of this magnitude associated with meteotsunami were observed in the area of Point Atkinson and Thetis Island [*Thomson et al.*, 2009; *Rabinovich et al.*, 2021].

REFERENCES

Abe, K. (1973), Tsunami and mechanism of great earthquakes, *Physics of the Earth and Planetary Interiors*, 7(2), 143-153.

Abe, K. (1979), Size of great earthquakes of 1873-1974 inferred from tsunami data, *Journal of Geophysical Research*, 84(B4), 1561-1568.

Atwater, B.F., Musumi-Rokkaku, S., Satake, K., Tsuji, Y., Ueda, K., and Yamaguchi, D.K. (2005), *The Orphan Tsunami of 1700—Japanese Clues to a Parent Earthquake in North America*, U.S. Geological Survey Professional Paper No. 1707, 133 p.

Berkman, S.C. and Symons, J.M. (1960), *The tsunami of May 22, 1960 as Recorded at Tide Gauge Stations*, U.S. Department of Commerce, Coast and Geodetic Survey, Washington, D.C., 79 p.

Bornhold, B.D. and Thomson, R.E. (2012), Tsunami hazard assessment related to slope failures in coastal waters. In *Landslides - Types Mechanisms and Modelling*, Eds. John Clague and Douglas Stead, Cambridge University Press, pp. 108-120.

Brideau, M.-A., Sturzenegger, M., Stead, D., Jaboyedoff, M., Lawrence, M., Roberts, N., Ward, B., Millard, T., and Clague, J. (2012), Stability analysis of the 2007 Chehalis Lake landslide based on long-range terrestrial photogrammetry and airborne LiDAR data, *Landslides*, 9, 75–91; doi: 10.1007/s10346-011-0286-4

Cherniawsky, J.Y., Titov, V.V., Wang, K., and Li, J.-Y. (2007), Numerical simulations of tsunami waves and currents for southern Vancouver Island from a Cascadia megathrust earthquake, *Pure and Applied Geophysics*, 164, 465–492; doi: 10.1007/s00024-006-0169-0.

Cheung, K.F., Wei, Y., Yamazaki, Y., and Yim, S.C.S. (2011), Modeling of 500-year tsunamis for probabilistic design of coastal infrastructure in the Pacific Northwest, *Coastal Engineering*, 58, 970–985.

Chillarige, A.V., Robertson, P.K., Morgenstern N.R., and Christian H.A. (1997a), Evaluation of the in situ state of Fraser River sand, *Canadian Geotechnical Journal*, 34, 510-519.

Chillarige, A.V., Morgenstern N.R., Robertson, P.K., and Christian H.A. (1997b), Seabed instability due to flow liquefaction in the Fraser River Delta, *Canadian Geotechnical Journal*, 34, 520-533.

Christian, H.A., Woeller, D.J., Robertson, P.K., and Courtney R.C. (1997a), Site Investigations to evaluate flow liquefaction slides at Sand Heads, Fraser River Delta, *Canadian Geotechnical Journal*, 34, 384-397.

Christian, H.A., Mosher, D.C., Mulder, T., J.V. Barrie, and Courtney R.C. (1997b), Geomorphology and potential slope instability on Fraser River Delta foreslope, Vancouver, British Columbia, *Canadian Geotechnical Journal*, 34, 432-446.

Clague, J.J. (2001), Tsunamis, in *A Synthesis of Geological Hazards in Canada*, edited by G.R. Brooks, Geol. Surv. Canada, Bull. 548, 27-42.

Clague, J.J., Bobrowsky, P.T., and Hutchinson, I. (2000), A review of geological records of large tsunamis at Vancouver Island, British Columbia, and implications for hazard, *Quaternary Science Reviews*, 19, 849-863.

Clague, J.J., Munro, A., and Murty, T.S. (2003), Tsunami hazard and risk in Canada, *Natural Hazards*, 28(2-3), 407-434.

Cornforth, D.H. and Lowell, J.A. (1996), The 1994 submarine slope failure at Skagway, Alaska. In *Landslides* (Balkema, Rotterdam, 1996), pp. 527-532.

Crawford, W.R. (1980), Sea level changes in British Columbia at periods of two days to a year, *Pacific Marine Science Report 80-8*, Institute of Ocean Sciences, Sidney, BC, 46 p.

Currie, R.G. and Mosher, D.C. (1996), Swath bathymetric surveys in the Strait of Georgia, British Columbia. In *Current Research, Part E*, Geological Survey of Canada, 33-40.

Dunbar, D.S. and Harper, J.R. (1993), Numerical simulation of tsunamigenic submarine slope failure in the Fraser River Delta, British Columbia, *Marine Geodesy*, 16, 101-108.

Eungard, D.W., Forson, C., Walsh, T.J., Gica, E., and Arcas, D. (2018), Tsunami hazard maps of the Anacortes–Bellingham area, Washington—Model results from a ~2,500-year Cascadia Subduction Zone earthquake scenario, Washington Geological Survey, Map Series 2018-02, Washington State Department of Natural Resources, Washington Geological Survey.

Evans, S.G. (2001), Landslides. In: *A Synthesis of Geological Hazards in Canada* (ed. Brooks, G. R.), Geological Survey of Canada, Bull. 548, 43–79.

Fine, I.V., Cherniawsky, J.Y., Rabinovich, A.B., and Stephenson F.E. (2008), Numerical modeling and observations of tsunami waves in Alberni Inlet and Barkley Sound, British Columbia, *Pure and Applied Geophysics*, 165(11/12), 2019-2044.

Fine, I.V., Thomson, R.E., Lupton, L.M., and Mundschutz, S. (2018a), *Numerical Modelling of an Alaska 1964-Type Tsunami at the Canadian Coast Guard Base in Victoria, British Columbia.* Can. Tech. Rep. Hydrogr. Ocean Sci. Fs97-18/323E-PDF; 978-0-660-25253-7.

Fine, I.V., Thomson, R.E., Lupton, L.M., and Mundschutz, S. (2018b), *Numerical Modelling of a Cascadia Subduction Zone Tsunami at the Canadian Coast Guard Base in Victoria, British Columbia*. Can. Tech. Rep. Hydrogr. Ocean Sci. Fs97-18/324E-PDF; 978-0-660-24928-5.

Fritz, H.M., Mohammed, F., and Yoo, J. (2009), Lituya Bay landslide impact generated mega-tsunami 50th anniversary, *Pure and Applied Geophysics*, 166, 153-175; doi:10.1007/s00024-008-0435-4.

Hamilton, T.S. and Luternauer, J.L. (1983), *Evidence of Sea Floor Instability in the Southcentral Strait of Georgia, British Columbia: A Preliminary Compilation*, Geological Survey of Canada, Pap.*83-1A*, 417-421.

Hamilton, T.S. and Wigen, S.O. (1987), The Foreslope Hills of the Fraser River Delta: Implication of tsunamis in Georgia Strait, *Science of Tsunami Hazards*, 5, 15-33.

Jiang, L. and LeBlond, P.H. (1992), The Coupling of a Submarine Slide and the Surface Waves which it Generates, *Journal of Geophysical Research*, 97(C8), 12,731-12,744.

Johns, M. W., Prior, D. B., Bornhold, B. D., Coleman, J. M., and Bryant, W. R. (1986), Geotechnical aspects of a submarine slope failure, Kitimat Fjord, British Columbia, *Marine Geotechnology*, 6, 243–279.

Johnson, J.M., Tanioka, Y., Ruff, L.J., Satake, K., Kanamori, H., and Sykes, L.R. (1994), The 1957 Great Aleutian earthquake. *Pure and Applied Geophysics*, 142(1), 3-28.

Johnson, J.M., Satake, K., Holdahl, S.R., and Sauber, J. (1996), The 1964 Prince William Sound earthquake – joint inversion of tsunami waveforms and geodetic data, *Journal of Geophysical Research*, 101 (B1), 523-532.

Kanamori, H. (1972), Tectonic implication of the 1944 Tonankai and the 1946 Nankaido earthquakes, *Physics of the Earth and Planetary Interiors*, 5(2), 129-139.

Kong, L.S.L., Dunbar, P.K., and Arcos, N. (2015), *Pacific Tsunami Warning System: A Half-Century of Protecting the Pacific*, 1965-2015, ITIC/NOAA, Honolulu, Hawaii, 188 pp.

Kulikov, E.A., Rabinovich, A.B., Thomson, R.E., and Bornhold, B.D. (1996), The Landslide Tsunami of November 3, 1994, Skagway Harbor, Alaska, *Journal of Geophysical Research*, 101 (C3), 6609-6615.

Kulikov, E.A., Rabinovich, A.B., Fine, I.V., Bornhold, B.D., and Thomson, R.E. (1998), Tsunami generation by landslides at the Pacific coast of North America and the role of tides, *Oceanology*, 38(3), 323-328.

Lander, J.F. (1996), *Tsunamis Affecting Alaska, 1737-1996*. USDC/NOAA, Boulder, CO, USA, 195 p.

Leonard, L.J. and Bednarski, J.M. (2014), Field survey following the 27 October 2012 Haida Gwaii tsunami. *Pure and Applied Geophysics*, 171, 3467-3482; doi: 10.1007/s00024-014-0792-0.

Leonard, L.J., Rogers, G.C., and Mazzotti, S. (2014), Tsunami hazard assessment of Canada, *Natural Hazards*, 70, 237-274.

Luternauer, J.L. and Finn, W.D.L. (1983), Stability of the Fraser River delta front, *Canadian Geotechnical Journal*, 20, 603-616.

Mathews, W.A. and Shepard, E.P. (1962), Sedimentation of the Fraser River Delta, British Columbia, *Bulletin of the American Association of Petroleum Geologists*, 46, 1416-1438.

McKenna, G.T. and Luternauer, J.L. (1987), *First Documented Large Failure at the Fraser River Delta Front, British Columbia*, Geological Survey of Canada, Pap. 87-1A, 919-924.

McKenna, G.T., Luternauer, J.L., and. Kostaschuk, R.A. (1992), Large-scale mass-wasting events on the Fraser River Delta near Sand Heads, British Columbia, *Canadian Geotechnical Journal*, 29, 151-156.

Murty, T.S. (1977), *Seismic Sea Waves - Tsunamis*. Bull. Fish. Res. Board Canada 198, Ottawa, 337 p.

Murty, T.S. (1984), *Storm Surges – Meteorological Ocean Tides*, No. 212 Canadian Bulletin of Fisheries and Aquatic Sciences, Ottawa, 897 pp.

Murty, T.S. and Crean, P.B. (1986), Numerical simulation of the tsunami of June 23,1946 in British Columbia, Canada, *Science of Tsunami Hazards*, 4(1), 15-24.

Murty T. S. and Hebenstreit G. T. (1989), Tsunami amplitudes from local earthquakes in the Pacific Northwest region of North America. Part 2: Strait of Georgia, Juan de Fuca Strait, and Puget Sound, *Marine Geodesy*, 13(3), 189-209, doi: 10.1080/15210608909379623

Myers, E.P., Baptista, A.M., and Priest, G.R. (1999), Finite element modelling of potential Cascadia subduction zone tsunamis, *Science of Tsunami Hazards*, 17, 3–18.

Myers, E.P. and Baptista, A.M. (2001), Analysis of factors influencing simulations of the 1993 Hokkaido Nansei-Oki and 1964 Alaska tsunamis, *Natural Hazards*, 23, 1–28.

Ng, M., LeBlond, P.H., and Murty, T.S. (1990), Numerical simulation of tsunami amplitudes on the coast of British Columbia due to local earthquakes, *Marine Geodesy*, 13, 101-146.

Prince Rupert Daily News (1964), Newspaper articles for March 30 – April 7, 1964.

Prior, D.B., Wiseman, W.J., and Bryant, W.R. (1981), Submarine chutes on the slopes of fjord deltas, *Nature*, 290, 5804, 326–328.

Prior, D. B., Bornhold, B. D., and Johns, M. W. (1984), Depositional characteristics of a submarine debris flow, *Journal of Geology*, 92, 707–727.

Pugh, D. and Woodworth, P. (2014), *Sea-Level Science: Understanding Tides, Surges, Tsunamis and Mean Sea-Level Changes*. Cambridge: Cambridge University Press.

Rabinovich, A.B. (2019), Twenty-seven years of progress in the science of meteorological tsunamis following the 1992 Daytona Beach event, *Pure and Applied Geophysics*, 177(3), 1193-1230; doi: 10.1007/s00024-019-02349-3.

Rabinovich, A.B., Thomson, R.E., Bornhold, B.D., Fine, I.V., and Kulikov, E.A. (2003), Numerical modelling of tsunamis generated by hypothetical landslides in the Strait of Georgia, British Columbia, *Pure and Applied Geophysics*, 160 (7), 1273-1313.

Rabinovich, A.B. and Stephenson, F.E. (2004), Longwave measurements for the coast of British Columbia and improvements to the tsunami warning capability, *Natural Hazards*, 32(3), 313-343.

Rabinovich, A.B., Thomson, R.E., and Stephenson, F.E. (2006), The Sumatra tsunami of 26 December 2004 as observed in the North Pacific and North Atlantic oceans, *Surveys in Geophysics*, 27, 647-677.

Rabinovich, A.B., Candella, R., and Thomson, R.E. (2011), Energy decay of the 2004 Sumatra tsunami in the world ocean, *Pure and Applied Geophysics*, 168(11), 1919-1950; doi 10.1007/s00024-01-0279-1.

Rabinovich, A.B., Thomson, R.E., and Fine, I.V. (2013), The 2010 Chilean tsunami off the west coast of Canada and the northwest coast of the United States, *Pure and Applied Geophysics*, 170, 1529-1565, doi 10.1007/s00024-012-0541-1.

Rabinovich, A.B., Thomson, R.E., Krassovski, M.V., Stephenson, F.E., and Sinnott, D.C. (2019), Five great tsunamis of the 20th century as recorded on the coast of British Columbia, *Pure and Applied Geophysics*, 176(7), 2887-2924; doi: 10.1007/s00024-019-02133-3.

Rabinovich, A.B., Šepić, J., and Thomson, R.E. (2021), The meteorological tsunami of 1 November 2010 in the southern Strait of Georgia: A case study, *Natural Hazards*, 106(2), 1503-1544; doi: 10.1007/s11069-020-04203-5.

Rabinovich, A.B., Šepić, J., and Thomson, R.E. (2023), Strength in numbers: The tail end of typhoon Songda combines with local cyclones to generate extreme sea level oscillations on the British Columbia and Washington Coasts during Mid-October 2016, *Journal of Physical Oceanography*, 53(1), 131-155; doi:10.1175/JPO-D-22-0096.1.

Ren, P., Bornhold, B.D., and Prior, D.B. (1996), Seafloor morphology and sedimentary processes, Knight Inlet, British Columbia, *Sedimentary Geology*, 103, 201-228.

Rogers, G.C. (1980), A documentation of soil failure during the British Columbia earthquake of 23 June, 1946, *Canadian Geotechnical Journal*, 17, 122–127.

Rogers, G.C. (1998), Earthquakes and earthquake hazard in the Vancouver area. In: J.J. Clague, J.L. Luternauer, and D.C. Mosher (Eds) *Geology and Natural Hazards of the Fraser River Delta, British Columbia*. Geological Survey of Canada, Bull. 525, pp.17–25.

Rogers, G C. and Hasegawa, H.S. (1978), A Second Look at the British Columbia earthquake of 23 June, 1946, *Bulletin of the Seismological Society of America*, 68(3), 653–675.

Salsman, G.G. (1959), *The Tsunami of March 9, 1957, as Recorded at Tide Stations*, U.S. Department of Commerce, Coast and Geodetic Survey, Techn. Bull. No.6, Washington, D.C., 18 p.

Satake, K., Shimazaki, K., Tsuji, K., and Ueda, K. (1996), Time and size of a giant earthquake in Cascadia earthquake inferred from Japanese tsunami records of January 1700, *Nature*, 379, 246–249.

Seemann, M., Onur, T., and Cloutier-Fisher, D. (2011), Earthquake shaking probabilities for communities on Vancouver Island, British Columbia, Canada, *Natural Hazards*, 58, 1253-1273; doi 10.1007/s11069-011-9727-6.

Sheppard, F.P., MacDonald, G.A., and Cox, D.C., (1950), The tsunami of April 1, 1946, *Bulletin of the Scripps Institution of Oceanography*, University of California, La Jolla, 5, 391-528.

Soloviev, S.L. and Go, Ch.N. (1975), *Catalogue of Tsunamis on the Eastern Shore of the Pacific Ocean*. (Nauka Publ. House, Moscow, 1975), 204 p. (in Russian; English translation: Canadian Transl. Fish. Aquatic Sci., No. 5078, Ottawa, 1984, 285 p.)

Spaeth, M.G. and Berkman, S.C. (1967), *The Tsunami of March 28, 1964, as Recorded at Tide Stations*, ESSA Technical Report C&GS 33, Rockville, Md, 86 p.

Stephenson, F.E., Rabinovich, A.B., Solovieva, O.N., Kulikov, E.A., and Yakovenko, O.I. (2007), *Catalogue of Tsunamis, British Columbia, Canada: 1700-2007*. Preprint. P.P. Shirshov Inst. Oceanology, Moscow, 134 p.

Stephenson F.E. and Rabinovich, A.B. (2009), Tsunamis on the Pacific coast of Canada recorded in 1994-2007, *Pure and Applied Geophysics*, 166(1/2), 177-210.

Suleimani, E.N., Nicolsky, D.J., and Koehler, R.D. (2013), *Tsunami Inundation Maps of Sitka, Alaska*, Report of Investigations 2013-3, State of Alaska, Department of Natural Resources, Division of Geological and Geophysical Surveys, Fairbanks, AK, 76 p.

Terzaghi, K. (1956), Varieties of submarine slope failures. In *8th Texas Conference on Soil Mechanics and Foundation Engineering* (Houston, Harvard Soil Mech. Comm., 1956), 41 p.

Thomson, R. E. (1981), *Oceanography of the British Columbia*, Coast. Can. Special Pub. Fish. Aquat. Sci., 56. Ottawa, 291 p.

Thomson, R.E., Rabinovich, A.B., Kulikov, E.A., Fine, I.V., and Bornhold, B.D. (2001), On numerical simulation of the landslide-generated tsunami of November 3, 1994 in Skagway Harbor, Alaska. In *Tsunami Research at the End of a Critical Decade*, edited by G. Hebenstreit, Kluwer Acad. Publ., Dordrecht, 243-282.

Thomson, R.E. and Spear, D.J. (2020), Gravity currents facilitate the generation and propagation of internal bores and solitons at the bottom of the Strait of Georgia, *Journal of Geophysical Research-Oceans*, 125(10); doi: 10.1029/2020JC016589 (submitted).

Tiffin, D.L., Murray, J.W., Myers, I.R., and Garrison, R.E. (1971), Structure and origin of the Foreslope Hills, Fraser Delta, British Columbia, *Bulletin of Canadian Petroleum Geology*, 19, 589-600.

Walsh, T.J., Titov, V.V., Venturato, A.J., Mofjeld, H.O., and González, F.I. (2003), *Tsunami Hazard Map of the Elliott Bay area, Seattle, Washington: Modeled Tsunami Inundation from*

a Seattle Fault Earthquake, Washington Division of Geology and Earth Resources, Open File Report 2003-14, NOAA TIME Center, PMEL, Seattle, WA.

Walsh, T.J., Arcas, D., Titov, V.V., and Chamberlin, C.C. (2014), *Tsunami Hazard Map of Everett, Washington: Model Results for Magnitude 7.3 and 6.7 Seattle Fault Earthquakes, Washington*, Division of Geology and Earth Resources, Open File Report 2014-03, NOAA Center for Tsunami Research, PMEL, Seattle, WA.

Wang, J., Ward, S.N., and Xiao, L. (2015), Numerical simulation of the December 4, 2007 landslide-generated tsunami in Chehalis Lake, Canada, *Geophysical Journal International*, 201, 372–376; doi: 10.1093/gji/ggv026

Wang, K., Wells, R., Mazzotti, S., Hyndman, R.D., and Sagiya T. (2003), A revised dislocation model of interseismic deformation of the Cascadia subduction zone, *Journal of Geophysical Research* 108(B1), doi:10.1029/2001JB001227.

Wang, K., and Tréhu, A.M. (2016), Invited review paper: Some outstanding issues in the study of great megathrust earthquakes—The Cascadia example, *Journal of Geodynamics*, 98, 1-18.

Wang, P-L., Engelhart, S.E., Wang, K., Hawkes, A.D., Horton, B.P., Nelson, A.R., and Witter, R.C. (2013), Heterogeneous rupture in the Great Cascadia earthquake of 1700 inferred from coastal subsidence estimates. *Journal of Geophysical Research*, 118, 2460-2473.

Weeks, S., and Studds, R.F.A. (1953), *The Tsunami of November 4, 1952 as Recorded at the Tide Gauges*. Spec. Publ. #300, U.S. Department of Commerce, Coast and Geodetic Survey, Washington, D.C., 62 p.

White, W.R.H. (1966), The Alaska earthquake – Its effect in Canada, *Canadian Geographical Journal*, 210–219.

Whitmore, P.M. (1993), Expected tsunami amplitudes and currents along the North American coast for Cascadia subduction zone earthquakes, *Natural Hazards*. 8, 59–73.

Wigen, S.O. (1960), *Tsunami of May 22, 1960. West Coast of Canada*, Unpublished Report, Canadian Hydrographic Service, Sidney, BC.

Wigen, S.O. (1983), Historical studies of tsunamis at Tofino, Canada, in *Tsunamis – Their Science and Engineering*, edited by K. Iida and T. Kawasaki, Terra Sci. Publ. Comp., Tokyo, Japan, 105-119.

Wigen, S.O. and White, W.R.H. (1964), *Tsunami of March 27-29, 1964, West Coast of Canada*, Dept. Mines Techn. Surv., Victoria, BC, Canada, 12 p.

Witter, R.C., Zhang, Y.J., Wang, K., Priest, G.R., Goldfinger, C., Stimely, L., English, J.T., and Ferro, P.A. (2013), Simulated tsunami inundation for a range of Cascadia megathrust earthquake scenarios at Bandon, Oregon, USA, Geosphere, *9*(6): 1783–1803; https://doi.org/10.1130/GES00899.1